Order Number 9408467

Critical behavior of rectangular frames considering the influence of non-linear flexible connections and lateral bracing in the presence of primary bending moments

Alkhatib, Ayman, Ph.D.

The University of Arizona, 1993

U·M·I
300 N. Zeeb Rd.
Ann Arbor, MI 48106

CRITICAL BEHAVIOR OF RECTANGULAR FRAMES CONSIDERING THE INFLUENCE OF NON-LINEAR FLEXIBLE CONNECTIONS AND LATERAL BRACING IN THE PRESENCE OF PRIMARY BENDING MOMENTS

by

Ayman Alkhatib

A Dissertation Submitted to the Faculty of the

DEPARTMENT OF CIVIL ENGINEERING AND ENGINEERING MECHANICS

In Partial Fulfillment of the Requirements
For the Degree of

DOCTOR OF PHILOSOPHY
WITH A MAJOR IN CIVIL ENGINEERING

In the Graduate College

THE UNIVERSITY OF ARIZONA

1 9 9 3

THE UNIVERSITY OF ARIZONA
GRADUATE COLLEGE

As members of the Final Examination Committee, we certify that we have read the dissertation prepared by Ayman Alkhatib

entitled Critical Behavior of Rectangular Frames Considering the Influence of Non-Linear Flexible Connections and Lateral Bracing in the Presence of Primary Bending Moments

and recommend that it be accepted as fulfilling the dissertation requirement for the Degree of Doctor of Philosophy

Dr. Donald A. DaDeppo	Date 8/10/93
Dr. Ralph Richard	Date 8/10/93
Dr. Panos Kiousis	Date 8/10/93
Dr. Dinshaw N. Contractor	Date 8/10/93
Dr. George Frantziskonis	Date 8/10/93

Final approval and acceptance of this dissertation is contingent upon the candidate's submission of the final copy of the dissertation to the Graduate College.

I hereby certify that I have read this dissertation prepared under my direction and recommend that it be accepted as fulfilling the dissertation requirement.

Dissertation Director	Date 8/10/93

STATEMENT BY AUTHOR

This dissertation has been submitted in partial fulfillment for an advanced degree at The University of Arizona and is deposited in the University Library to be made available to borrowers under rules of the library.

Brief quotations from this dissertation are allowable without special permission, provided that accurate acknowledgement of source is made. Requests for permission for extended quotation from or reproduction of this manuscript in whole or in part may be granted by the head of the major department or the Dean of the Graduate College when in his or her judgement the proposed use of the material is in the interest of scholarship. In all other instances, however, permission must be obtained from the author.

SIGNED: Ayman Alkhatib

ACKNOWLEDGEMENTS

The author would like to convey his genuine gratitude and sincere appreciation to his advisor and major professor, Dr. Donald A. DaDeppo, for his ingenuous guidance and support throughout this study.

The author wishes to express his sincere gratefulness to Professor Ralph M. Richard for the valuable suggestions and generous contributions to this study.

Sincere thanks are extended to Dr. Panos D. Kiousis and to the graduate committee members.

The author would like to acknowledge his indebtedness to his father, Dr. Mohammad M. Alkhatib, for his ultimate devotion and inspiration, and his wife, daughters, sisters and brothers for their love and support.

Finally, the support of The University of Damascus is greatly appreciated.

To the memory of

MY MOTHER

Raga` Habbab

TABLE OF CONTENTS

Page

TABLE OF CONTENTS (Cont'd.)

Page

LIST OF ILLUSTRATIONS

Page

LIST OF ILLUSTRATIONS (Cont'd.)

Page

LIST OF ILLUSTRATIONS (Cont'd.)

Page

LIST OF ILLUSTRATIONS (Cont'd.)

Page

LIST OF TABLES

ABSTRACT

In almost all investigations on stability of frames having flexible connections, it has been assumed that frames are loaded in such a manner that no bending moments are present when instability is initiated. Apparently, this condition is not fulfilled for many frame work systems that are designed in principle to undertake bending moment. The question arises as to how the combined influence of connection stiffness and primary bending moments affect the buckling strength of a structure and how to account for these factors.

To answer this question a Fortran program is developed for the analysis of flexibly jointed symmetric one-story frames and two-story frames. The well known slope-deflection equations are utilized in the analysis. The exact moment-rotation attributes of several connections are used in the analysis. Iterative procedures are implemented to permit reducing the stiffnesses of the compression members according to the values of their axial forces and to find the connection rotations that correspond to the pertinent bending moments. The elastic critical load of the structure is found by tracing its load-deflection behavior throughout the entire range of loading up to the critical load.

Further studies include the effect of lateral bracing on the critical behavior of framed structures. Both modes of buckling, symmetrical and anti-symmetrical, are considered. The critical load for the anti-symmetrical mode of buckling is found to be

considerably lower than that corresponding to the symmetrical mode. When sufficient lateral bracing is provided, the frame buckles only in a symmetrical mode. Values for the minimum ratios of brace-to-frame stiffness required to prevent lateral instability are given for several cases.

Diverse numerical applications are presented to show the impact of the presence of flexible connections and lateral bracing on the critical behavior of frames. The proposed analysis, utilizing the slope-deflection equations in a unique way and implementing the Newton-Raphson procedure to solve the related non-linear equations for multi-story frames, is found to be both simple and efficient.

CHAPTER 1

INTRODUCTION

1.1. General

In practical frame design, connections are assumed to be pinned or rigid. A rigid connection is defined as a connection that provides moment resistance and has no flexibility. A pinned connection is known as a connection that features zero moment resistance. In reality, a rigid connection exhibits some flexibility, and a connection regarded as pinned possesses some rotational stiffness.

Numerous studies conducted on the design of frames call attention to the substantial economy resulting when the actual behavior of the connections is considered. One advantage of utilizing a semi-rigid connection in design is the cutback of beam moment, leading to lighter beams. This improved economy would only have meaning if the stability of the structure is still preserved. Studies on elastic stability of frames regarding the realistic behavior of the connection are reviewed in the next chapter. The conclusion drawn from these studies is that stiffer connections enhance the stability of the structure. In other words, the critical load increases with the connection stiffness.

In almost all investigations on stability of frames having flexible connections, it has been assumed that frames are loaded in such a manner that no bending moments are present when instability is initiated. Apparently, this condition is not fulfilled for many framework systems that are designed in principle to undertake bending moment. In fact, when primary bending moments are ignored in the analysis, the conclusion that

stiffer connections yield higher buckling load is obvious. It is merely rational that the increase in the connection stiffness, which in turn increases the structural stiffness, can only enhance the stability of the structure. However, when primary bending moments are taken into consideration, increasing connection stiffness permits a higher moment at the top of the column, which may impair the stability of the structure. The question arises as to how the combined influence of connection stiffness and primary bending moments affect the buckling strength of a structure and how to account for these factors. The concern that an increase in connection stiffness may impair the stability of the structure is legitimate. An increase in connection stiffness over the design value may be the result of a customary shop practice or a practical frame design. It is common shop practice to use a connection stronger (and probably stiffer) than that specified in the design because of lack of availability. It is also common in practical frame design to consider that a semi-rigid connection behaves like a pin. This concern may be negated if one could establish that stiffer connections enhance the stability of the structure, even in the presence of primary bending moments. Therefore, one objective of this investigation is to determine whether stiffer and stronger connections are better.

This study is concerned with elastic instability. The well-known slope-deflection equations are utilized to determine the elastic critical behavior of frames having flexible beam-to-column connections. The exact moment-rotation attributes of connections are used in the analysis. Iterative procedures are implemented to take into account the stiffness-reducing effect of axial force. The load-deflection approach is used in this analysis. The buckling load of the structure is found by tracing its load-deflection behavior

throughout the entire range of loading up to the critical load.

1.2. Scope and Objective:

The objectives of this research work are:

1. To study the influence of non-linear flexible end restraint on the critical behavior of frames in the presence of primary bending moments. The frame critical behavior is considered for both symmetrical and anti-symmetrical modes of buckling. For a column buckled in the elastic range, the magnitude of the buckling load has a unique value, but in the inelastic range this magnitude depends on the particular loading path. The critical load associated with the tangent-modulus is such that it is the largest load at which a column can buckle without strain reversal in the cross sections. In Technical Memorandum No.1 entitled " The Basic Column Formula."(issue May 19, 1952), the Column Research Council recommended use of the tangent modulus in stability analysis. The following key sentence in the memorandum sums this up:

It is the considered opinion of the Column Research Council that the tangent modulus formula for the buckling strength affords a proper basis for the establishment of working load formula.

Against this background Joseph A. Yura (1971) suggested an iteration procedure to find the effective length of an inelastic column where the flexural rigidity of a compression member is taken as the product of the tangent-modulus E_t and the moment of inertia I. The tangent-modulus at any stress level may be obtained from the AISC stress-strain curve or any other assumed curve.

It is not in the scope of this study to launch into a full investigation concerning the effect of inelastic behavior.

2. To study the effect of lateral bracing on the critical load value for a multi-story frame.

Frames that are not braced will buckle in an anti-symmetrical mode. The critical load in this case is considerably lower than for the critical load corresponding to the symmetrical mode of buckling. It is of interest to verify this fact and to find the minimum ratio of frame-to-brace stiffness that will prevent lateral instability.

The analysis for a simple portal frame and a two-story frame is performed in the cases of symmetrical and anti-symmetrical buckling modes. The method of the slope-deflection equations is used in a unique way as the basis for the analysis to account for both primary bending moments and the non-linear behavior of the flexible connections.

The outcome of this research work should provide a thorough understanding of the effect of the realistic behavior of flexible connections and the effect of lateral bracing on the critical behavior of frames.

The work done covers the cases of both single-bay portal frames and two-story frames. The analysis for multi-story frames of more than two stories can be accomplished by proceeding along the same lines for two-story frames after adding the appropriate equations, but with no new elements involved in the analysis. Hence, the analysis and numerical application given for two-story frames are taken as representative of the case of multi-story frames.

CHAPTER 2

LITERATURE REVIEW

The influence of flexible connections on frame stability has been studied by many scholars. Chen in 1993 presented a book which includes an extensive review of the work done in the area of flexible connections. The papers presented in the book dealt with three subjects on flexible connections. First, the analysis and design of flexible frames. Second, buckling load analysis of flexible frames. Third, behavior and modeling of semi-rigid connections. In this chapter, a few selected papers on the buckling load analysis of flexible frames and on the behavior and modeling of flexible connections are referenced.

2.1. Buckling Load Analysis of Flexible Frames

Simitses and Vlahinos (1982) presented a method to assess the critical behavior of a two-bar frame with a flexible joint, as shown in Figure 2.1. The frame was subjected to an eccentric concentrated load near the joint. The flexible joint was modelled by a linear elastic torsion spring connecting the two members. The study included an assessment of the effect of increasing the stiffness of the flexible joint on the critical behavior of the frame. Figure 2.2 was presented by Simitses and Vlahinos to illustrate the effect of the joint stiffness K on the critical load value.

A buckling load analysis based on the slope-deflection equations was presented by Ackroyed and Gerstle in 1983. The analysis was for the flexible frame shown in Figure 2.3. The flexible connections were modelled as linear elastic torsion springs.

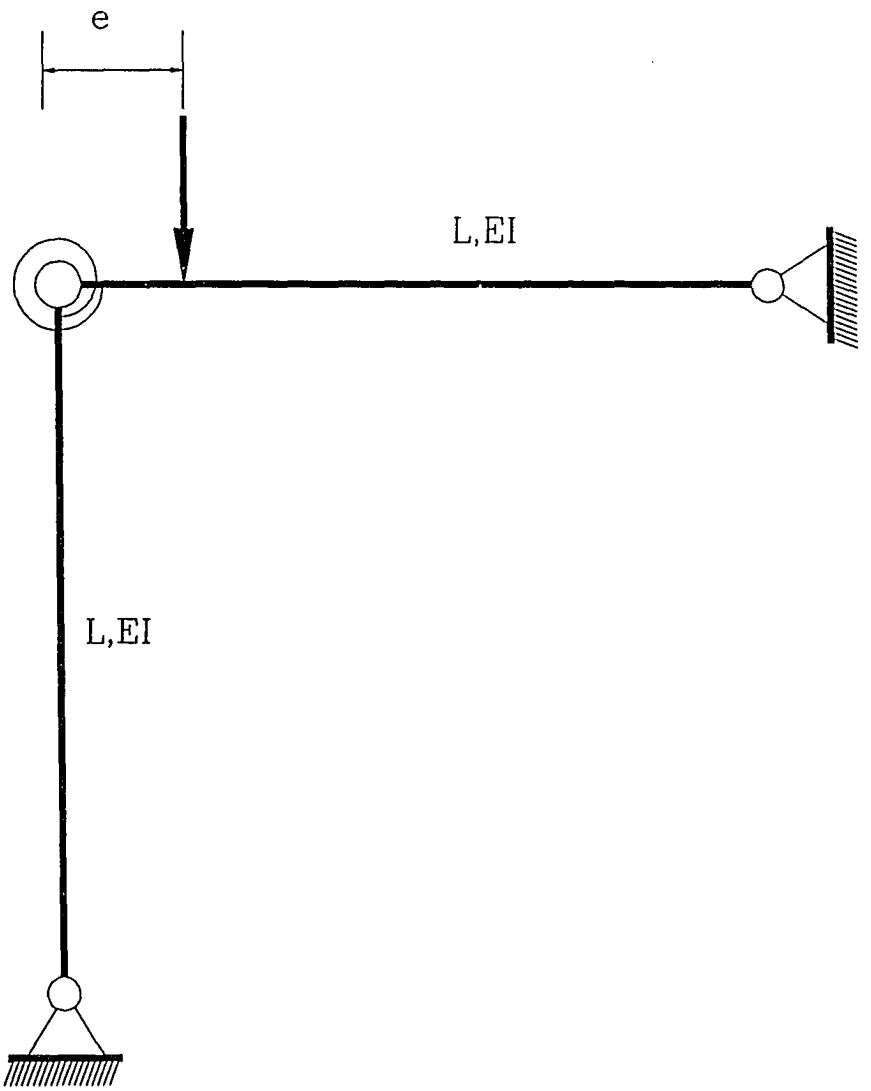

Figure 2.1, Frame Studied by Simitses and Vlahinos

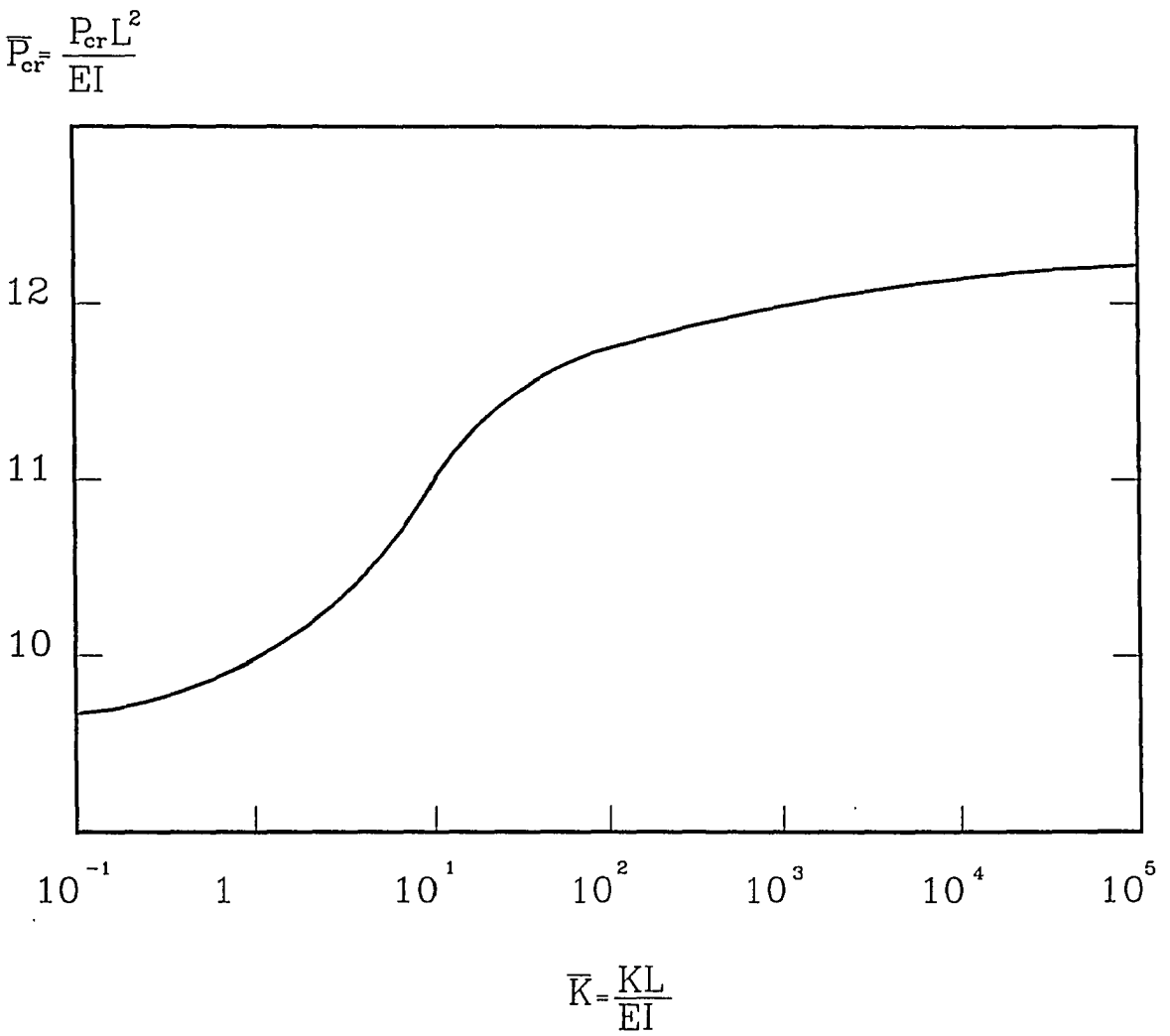

Figure 2.2, Effect of Stiffness K on The Critical Load (e = 0)

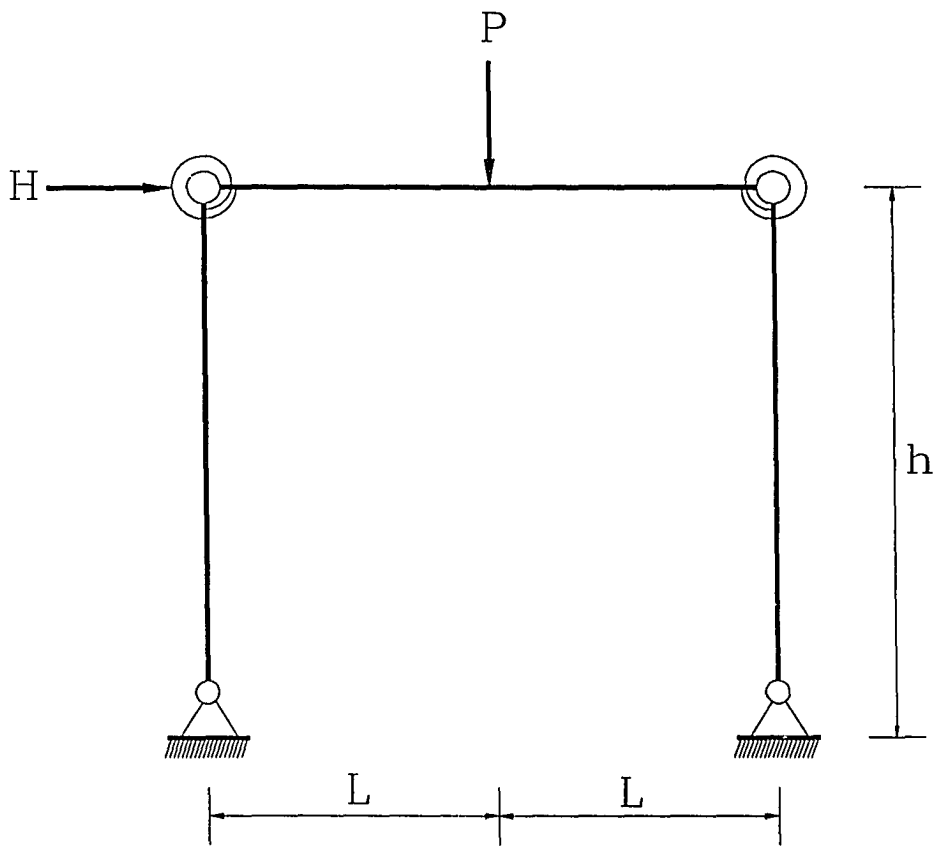

Figure 2.3, Pinned Base Portal Frame (Ackroyed and Gerstle, 1983)

The stiffness coefficients and rotations of the beam were modified for the presence of the flexible connections. The results obtained for the frame shown in Figure 2.3 indicate that the buckling capacity of the frame increases with the stiffness of beam-to-column connection.

Grundy (1985) proposed a method of the analysis and design of frames with flexible connections. The stiffness of the connection was approximated by the secant stiffness that accommodates each connection type and beam size at working load. The method was extended to check the stability of the structure. The contributions of flexible connections and flexure to the stiffness of the structure were appropriately considered. A classical bifurcation analysis was executed to find the elastic critical load. The study found that stiffer connections yield a higher critical load. The study does not consider the primary bending moment effect on the critical load. Moreover, the use of the secant stiffness of the connection instead of the tangent stiffness is inconsistent with basic concepts appropriate to a stability analysis.

Yu and Shanmugam (1986) presented an analysis to find the critical buckling load of a rectangular frame with semi-rigid connections. The stiffness of a member with flexible end connections and under axial force was employed to construct a modified stiffness matrix for the structure. The stiffness matrix is a function of axial force. When the matrix becomes singular due to the increase of axial force, the structure becomes unstable. Figures 2.4 and 2.5 show some of the results obtained in this study. In Figures 2.4 and 2.5, p_i and p_j are called the fixity factors (Wang, 1983). For a pin connection, p is zero and for a rigid connection p is 100 percent. The study has two

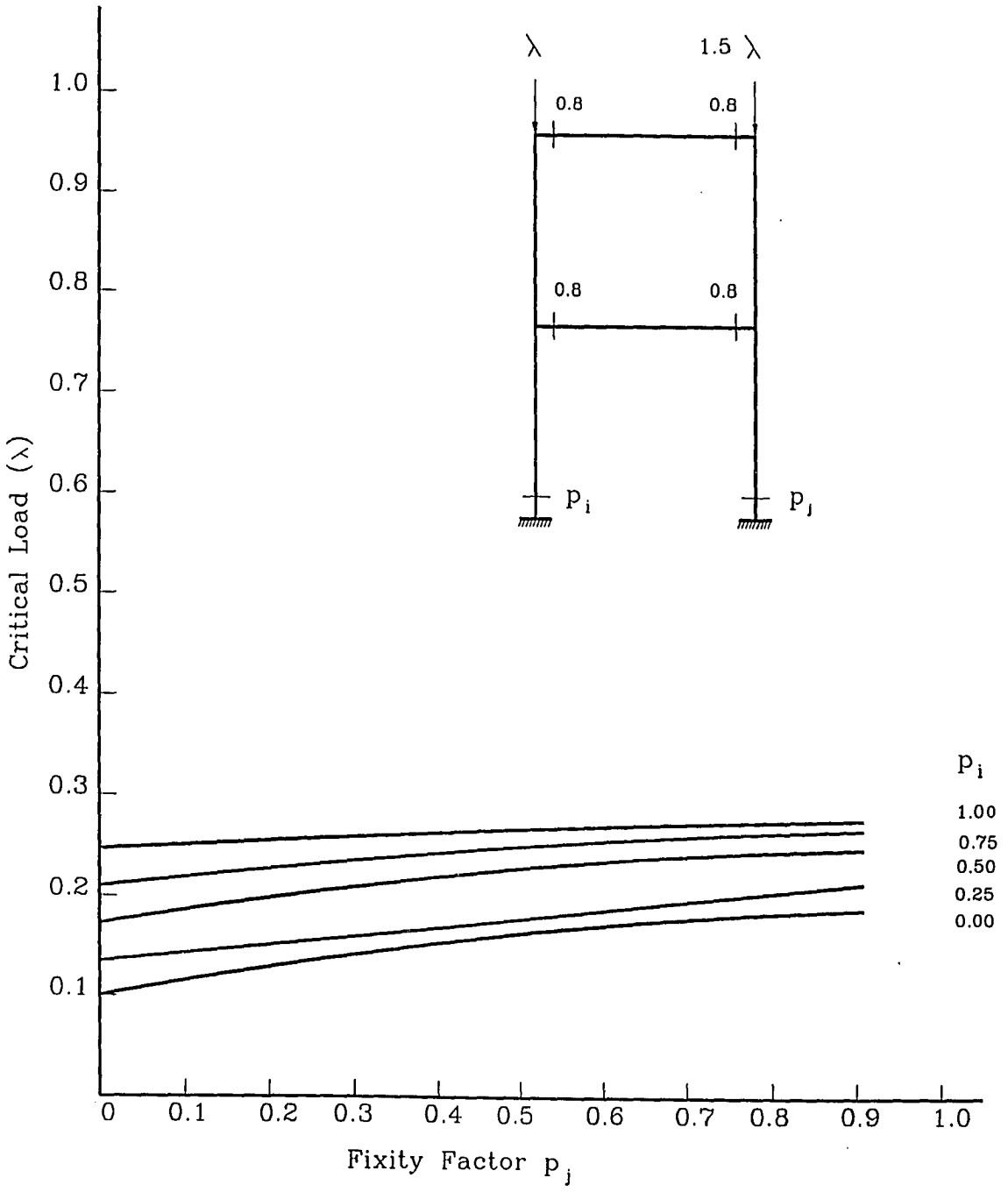

Figure 2.4, Variation of Critical Load with Rigidity of Column to Base Connection

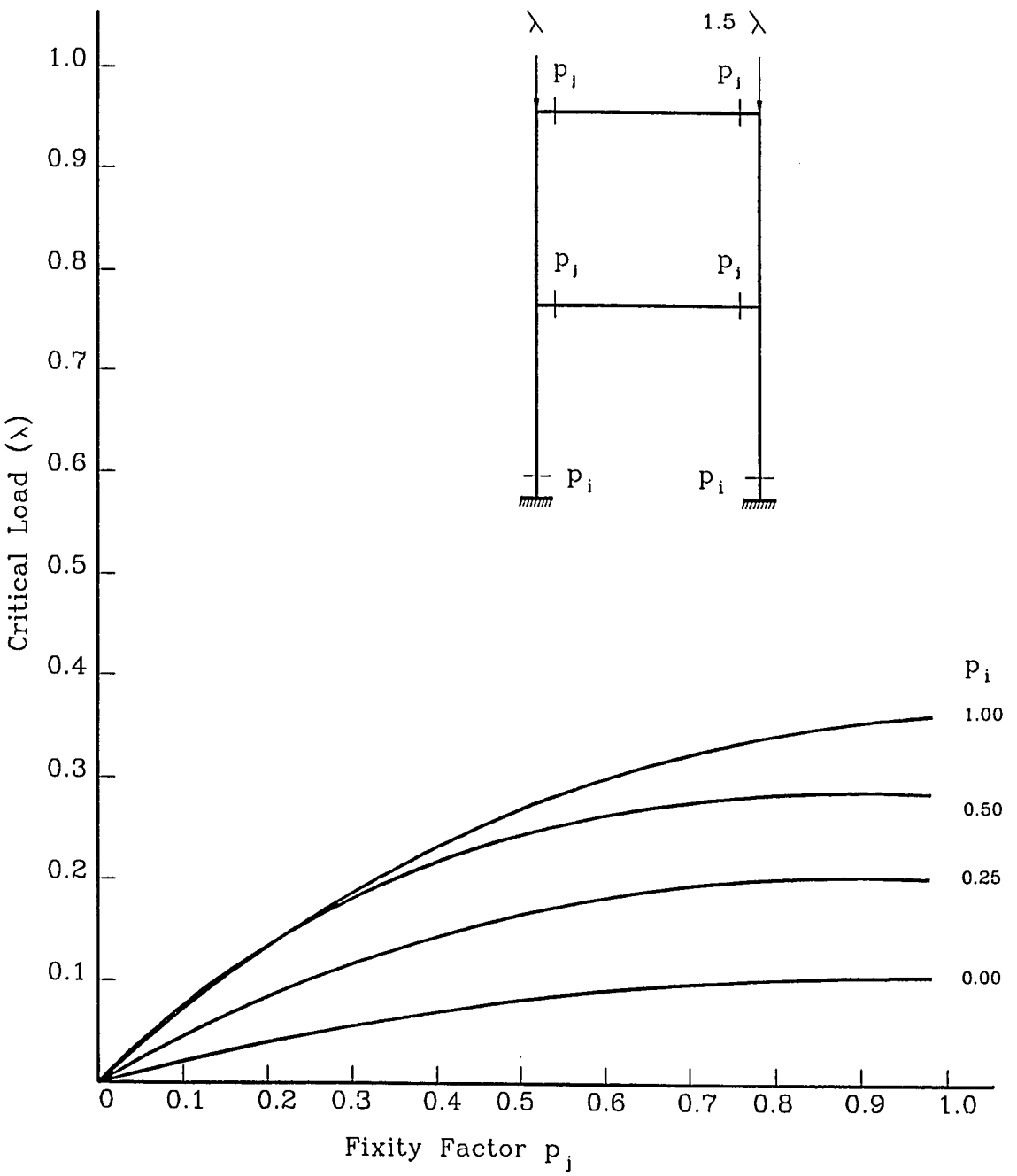

Figure 2.5, Variation of Critical Load with Rigidities at Beam to Column and Column to base Connections

major deficiencies. First, the loads are applied as concentrated loads on columns, so no primary bending moment is present. However, considering primary bending moment is essential to assess the actual critical behavior of the structure, as explained in Chapter one. Second, the connection behavior is regarded as linear, which results in overestimating the stiffness of the connection, particularly around the critical load value. This study justifies the linear modeling of the connection behavior by the use of test results that show the connection behavior to be linear. To demonstrate why these test results are deceptive, the method of applying the loads on the structure is relevant. When the loads are applied as concentrated loads on columns, the connections are not loaded as long as the structure is stable. Therefore, the stiffnesses of the connections coincide with the initial stiffnesses taken from their moment-rotation curves. Thus, the test results indicate the linear behavior for the connections.

Yu and Shanmugam (1988) extended their study to space frames with semi-rigid connections. The conclusion of their studies is that critical load increases with connection stiffness.

Rashed, Machaly and Niazy (1989) developed a Fortran program to analyze steel space frames having semi-rigid connections. They implemented the modified stiffness matrix approach. Connections were modeled as linear elastic torsion springs at the ends of each beam. Loads were applied as concentrated loads on columns. The conclusions of the study agree with the conclusions of the study done by Yu and Shanmugam in 1986.

2.2. Behavior of Semi-Rigid Connections

The AISC specifications consider three types of connections:

A. Type 1 Rigid Connection

B. Type 2 Pinned Connection

C. Type 3 Semi-Rigid Connection

In practical frame design, connections are assumed to be pinned or rigid. A rigid connection is defined as a connection that provides moment resistance and has no flexibility. In other words, a rigid connection enforces the condition that the rotations of the tangents of the reference axes of the members at the connection have a common value. A pinned connection is understood to be a connection that displays zero moment resistance. In reality, a rigid connection exhibits some flexibility and a connection regarded as pinned possesses some rotational stiffness. Common types of actual beam-to-column connections regarded as pins are the double web angle, the single web angle and the header plate connection, as shown in Figure 2.6. These flexible connections may transmit between 5% and 20% of the moment that a rigid connection can transmit. Therefore, the assumption that connections behave like either pins or as being rigid is not true. It is intuitively clear that semi-rigid connections could have a beneficial effect on frame design.

2.2.1. Moment-Rotation Curve

Beam-to-column connections transmit a set of forces that includes shearing force, axial force, torsion and bending moment. For in-plane study, the torsion effect is neglected. Moreover, the effects of axial and shear forces in determining the rotational

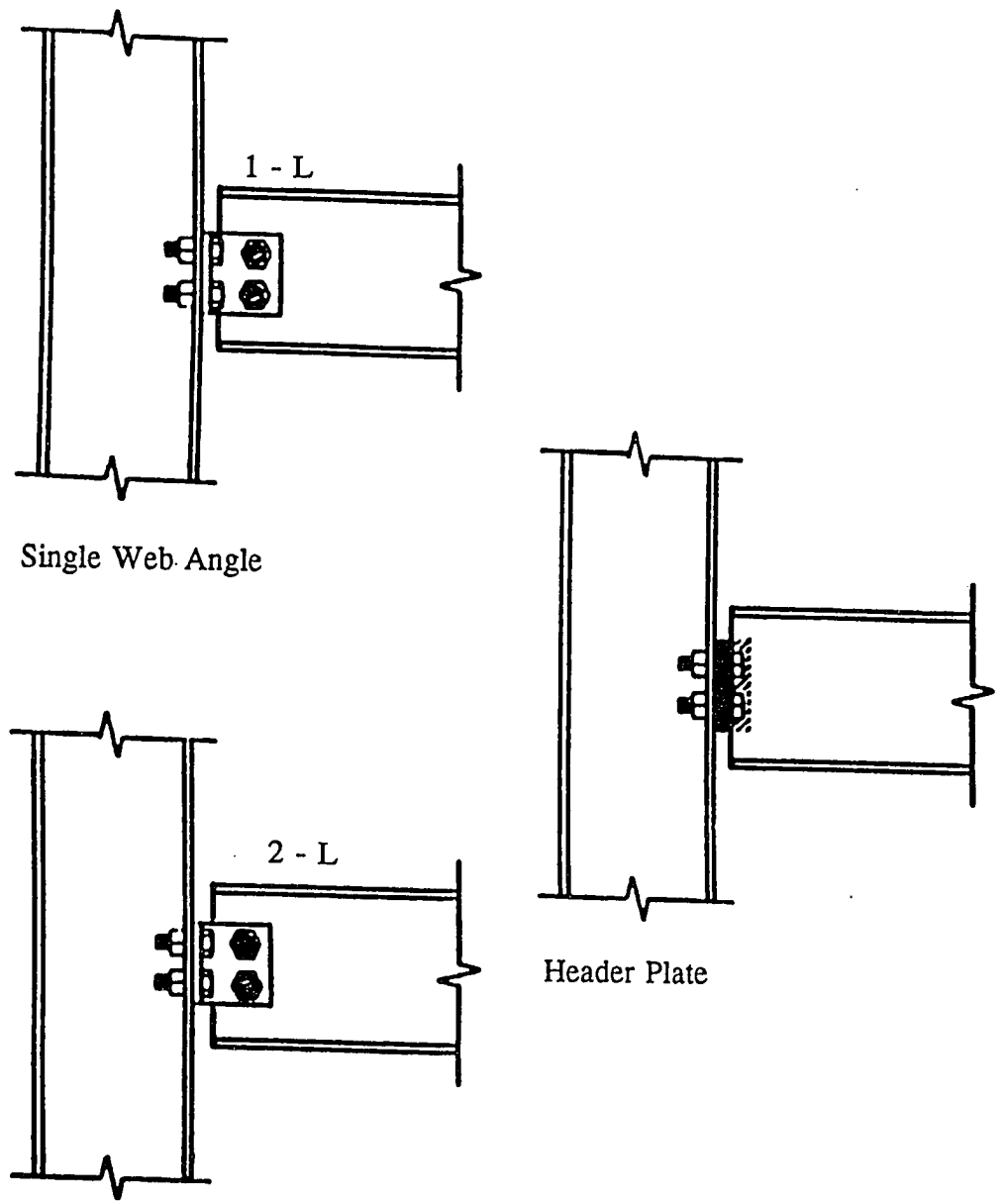

Figure 2.6, Some Types of Connections Regarded as Pins

deformation for most connections are insignificant. Consequently, a moment-rotational deformation curve can best illustrate the behavior of a flexible connection. The moment-rotation behavior of some commonly used connections are shown in Figure 2.7. The slope of the moment-rotation curve at the origin, which represents the initial stiffness of the connection, is defined as the connection rotational stiffness. Figure 2.7 shows that the maximum moment that a connection can transmit decreases with increasing connection flexibility. The connections also display a non-linear moment-rotation behavior almost from the beginning and over the entire range of loading.

Figure 2.8 shows the moment-rotation relationships as defined by Richard in 1975. This equation is used in this analysis to define the moment-rotation curve for the connections used in the numerical applications.

2.2.2. Load Deflection Curve

Figure 2.9 shows typical non-dimensional load-deflection curves for columns with different end restraints. A pin connection, a double web angle and a top and seat angle were used to fix both ends of each column. The data was generated using British wide-flange shapes. Data was obtained for an initial out of straightness equal to $\Delta_i = L/1000$, in which L is the column length and slenderness ratio of 120. The deflections Δ were measured at the column mid point. These load-deflection curves demonstrate that deflection is decreased by using a stiffer connection and the load carrying capacity is increased. In 1980 Jones, Kirby and Nethercot found that the increase in maximum load that can be carried when a stiffer connection is used compared to the perfect pin connection decreases as the slenderness ratios goes towards values of 50 and less.

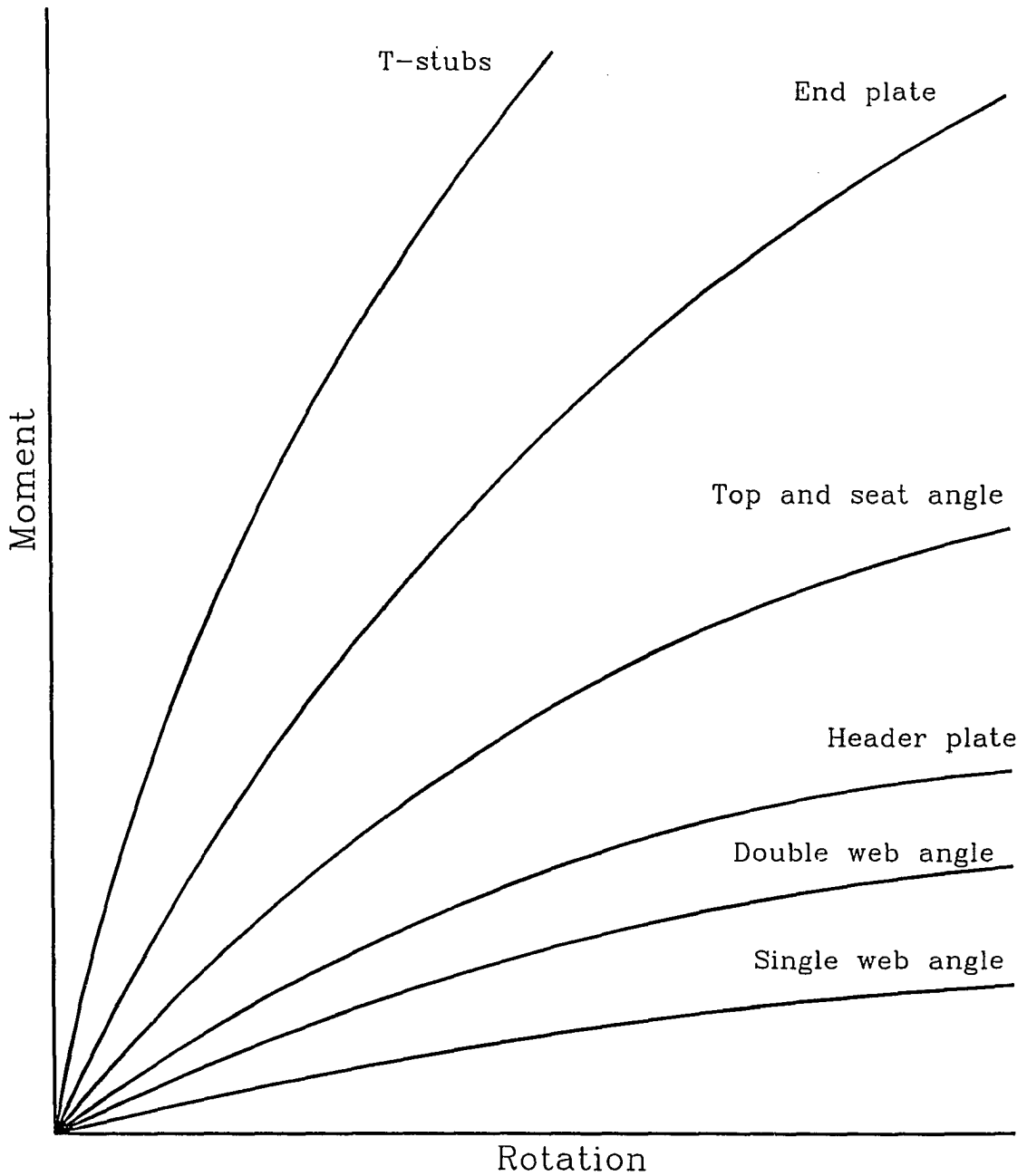

Figure 2.7, Moment-Rotation Curves for Some Commonly Used Connections

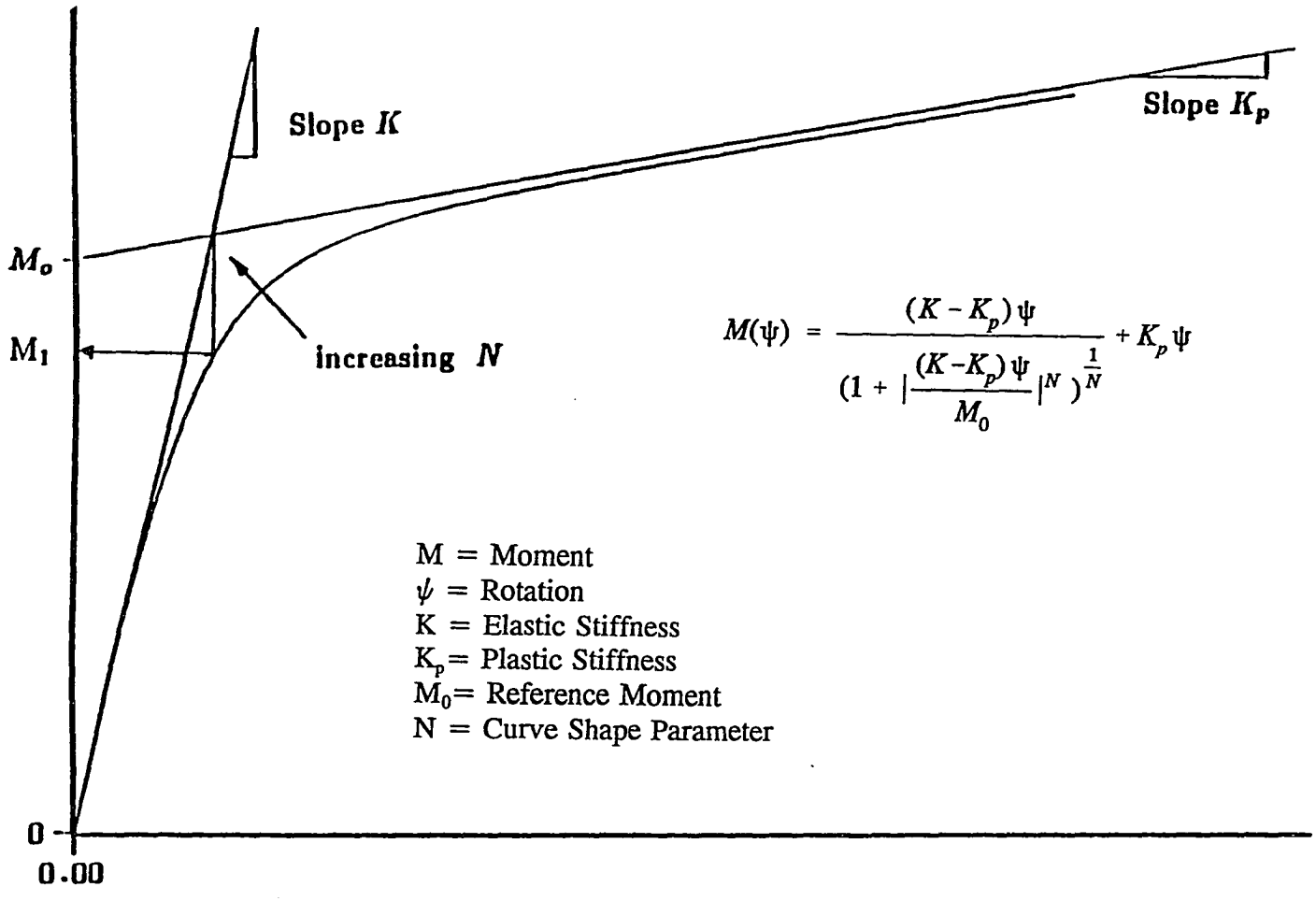

Figure 2.8, Richard Equation for Defining Moment-Rotation Relationships

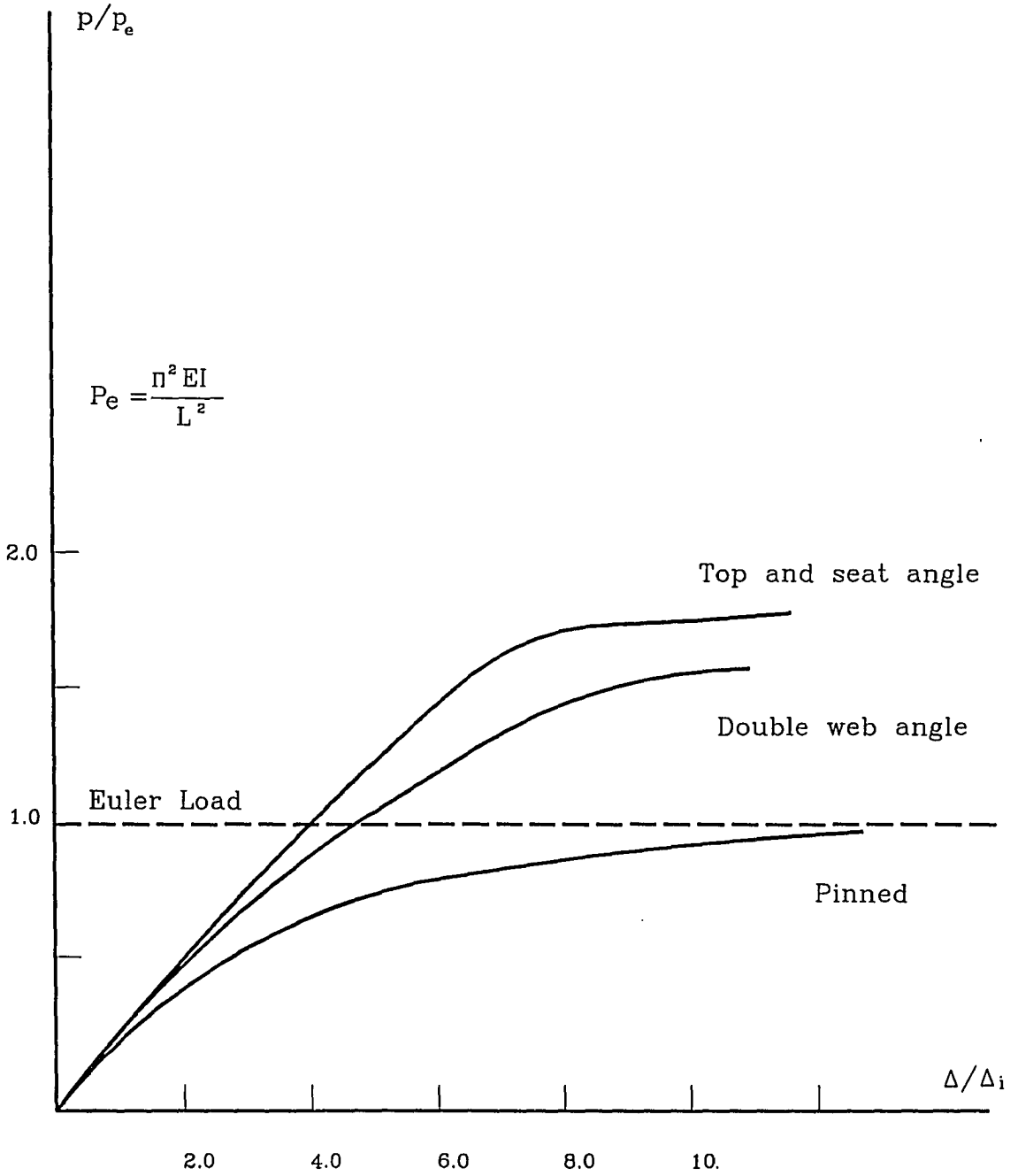

Figure 2.9, Typical Load-Deflection Curves for Columns
(Jones, Kirby and Nethercot, 1981)

2.3. Some Data on the Behavior of Connections

The rotational stiffness C represents the initial stiffness of the connection. It is defined as the slope of the moment-rotation curve at the origin. Studies by Johnston in 1976, Chapuis and Galambos in 1982 have provided data and methods for finding the rotational stiffness C. The rotational stiffness is zero for a perfect pin. Table 2.1 provides the actual C-values for some simple connections (Jones, Kirby and Nethercot, 1981).

Table 2.1

Connection Data	Value of C (kips-in/rad)
Double angle, 3 bolts	3.23×10^4
Double angle, 5 bolts	28.6×10^4
Double angle, 7 bolts	90.9×10^4
6 x4 x 3/4 top and seat angle with:	
12" beam depth	357×10^4
16" beam depth	556×10^4
21" beam depth	833×10^4

The slope of the moment-rotation curve decreases with increasing rotation. This means that the rigidity of a connection reduces with increasing load since the slope represents the stiffness of the connection at any particular value of rotation.

2.4. End Restraint Modeling

For the purpose of accounting for connection rigidity in design, different simplified approaches have been employed.

2.4.1. Linear Approach

To simplify the problem of the semi-rigid connection, a linear response is assumed. As the moment increases the linear assumption overestimates the connection rigidity. In limit design the linear approach becomes undesirable, because it does not adequately represent the behavior of the connection near the limit load.

Lionberger (1967, 1969), and Romstad and Subramanian in 1970, improved the linear model by using a bi-linear model. At a certain point of loading they reduce the slope of the moment-rotation curve to follow the curve obtained from experimental data. This is illustrated in Figure 2.10.

2.4.2. Polynomial Curve Fitting Models

Connection stiffness is determined by variety of factors. Hence, the moment-rotation curve of a connection does not follow any simple mathematical function. Sommer in 1969 used a fit curve for available experimental data and arrived at the standard polynomial non-dimensional function of the form: θ = f(CM) where C is factor to account for size of connection.

Another contribution to Sommer's work was added by Frye (1971), and Frye and Morris (1975). Using available data from experiments, they standardized the moment function for the following connections:

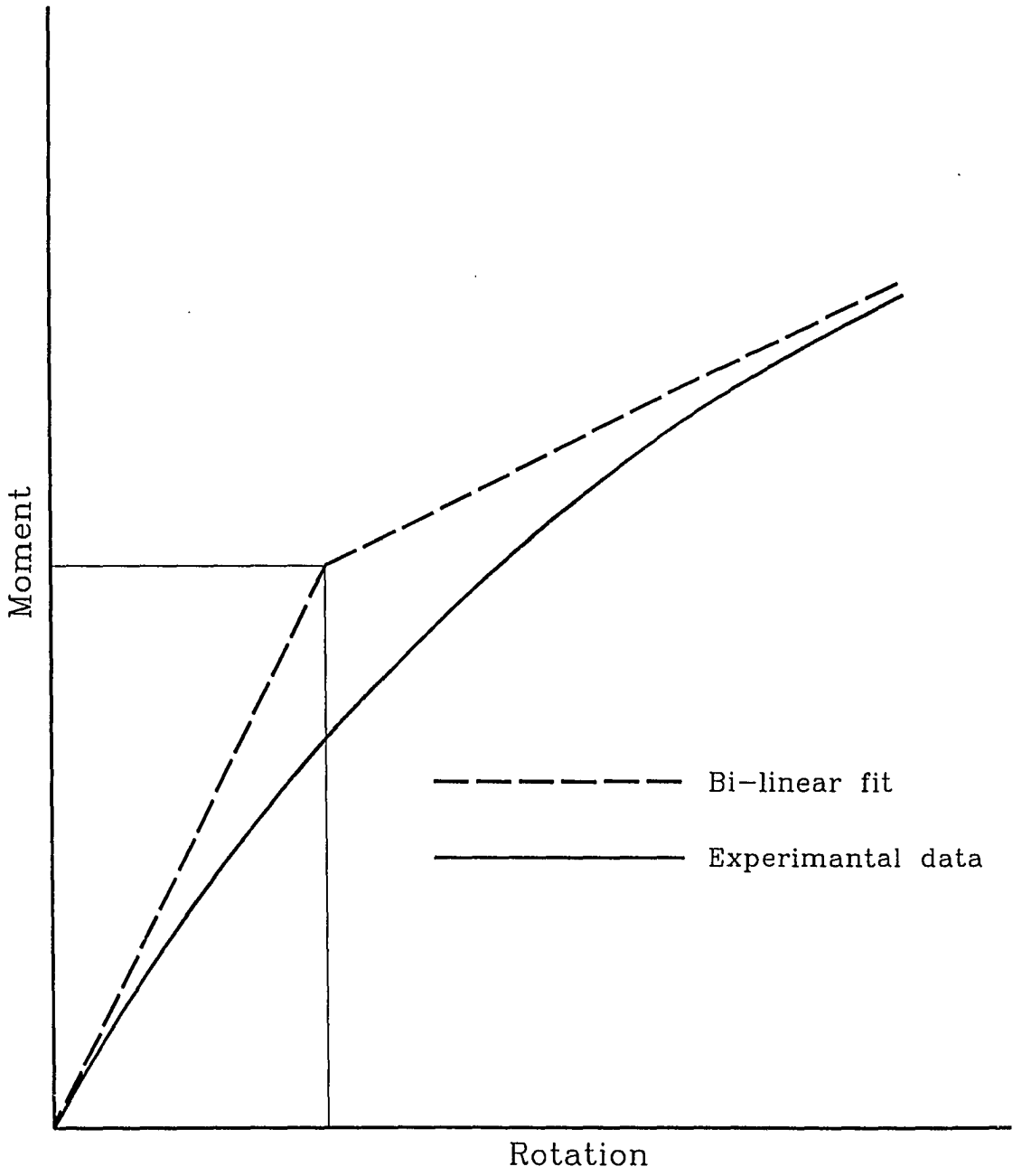

Figure 2.10, Bi-Linear Moment-Rotation Model

Double web angle

Single web angle

Header plate

Top and seat angle

End plates - no column stiffener

End plates - with column stiffener

T-stubs

The form of the function for these simple connections is given by:

$$\theta = \Sigma^{n}_{i=1} C_i(KM)_i$$

where: θ = Connection rotation in radian

C = Constant

K = non-dimensional factor whose value depends on the size parameters for the particular connection under consideration

An error of less than 12% was reported for this approach. The curve fitting technique was successfully applied by Frye to calculate the increase in sway due to connection flexibility of a multi-story frame under lateral loads. Compared to a rigid frame, the increase was found to be around 21%.

Romstad and Subramanian (1970) used the work of Frye and Morris to generate the moment-rotation curve and then fitted it with a bi-linear curve. The bi-linear fit does not accurately represent the behavior of the connection. However, Bergquist (1977) demonstrated the acceptability of Romstad's work by checking it against the experimental data.

2.4.3. B-Spline Curve Fitting Technique

The polynomial curve fitting technique has the disadvantage of producing a moment-rotation curve that has peaks and troughs. Therefore, the slope of the moment-rotation curve in some ranges is negative. Since the slope of the moment-rotation curve represents the stiffness of the connection, the stiffness is negative at some ranges which is not realistic. In 1980, Jones et al. overcame this problem by using B-spline curve-fitting techniques (Chen, 1986).

This approach requires the division of the connection's rotation range into a finite number of small ranges. Each small range has to be fitted to a cubic equation. Continuity of the first and second derivative is maintained. This approximation produces a smooth moment-rotation curve that is very close to the experimental data.

2.4.4. Exponential Connection

Although the B-spline curve-fitting technique gives a very accurate representation for the behavior of the connection, it has the disadvantage of requiring a large number of data points along the deformation range.

Lui (1984) developed an exponential model that needs fewer data points without compromising accuracy. The exponential function has a positive derivative along the deformation range. The model also accounts for unloading of the joint. This model is expected to be one of the best developments in connections modeling, since it has the merit of practicality and accuracy.

Flexible joint modeling has been given considerable attention recently. However, more data and studies are still needed to insure that practical design can be performed.

CHAPTER 3

PARAMETERS INVOLVING STABILITY ANALYSIS OF FRAMES

3.1. Stiffness Matrix for Element with no Axial Force

The relations between end moments and rotations of a prismatic bar in flexure, without considering the influence of the secondary moment, $P_i Y$ in Figure 3.1a, are well documented. These relations can be expressed either by the flexibility matrix or by the stiffness matrix; thus:

Flexibility Matrix:
$$[F] = \begin{bmatrix} \frac{1}{3} & -\frac{1}{6} \\ -\frac{1}{6} & \frac{1}{3} \end{bmatrix} \times \frac{L}{EI} \qquad (3.1)$$

Stiffness Matrix:
$$[S] = \begin{bmatrix} 4 & 2 \\ 2 & 4 \end{bmatrix} \times \frac{EI}{L} \qquad (3.2)$$

3.2. Effect of Axial Force on Member Flexure

When the secondary moment, $P_i Y$, is included in the differential equation of the elastic curve, the flexibility is increased (stiffness is decreased). Equations (3.1) and (3.2), when considering the axial compressive force, become Equations (3.3) and (3.4), respectively.

$$[F] = \begin{bmatrix} f_{ii} & f_{ij} \\ f_{ji} & f_{jj} \end{bmatrix} \times \frac{L}{EI} = \begin{bmatrix} \frac{\sin\mu - \mu\cos\mu}{\mu^2\sin\mu} & -\frac{\mu - \sin\mu}{\mu^2\sin\mu} \\ -\frac{\mu - \sin\mu}{\mu^2\sin\mu} & \frac{\sin\mu - \mu\cos\mu}{\mu^2\sin\mu} \end{bmatrix} \times \frac{L}{EI} \qquad (3.3)$$

$$[S] = \begin{bmatrix} S_{ii} & S_{ij} \\ S_{ji} & S_{jj} \end{bmatrix} \times \frac{L}{EI} = \begin{bmatrix} \frac{\mu\sin\mu - \mu^2\cos\mu}{2 - 2\cos\mu - \mu\sin\mu} & \frac{\mu^2 - \mu\sin\mu}{2 - 2\cos\mu - \mu\sin\mu} \\ \frac{\mu^2 - \mu\sin\mu}{2 - 2\cos\mu - \mu\sin\mu} & \frac{\mu\sin\mu - \mu^2\cos\mu}{2 - 2\cos\mu - \mu\sin\mu} \end{bmatrix} \times \frac{EI}{L} \qquad (3.4)$$

In Equations (3.3) and (3.4),

$$\mu = L\sqrt{\frac{P}{EI}}$$

3.3. Effect of Semi-Rigid Connection on Member Flexure

Figure 3.1a shows the deformation of a beam with rigid joints. $(\phi_i+\rho)$ and $(\phi_j+\rho)$ represent the beam end rotations. ρ is the chord rotation. Figure 3.1b shows the deformation of a beam with flexible joints. $(\phi_i+\rho)$ and $(\phi_j+\rho)$ are the member end rotations. θ_i and θ_j are the rotations at the ends of the beam from the chord connecting ends i and j. ψ_i and ψ_j are the rotational slips of the beam at ends i and j, respectively.

The flexibility matrix of a member with rigid joints expresses the end rotations ϕ_i and ϕ_j, as they are defined in Figure 3.1a, in terms of the member-end moments M_i and M_j.

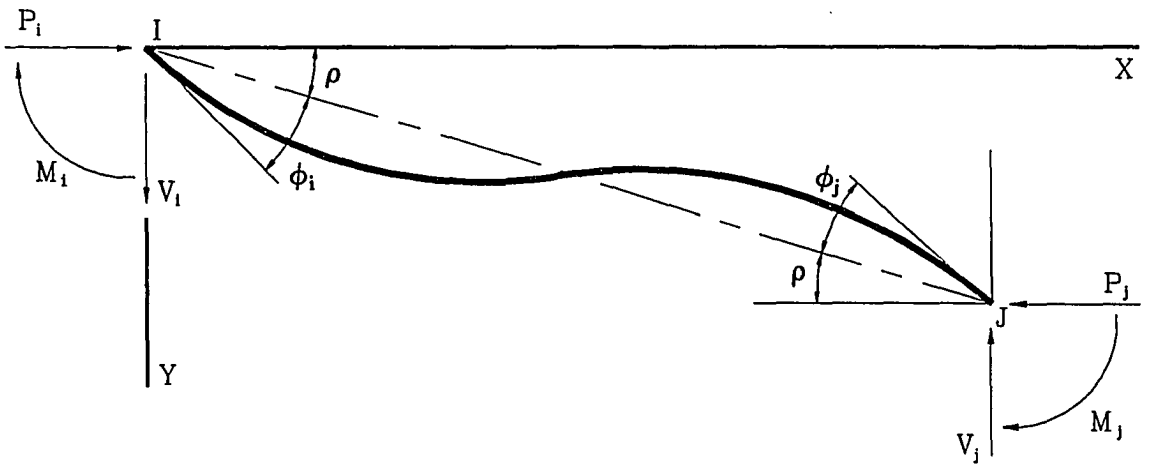

Figure 3.1a, Deformation of a Member with Rigid Joints

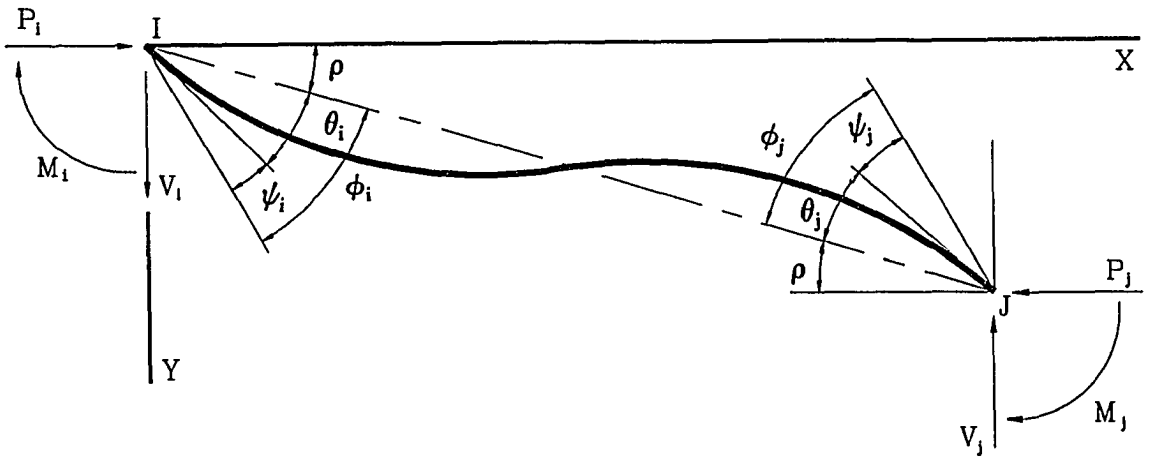

Figure 3.1b, Deformation of a Member with Flexible Connections

The elements in the flexibility matrix, [F], can be derived by virtual work, the M-A theorems, or conjugate-beam method. The results are of the form:

$$\begin{Bmatrix} \phi_i \\ \phi_j \end{Bmatrix} = \begin{bmatrix} f_{ii} & f_{ij} \\ f_{ji} & f_{jj} \end{bmatrix} \times \frac{L}{EI} \times \begin{Bmatrix} M_i \\ M_j \end{Bmatrix} \tag{3.5}$$

The elements of the above flexibility matrix, f_{ii}, f_{ij}, f_{ji} and f_{jj}, which are derived for a beam with rigid joints, Figure 3.1a, represent the coefficients of Equation (3.1) or Equation (3.3).

The modified member flexibility matrix, $[F^s]$, for a member with semi-rigid connections expresses the end rotations ϕ_i and ϕ_j, as they are defined in Figure 3.1b, in terms of the member-end moments M_i and M_j in the form

$$\begin{Bmatrix} \phi_i \\ \phi_j \end{Bmatrix} = \begin{bmatrix} f^s_{ii} & f^s_{ij} \\ f^s_{ji} & f^s_{jj} \end{bmatrix} \times \frac{L}{EI} \times \begin{Bmatrix} M_i \\ M_j \end{Bmatrix} \tag{3.6}$$

From Figure 3.1b, the following relation is obtained,

$$\begin{Bmatrix} \phi_i \\ \phi_j \end{Bmatrix} - \begin{Bmatrix} \psi_i \\ \psi_j \end{Bmatrix} = \begin{Bmatrix} \theta_i \\ \theta_j \end{Bmatrix} \tag{3.7}$$

Substituting for $\{\theta\}$ and expressing $\{\psi\}$ in terms of the end moment gives

$$\begin{Bmatrix} \phi_i \\ \phi_j \end{Bmatrix} = \begin{bmatrix} f_{ii} & f_{ij} \\ f_{ji} & f_{jj} \end{bmatrix} \begin{Bmatrix} M_i \\ M_j \end{Bmatrix} + \begin{Bmatrix} M_i / K_{si} \\ M_j / K_{sj} \end{Bmatrix} \tag{3.8}$$

Therefore, the modified member flexibility matrix for the beam with the connections (or for the beam-connection element) is

$$[F^s] = \begin{bmatrix} \frac{1}{K_{si}} + f_{ii} & f_{ij} \\ f_{ji} & \frac{1}{K_{sj}} + f_{jj} \end{bmatrix} \times \frac{L}{EI} \tag{3.9}$$

in which K_{si} and K_{sj} are the normalized secant stiffnesses of the connections at ends i and j corresponding to end moments equal to M_i and M_j, respectively. The stiffness matrix for the beam-connection element is the inverse of the flexibility matrix given in Equation (3.9). It takes the form

$$[S^s] = \begin{bmatrix} S^s_{ii} & S^s_{ij} \\ S^s_{ji} & S^s_{jj} \end{bmatrix} \times \frac{EI}{L}$$

Thus, in terms of the elements in [F^s]

$$S^s_{ii}=\frac{\frac{1}{K_{sj}}+f_{jj}}{(\frac{1}{K_{si}}+f_{ii})(\frac{1}{K_{sj}}+f_{jj})-(f_{ij})^2}$$

$$S^s_{jj}=\frac{\frac{1}{K_{si}}+f_{ii}}{(\frac{1}{K_{si}}+f_{ii})(\frac{1}{K_{sj}}+f_{jj})-(f_{ij})^2}$$

$$S_{ij}=\frac{-f_{ij}}{(\frac{1}{K_{si}}+f_{ii})(\frac{1}{K_{sj}}+f_{jj})-(f_{ij})^2}$$

Employing the relation between the stiffness and the flexibility matrices for the beam alone, the foregoing can be expressed in the form

$$S^s_{ii}=\frac{\frac{1}{K_{sj}}+\frac{S_{ii}}{S_{ii}S_{ij}-S^2_{ij}}}{(\frac{1}{K_{si}}+\frac{S_{jj}}{S_{ii}S_{ij}-S^2_{ij}})(\frac{1}{K_{sj}}+\frac{S_{ii}}{S_{ii}S_{ij}-S^2_{ij}})-(\frac{S_{ij}}{S_{ii}S_{ij}-S^2_{ij}})^2}$$

$$S^s_{jj}=\frac{\frac{1}{K_{si}}+\frac{S_{jj}}{S_{ii}S_{ij}-S^2_{ij}}}{(\frac{1}{K_{si}}+\frac{S_{jj}}{S_{ii}S_{ij}-S^2_{ij}})(\frac{1}{K_{sj}}+\frac{S_{ii}}{S_{ii}S_{ij}-S^2_{ij}})-(\frac{S_{ij}}{S_{ii}S_{ij}-S^2_{ij}})^2}$$

$$S^s_{ij}=\frac{\dfrac{S_{ij}}{S_{ii}S_{ij}-S^2_{ij}}}{(\dfrac{1}{K_{si}}+\dfrac{S_{jj}}{S_{ii}S_{ij}-S^2_{ij}})(\dfrac{1}{K_{sj}}+\dfrac{S_{ii}}{S_{ii}S_{ij}-S^2_{ij}})-(\dfrac{S_{ij}}{S_{ii}S_{ij}-S^2_{ij}})^2}$$

Introducing $D = S_{ii}S_{ij} - (S_{ij})^2$ and further simplifying, the following relations which were derived by the author in 1987 are obtained:

$$S^s_{ii}=\frac{\dfrac{D}{K_{sj}}+S_{ii}}{1+\dfrac{S_{ii}}{K_{si}}+\dfrac{S_{jj}}{K_{sj}}+\dfrac{D}{K_{si}K_{sj}}} \tag{3.10}$$

$$S^s_{jj}=\frac{\dfrac{D}{K_{si}}+S_{jj}}{1+\dfrac{S_{ii}}{K_{si}}+\dfrac{S_{jj}}{K_{sj}}+\dfrac{D}{K_{si}K_{sj}}} \tag{3.11}$$

$$S^s_{ij}=\frac{S_{ij}}{1+\dfrac{S_{ii}}{K_{si}}+\dfrac{S_{jj}}{K_{sj}}+\dfrac{D}{K_{si}K_{sj}}} \tag{3.12}$$

Equations (3.10), (3.11), and (3.12) express the stiffness coefficients for a member with semi-rigid connections in terms of its stiffness coefficients when it has rigid joints.

3.4. The Modified Fixed-End Moment

The stiffness coefficients for a member with semi-rigid connections are given by Equations (3.10), (3.11), and (3.12); only these equations are to be used to calculate the stiffness of members having flexible connections. In the case of symmetric frames, the stiffness coefficients of the beam are $C^s = S^s_{ii} = S^s_{jj}$ in Equations (3.10) and (3.11), and $S^s = S^s_{ij}$ in Equation (3.12). C^s and S^s are used, as defined here, in the following slope-deflection equation analysis. The fixed end moment at end a of member ab, Figure 4.1, can be expressed in the form:

$$M^s_{fab} = -\frac{EI}{L}\,(C^s\,\lambda_a + S^s\,\lambda_b) \tag{3.13}$$

in which λ_a and λ_b represent the end rotations of the member when it is simply supported. Expressions for the λ's for a number of loading cases have been derived explicitly by S.P. Timoshenko and J.M. Gere (1961). For the case of a uniformly distributed lateral load throughout the entire length of the member, the values of λ are:

$$\lambda_a = -\lambda_b = \frac{WL^3}{24EI}\,\frac{3(\tan\frac{\mu}{2}-\frac{\mu}{2})}{(\frac{\mu}{2})^3} \tag{3.14}$$

where W is the intensity of the distributed load.

CHAPTER 4

SYMMETRICAL MODE OF BUCKLING

Herein, a theoretical solution based on the slope-deflection approach is developed to find the elastic critical load for frames with flexible connections. This approach follow the method produced by Chang (1958); Masur, Chang and Donnell (1961); and later explored by Le-Wu Lu (1963); to find the elastic critical load for rigid frames with primary bending moments.

4.1. One-Story Frame with Flexible Beam-to-Column Connections

The moment at the "a" end of a prismatic member ab composed of a beam with flexible connections at its ends and loaded as shown in Figure 4.1, is provided by the following equation:

$$M_{ab}=\frac{EI}{L}[C^s\phi_a+S^s\phi_b-(C^s+S^s)\rho]+M^s_{fab} \qquad (4.1)$$

in which $\phi_a = \psi_a + \theta_a$ is the rotation of the member (i.e, beam with connections) at end "a". $\phi_b = \psi_b + \theta_b$ is the rotation of the member at end "b", and ρ is the rotation of the member with respect to the undeformed position. The stiffness coefficients C^s and S^s, as defined in Section 3.4, are functions of axial force. Clockwise moments acting at the member ends are considered to be positive. Clockwise joint rotations are considered to be positive. The frame shown in Figure 4.2 is now analyzed for its symmetrical mode of buckling.

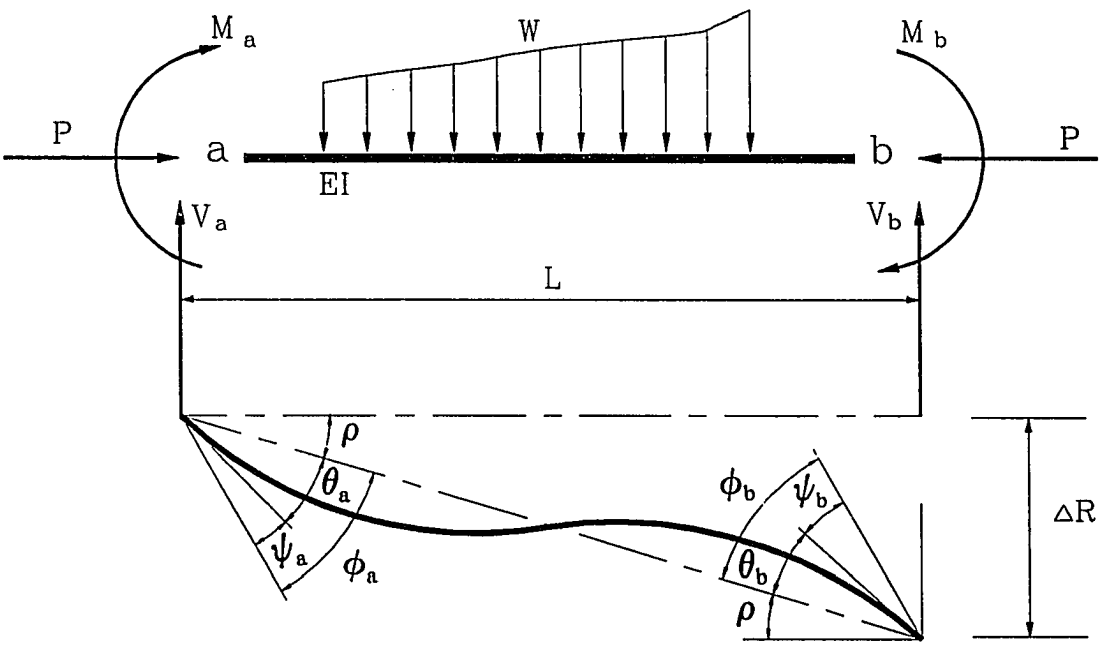

Figure 4.1, Member ab

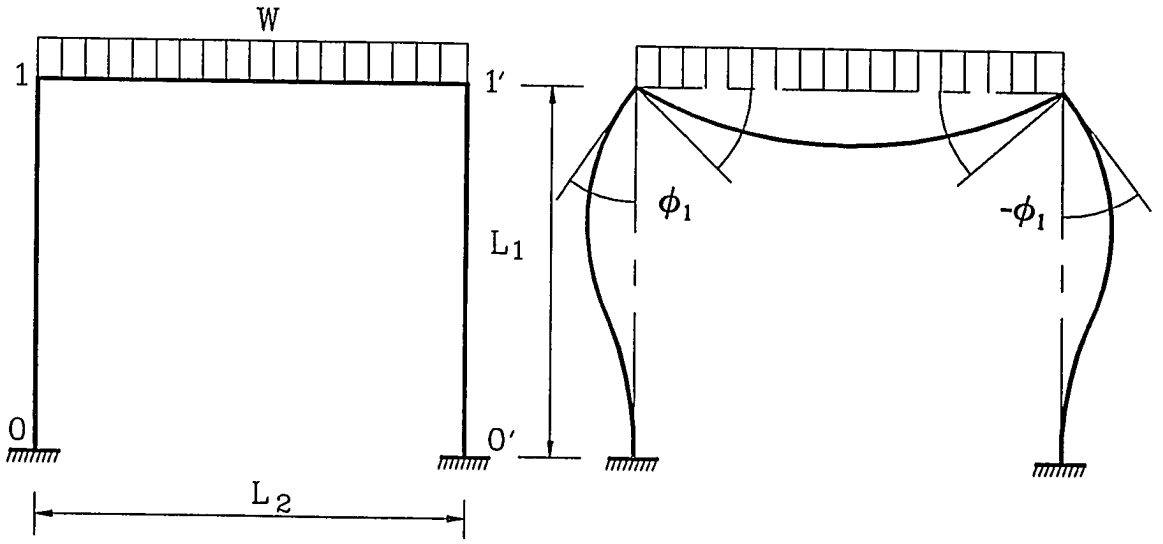

Figure 4.2, One-Story Symmetrical Buckling

For symmetric deformation $\rho = 0$ for the columns and because the column bases are fixed, for column 0-1

$$M_{0-1} = \frac{EI_1}{L_1} S_1 \phi_1 \tag{4.2a}$$

$$M_{1-0} = \frac{EI_1}{L_1} C_1 \phi_1 \tag{4.2b}$$

and for column 0′-1′

$$M_{0'-1'} = \frac{EI_1}{L_1} S_1 \phi_1' \tag{4.3a}$$

$$M_{1'-0'} = \frac{EI_1}{L_1} C_1 \phi_1' \tag{4.3b}$$

Because of the symmetry of the deformation, the rotation at joint 1 must be equal and of an opposite sign to that at joint 1′; that is; $\phi_1 = -\phi_{1'}$. The moment at the left end of beam 1-1′ is therefore equal to:

$$M_{1-1'} = \frac{EI_2}{L_2} (C^s{}_2 \phi_1 + S^s{}_2 \phi_1') + M^s{}_{f1-1'}$$

$$M_{1-1'} = \frac{EI_2}{L_2} (C^s{}_2 - S^s{}_2) \phi_1 + M^s{}_{f1} \tag{4.4}$$

Joint equilibrium at 1 requires that:

$$M_{1\text{-}0} + M_{1\text{-}1'} = 0 \tag{4.5}$$

Substitution for $M_{1\text{-}0}$ from Equation (4.3b), and $M_{1\text{-}1'}$ from Equation (4.4), in Equation (4.5) leads to:

$$[K_1C_1+K_2(C^s{}_2-S^s{}_2)]\phi_1+M^s{}_{f1\text{-}1'}=0 \tag{4.6}$$

in which $K = \frac{EI}{L}$.

The equilibrium of column 0-1, Figure 4.3, requires that:

$$HL_1=M_{0\text{-}1}+M_{1\text{-}0}$$

$$HL_1=K_1C_1\phi_1+K_1S_1\phi_1$$

$$HL_1=K_1(C_1+S_1)\phi_1$$

from which

$$\phi_1 = \frac{HL_1}{K_1(C_1+S_1)} \tag{4.7}$$

Substituting for ϕ_1 in Equation (4.6) produces the following characteristic equation:

$$[K_1C_1+K_2(C^s{}_2-S^s{}_2)]\frac{HL_1}{K_1(C_1+S_1)}+M^s{}_{f1\text{-}1'}= 0 \tag{4.8}$$

Equation (4.8) is the characteristic equation for the symmetrical buckling of one-story frames having flexible beam-to-column connections and primary bending moment. Equation (4.8) is solved numerically by Newton's method to establish the equilibrium path from which the buckling load is obtained.

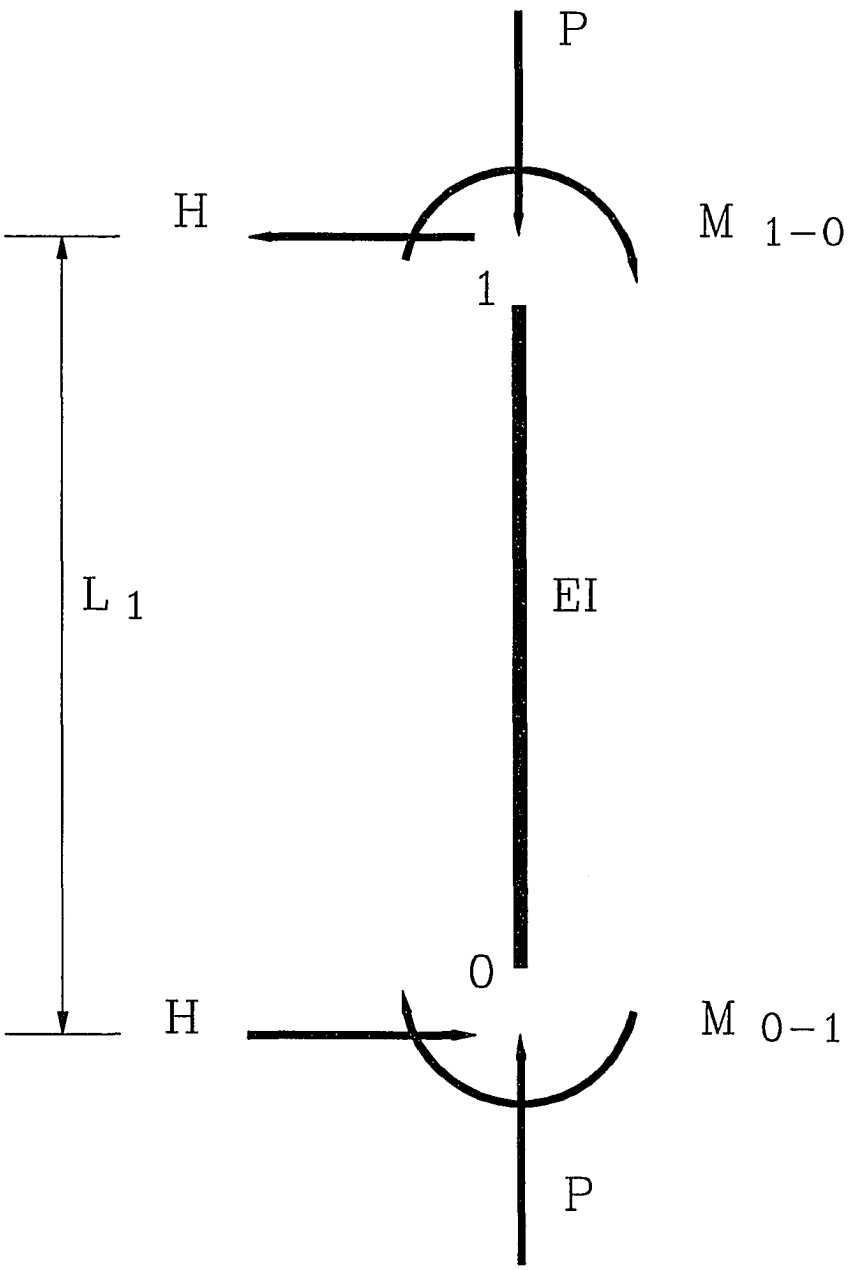

Figure 4.3, Equilibrium of Column 0-1

4.2. TWO-STORY FRAMES

4.2.1. Rigid Connections

Consider the two-story frame that is loaded as shown in Figure 4.4. It is assumed that sidesway is prevented. Because of the symmetry, only half of the frame needs to be considered in the analysis. Letting $K=\frac{EI}{L}$, $L_1 = L_3$ and numbering the different members as indicated in Figure 4.4, , the moments according to Equation (4.1) are:

$$M_{1\text{-}0} = K_1[S_1\phi_0+C_1\phi_1-(C_1+S_1)\rho_1] \tag{4.9a}$$

$$M_{1\text{-}2} = K_3[C_3\phi_1+S_3\phi_2-(C_3+S_3)\rho_2] \tag{4.9b}$$

$$M_{2\text{-}1} = K_3[S_3\phi_1+C_3\phi_2-(C_3+S_3)\rho_2] \tag{4.9c}$$

in which $\phi_0=0$ and $\rho_1=\rho_2=0$

$$M_{1\text{-}1'}=K_2[C_2\phi_1+S_2\phi_{1'}]+M_{f1} \tag{4.9d}$$

$$M_{2\text{-}2'}=K_4[C_4\phi_2+S_4\phi_{2'}]+M_{f2} \tag{4.9e}$$

in which $\phi_1=-\phi_{1'}$ and $\phi_2=-\phi_{2'}$. Therefore,

$$M_{1\text{-}0}=K_1C_1\phi_1 \tag{4.10a}$$

$$M_{1\text{-}2}=K_3[C_3\phi_1+S_3\phi_2] \tag{4.10b}$$

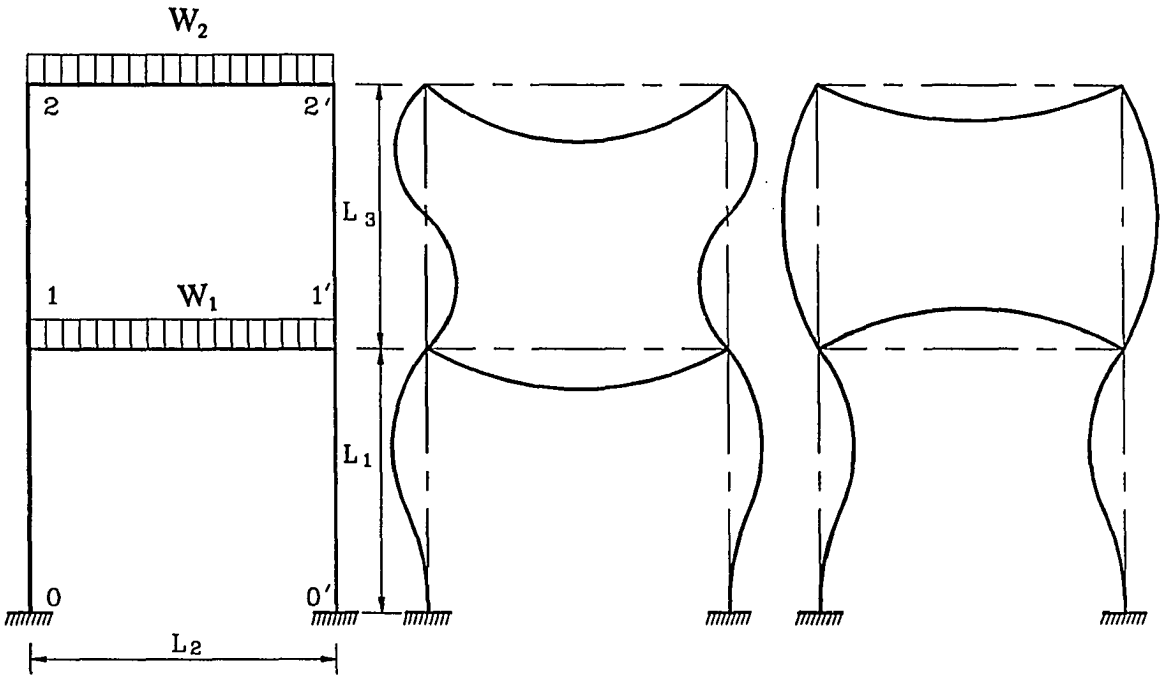

Figure 4.4, Two-Story Symmetrical Buckling

$$M_{2\text{-}1} = K_3[S_3\phi_1 + C_3\phi_2] \tag{4.10c}$$

$$M_{1\text{-}1'} = K_2(C_2 - S_2)\phi_1 + M_{f1} \tag{4.10d}$$

$$M_{2\text{-}2'} = K_4(C_4 - S_4)\phi_2 + M_{f2} \tag{4.10e}$$

The equations of moment equilibrium at joints 1 and 2 are:

$$M_{1\text{-}0} + M_{1\text{-}1'} + M_{1\text{-}2} = 0 \tag{4.11a}$$

$$M_{2\text{-}1} + M_{2\text{-}2'} = 0 \tag{4.11b}$$

Substitution of Equations (4.10a) through (4.10e) into (4.11a) and (4.11b) yields:

$$[K_1C_1 + K_3C_3 + K_2(C_2 - S_2)]\ \phi_1 + K_3S_3\ \phi_2 + M_{f1} = 0 \tag{4.12a}$$

$$K_3S_3\ \phi_1 + [K_3C_3 + K_4(C_4 - S_4)]\ \phi_2 + M_{f2} = 0 \tag{4.12b}$$

The following relation is obtained from the equilibrium of columns 0-1, Figure 4.5,

$$\begin{aligned} H_1L_1 &= M_{0\text{-}1} + M_{1\text{-}0} \\ H_1L_1 &= K_1C_1\phi_1 + K_1S_1\phi_1 \\ \phi_1 &= \frac{H_1L_1}{K_1(C_1 + S_1)} \end{aligned} \tag{4.13}$$

The following relation is obtained from the equilibrium of columns 1-2, Figure 4.5,

$$\begin{aligned} H_2L_1 &= M_{1\text{-}2} + M_{2\text{-}1} \\ H_2L_1 &= K_3[(C_3\phi_1 + S_3\phi_2) + (S_3\phi_1 + C_3\phi_2)] \\ \phi_2 &= \frac{H_2L_1}{K_3(C_3+S_3)} - \phi_1 \end{aligned} \tag{4.14}$$

Equations (4.13) and (4.14) may be used to eliminate ϕ_1 and ϕ_2 from the system of non-linear equations, Equations (4.12a) and (4.12b). The system of equations is solved numerically by Newton's method. Hence, the equilibrium path is established from the onset of loading up to the critical load.

4.2.2. Flexible Connections

Considering the two-story frame studied in Section 4.2.1, Equations (4.10a) through (4.10e) become, after substituting flexible connections for the rigid connections:

$$M_{1\text{-}0} = K_1C_1\phi_1 \tag{4.15a}$$

$$M_{1\text{-}2} = K_3[C_3\phi_1 + S_3\phi_2] \tag{4.15b}$$

$$M_{2\text{-}1} = K_3[S_3\phi_1 + C_3\phi_2] \tag{4.15c}$$

$$M_{1\text{-}1'} = K_2(C^s{}_2 - S^s{}_2)\phi_1 + M^s{}_{f1} \tag{4.15d}$$

$$M_{2\text{-}2'} = K_4(C^s{}_4 - S^s{}_4)\phi_2 + M^s{}_{f2} \tag{4.15e}$$

Substitution of Equations (4.15a) through (4.15e) into the equilibrium Equations (4.11a) and (4.11b) produces:

$$[K_1C_1+K_3C_3+K_2(C^s{}_2-S^s{}_2)]\phi_1+K_3S_3\phi_2+M^s{}_{f1}=0 \tag{4.16a}$$

$$K_3S_3\ \phi_1+[K_3C_3+K_4(C^s{}_4-S^s{}_4)]\phi_2+M^s{}_{f2}=0 \tag{4.16b}$$

The following relation is obtained from the equilibrium of columns 0-1 and 1-2,

$$\phi_1=\frac{H_1L_1}{K_1(C_1+S_1)} \tag{4.17}$$

$$\phi_2=\frac{H_2L_1}{K_3(C_3+S_3)}-\phi_1 \tag{4.18}$$

After substitution of Equations (4.17) and (4.18) into (4.16a) and (4.16b), the system of non-linear equations is solved numerically by Newton's method. Hence, the equilibrium path is established from the onset of loading up to the critical load.

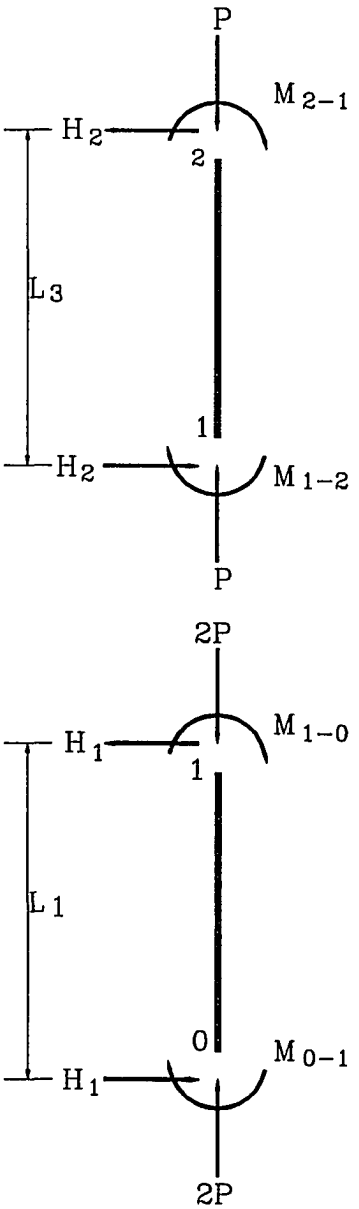

Figure 4.5, Equilibrium of Column 0-1 and 1-2

CHAPTER 5

ANTI-SYMMETRICAL MODE OF BUCKLING

5.1. One-Story Frames

5.1.1 General

A symmetric frame under symmetric loads may exhibit an anti-symmetrical mode of buckling. The load at which such buckling becomes possible defines a bifurcation point on the load path for the structure. Generally, the load at which sidesway or anti-symmetric buckling occurs is less than the critical load for symmetric buckling. The equilibrium of a slightly buckled frame is considered to establish the conditions under which the structure initiates lateral instability. This state of equilibrium, as shown in Figure 5.1, is achieved by superimposing on the symmetrical deflection shape an infinitely small anti-symmetrical deformation associated with a lateral displacement ΔR of joints 1 and 1′. The anti-symmetrical configuration corresponds to a set of small variations in end rotation, $\Delta\phi$, and the bar rotation, $\Delta\rho$, as shown in Figure 5.1. Connected with these variations in deflection shape is a change in axial force equal to ΔP, which in turn causes changes in the stiffness coefficients equal to ΔS and ΔC. Due to these modifications, the variation in moment at end "a" of member ab shown in Figure 4.1 may be expressed in the following form

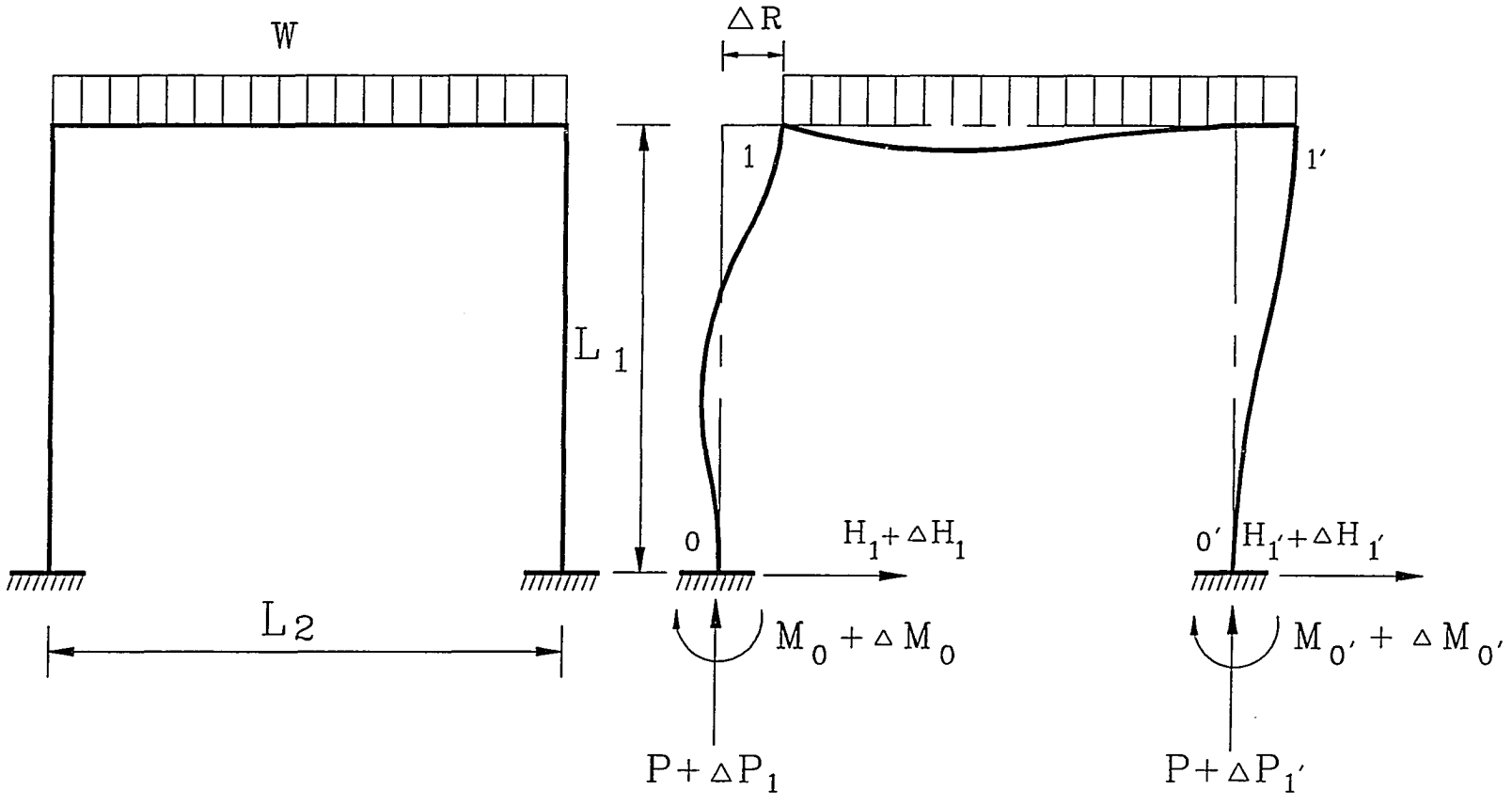

Figure 5.1, One-Story Anti-Symmetrical Mode

$$M_{ab} = K[(C\phi_a + S\phi_b) - (C+S)\rho] + M_{fa}$$
$$\Delta M_{ab} = K[C\Delta\phi_a + \Delta C\phi_a + S\Delta\phi_b + \Delta S\phi_b - (\Delta C + \Delta S)\rho - (C+S)\Delta\rho] + \Delta M_{fa} \quad (5.1)$$

in which

$$K = \frac{EI}{L}\ ,\quad \Delta S = S'\Delta P\ ,\quad \Delta C = C'\Delta P\ ,\quad \Delta M^s_{fab} = M'_{fa}\Delta P \quad (5.2a)$$

$$S' = \frac{dS}{dP}\ ,\quad C' = \frac{dC}{dP}\ ,\quad M'_{fa} = \frac{dM_{fa}}{dP} \quad (5.2b)$$

The influence of pre-buckling deformation, induced by the principal bending moment, is accounted for in the terms involving ϕ_a , ϕ_b , ρ and ΔM_{fab}. The terms $\frac{dS}{dP}$ and $\frac{dC}{dP}$ represent the rate of change of the coefficients S and C, respectively, with respect to the axial force P. Similarly, $\frac{dM_{fa}}{dP}$ is the rate of change of the fixed end moment with respect to P. If the member shown in Figure 4.1 is not submitted to any lateral loads, the expression for the change of moment takes the form

$$M_{ab} = K[(C\phi_a + S\phi_b) - (C+S)\rho]$$
$$\Delta M_{ab} = K[\Delta C\phi_a + C\Delta\phi_a + \Delta S\phi_b + S\Delta\phi_b - (\Delta C + \Delta S)\rho - (C+S)\Delta\rho] \quad (5.3)$$

This expression may be used to evaluate the change in moment at the top of the column due to the imposed lateral displacement ΔR.

5.1.2. Derivation of the Characteristic Equation (Rigid Frames)

The condition for lateral instability is established by superimposing on the symmetrical deflection form an infinitely small anti-symmetrical deformation. For the symmetrical deflection in Figure 5.1, the vertical reactions at the supports 0 and 0′ are equal to the axial forces in columns 0-1 and 0′-1′, that is

$$V_1 = P = \frac{WL_2}{2} \qquad (5.4a)$$

$$V_{1'} = P$$

Equilibrium using summation of moments about point 0′ of Figure 5.1, the distributed load is lumped at joints 1 and 1′, gives

$$(V_1 + \Delta V_1)L_2 - P(L_2 - \Delta R) + P\Delta R + M_{0\text{-}1} + M_{0'\text{-}1'} + \Delta M_{0\text{-}1} + \Delta M_{0'\text{-}1'} = 0 \qquad (5.4b)$$

In Equation (5.4b), symmetry requires that

$$M_{0\text{-}1} = -M_{0'\text{-}1'}$$

In Equation (5.4b) $\Delta M_{0\text{-}1}$ and $\Delta M_{0'\text{-}1'}$ are the moment reactions induced at the supports 0 and 0′, respectively, due to lateral displacement ΔR. $\Delta M_{0\text{-}1}$ and $\Delta M_{0'\text{-}1'}$ can be written in terms of ΔR and a multiplier η. , that is

$$\Delta M_{0\text{-}1} = \Delta M_{0'\text{-}1'} = -\eta\frac{\Delta R}{L_1}$$

The following procedure which utilizes the moment distribution method is applied in this analysis to calculate the multiplier η :

1. A joint translation ΔR is applied at joints 1 and 1′ of the frame in Figure 5.1.

2. At this instant the frame is departing from its current symmetric deformation into a new non-symmetric configuration.

3. The fixed-end moments for columns 0-1 and 0′-1′, due to the applied lateral displacement, at each equilibrium state examined take the following form

$$FEM_{0\text{-}1} = FEM_{1\text{-}0} = FEM_{0'\text{-}1'} = FEM_{1'\text{-}0'} = -(6\,EI_1/L^2_1)\,\Delta R$$

4. The fixed end moments for the beam $FEM_{1\text{-}1'} = FEM_{1'\text{-}1} = 0$.

5. Stiffness coefficients C_1 and S_1 for the columns and C_2 and S_2 for the beam at the current equilibrium state are used to calculate the distribution factors and the carry over factors for each member.

6. In the case of flexible connections the stiffnesses for the beam-connection element are to be evaluated as follows

a. The stiffness coefficients for the beam C_2 and S_2 that correspond to the current value of the axial force in the beam are used with the tangent stiffnesses of the connections that correspond to the current loading condition in order to obtain C^t_2 and S^t_2. C^t_2 and S^t_2 are the stiffness coefficients of the beam-connection elements that are to be used in the moment distribution procedure.

b. The connections are assumed to have an elastic response over the entire range of loading, which includes possible loading of joint 1 and unloading of joint 1′ use the same tangent stiffness for the connection at either end of the

beam-connection element.

7. Solving the structure by performing the moment distribution for the applied displacement, the moments at the supports, $\Delta M_{1\text{-}0}$ and $\Delta M_{0'\text{-}1'}$, are found in terms of ΔR from which η is obtained.

Consequently, Equation (5.4b) reduces to the following

$$V_1+\Delta V_1 = P-2P\frac{\Delta R}{L_2}+\frac{2}{L_1}\eta\frac{\Delta R}{L_2} \tag{5.5a}$$

Similarly, summation of moments about point 0 gives

$$V_{1'}+\Delta V_{1'}=P+2P\frac{\Delta R}{L_2}-\frac{2}{L_1}\eta\frac{\Delta R}{L_2} \tag{5.5b}$$

Combining Equations (5.4a), (5.5a) and (5.5b), the following is obtained

$$\begin{aligned}\Delta V_1=\Delta P_1&=(-2PL_1+2\eta)\frac{1}{L_2}\frac{\Delta R}{L_1}\\ \Delta V_{1'}=\Delta P_{1'}&=(2PL_1-2\eta)\frac{1}{L_2}\frac{\Delta R}{L_1}\end{aligned} \tag{5.6}$$

in the above equations, ΔP_1 and $\Delta P_{1'}$ are the changes in axial force in the left and right columns respectively, due to the imposed anti-symmetrical deformation. The variation in end moment of the left column can be expressed by implementing Equation (5.3)

$$M_{1\text{-}0} = K_1[C_1\phi_1 - (C_1 + S_1)\rho]$$

$$\Delta M_{1\text{-}0} = K_1[C_1\Delta\phi_1 + \Delta C_1\phi_1 - (\Delta C_1 + \Delta S_1)\rho - (C_1 + S_1)\Delta\rho]$$

$$\Delta S_1 = S'_1\,\Delta P_1 \quad , \quad \Delta C_1 = C'_1\,\Delta P_1$$

in which S´ and C´ are the derivatives with respect to the axial force in column 0-1, P, and can be expressed in the form

$$\Delta S_1 = S'_1\,\Delta P_1 \quad , \quad \Delta C_1 = C'_1\,\Delta P_1$$

$$S'_1 = \frac{dS_1}{dP} \quad , \quad C'_1 = \frac{dC_1}{dP}$$

Consequently, $\Delta M_{1\text{-}0}$ takes the following form

$$\Delta M_{1\text{-}0} = K_1C_1\Delta\phi_1 + K_1[C'_1\phi_1(2\eta - 2PL_1)\frac{1}{L_2} - (C_1 + S_1)]\frac{\Delta R_1}{L_1} \qquad (5.7a)$$

Similarly

$$\Delta M_{0\text{-}1} = K_1S_1\Delta\phi_1 + K_1[S'_1\phi_1(2\eta - 2PL_1)\frac{1}{L_2} - (C_1 + S_1)]\frac{\Delta R_1}{L_1} \qquad (5.7b)$$

in the above equation $\Delta\rho = \dfrac{\Delta R}{L_1}$, $\rho = 0$.

Expressions for the changes in moments at the ends of member 1-1′ may be obtained by using Equation (5.1) after considering the following relations

$$\rho = \Delta\rho = 0$$

$$\phi_1 = -\phi_{1'} \quad , \quad \Delta\phi_1 = \Delta\phi_{1'}$$

$$\Delta S_2 = S'_2\,\Delta H \quad , \quad \Delta C_2 = C'_2\,\Delta H \quad , \quad \Delta M_f = M'_f\,\Delta H$$

in which S'_2, C'_2 and M'_f are the derivatives with respect to the axial force in member 1-1′, H, and can be expressed in the form

$$S'_2 = \frac{dS_2}{dH} \quad , \quad C'_2 = \frac{dC_2}{dH} \quad , \quad M'_f = \frac{dM_f}{dH}$$

Summation of horizontal forces requires

$$\Delta H_1 + \Delta H_{1'} = 0 \tag{5.8a}$$

Moreover, the assumed anti-symmetric configuration requires

$$\Delta H_1 = \Delta H_{1'} \tag{5.8b}$$

Therefore because there is no net external horizontal force, the change in horizontal reaction at the support 1, ΔH_1, must be zero and the change in horizontal reaction at the support 1′, $\Delta H_{1'}$, must also be zero in order to satisfy both the equilibrium of summation of horizontal forces, Equation (5.8a), and the condition for anti-symmetric configuration,

Equation (5.8b). Consequently, ΔS^s_2, ΔC^s_2 and ΔM^s_f are all zero. The expressions for $\Delta M_{1\text{-}1'}$ and $\Delta M_{1'\text{-}1}$ are thus simplified to the following form

$$\Delta M_{1\text{-}1'} = K_2(C_2 + S_2)\Delta\phi_1 \tag{5.9a}$$

$$\Delta M_{1'\text{-}1} = K_2(C_2 + S_2)\Delta\phi_{1'} \tag{5.9b}$$

The deformation configuration requires that $\phi_1 = -\phi_{1'}$ before buckling, since the loading and dimensions are symmetrical. Moreover, $\Delta\phi_1$ should be equal to $\Delta\phi_{1'}$ for the anti-symmetrical configuration. Consequently, expressions for $\Delta M_{0\text{-}1}$, $\Delta M_{1\text{-}0}$ and $\Delta M_{1\text{-}1'}$, from the left, become essentially the same as $\Delta M_{0'\text{-}1'}$, $\Delta M_{1'\text{-}0}$ and $\Delta M_{1'\text{-}1}$, from the right, respectively. Hence, there are only three independent equations involved in this problem. The equilibrium equations are

$$\begin{aligned} \Delta M_{0\text{-}1} + \Delta M_{1\text{-}0} &= -P\Delta R_1 \\ \Delta M_{1\text{-}0} + \Delta M_{1\text{-}1'} &= 0 \end{aligned} \tag{5.10}$$

Substitution of Equations (5.7a), (5.7b) and (5.8a) in the equilibrium Equations (5.10) yields the following set of equations

$$K_1(C_1+S_1)\Delta\phi_1 + \{K_1[(C'_1+S'_1)\phi_1(2\eta - 2PL_1)\frac{1}{L_2} - 2(C_1+S_1)] + PL_1\}\frac{\Delta R_1}{L_1} = 0 \tag{5.11}$$

$$[K_1C_1 + K_2(C_2+S_2)]\Delta\phi_1 + K_1[C'_1\phi_1(2\eta - 2PL_1)\frac{1}{L_2} - (C_1+S_1)]\frac{\Delta R_1}{L_1} = 0 \tag{5.12}$$

In the case of frames with flexible connections the above equations apply after modifying the stiffness coefficients and the fixed-end moments as defined in Chapter 3.

The vanishing of the determinant of the coefficients of Equations (5.11) and (5.12) produces the equation for the stability condition. The appropriate expression for ϕ_1 is taken from Equation (4.7), which is repeated below

$$\phi_1 = \frac{HL_1}{K_1(C_1+S_1)}$$

The equation for the stability condition asserts the value of H, as a function of P, at the instant sidesway movement becomes possible. To compute the anti-symmetrical buckling load of the frame, this equation is solved simultaneously with the governing equation for the symmetrical deformation case. This means anti-symmetrical deformation becomes feasible when the applied load attains a value at which all equations, Equation (4.8) and Equations (5.11) and (5.12), are simultaneously satisfied.

Therefore, at each equilibrium state of the symmetrical configuration, found by solving Equation (4.8), the determinant of Equations (5.11) and (5.12) is calculated to check if that equilibrium state is stable with regard to the anti-symmetrical configuration.

In the following flow-chart, Flow-chart 1, the procedure for the calculation to establish the equilibrium path and to find the anti-symmetric buckling load for a one-story frame is presented. A second flow-chart is given to illustrate the procedure to find the stiffnesses of the connections at each possible equilibrium state.

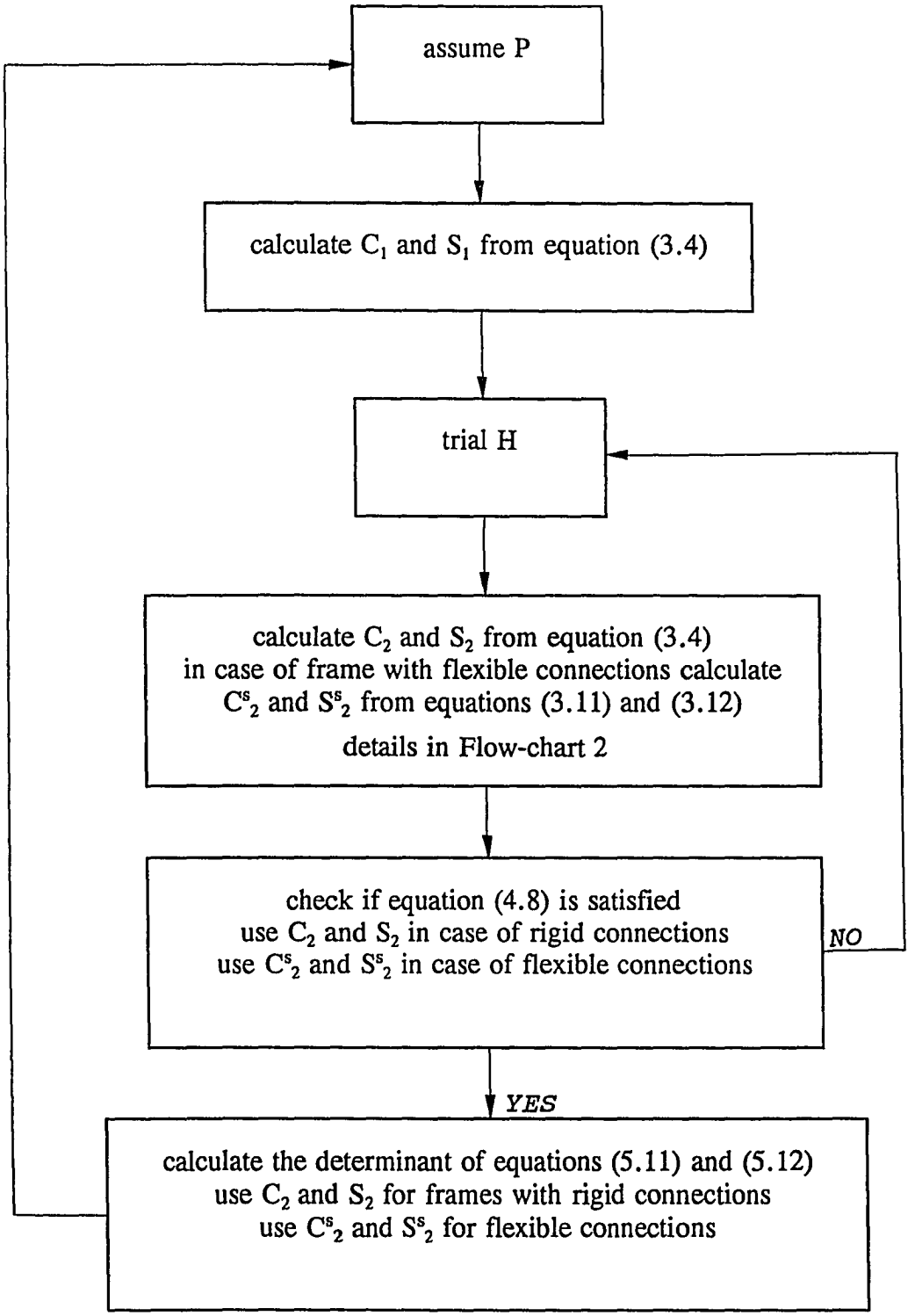
assume P
calculate C_1 and S_1 from equation (3.4)
trial H
calculate C_2 and S_2 from equation (3.4)
in case of frame with flexible connections calculate
C^s_2 and S^s_2 from equations (3.11) and (3.12)
details in Flow-chart 2
check if equation (4.8) is satisfied
use C_2 and S_2 in case of rigid connections
use C^s_2 and S^s_2 in case of flexible connections
NO
YES
calculate the determinant of equations (5.11) and (5.12)
use C_2 and S_2 for frames with rigid connections
use C^s_2 and S^s_2 for flexible connections

Flow-chart 1

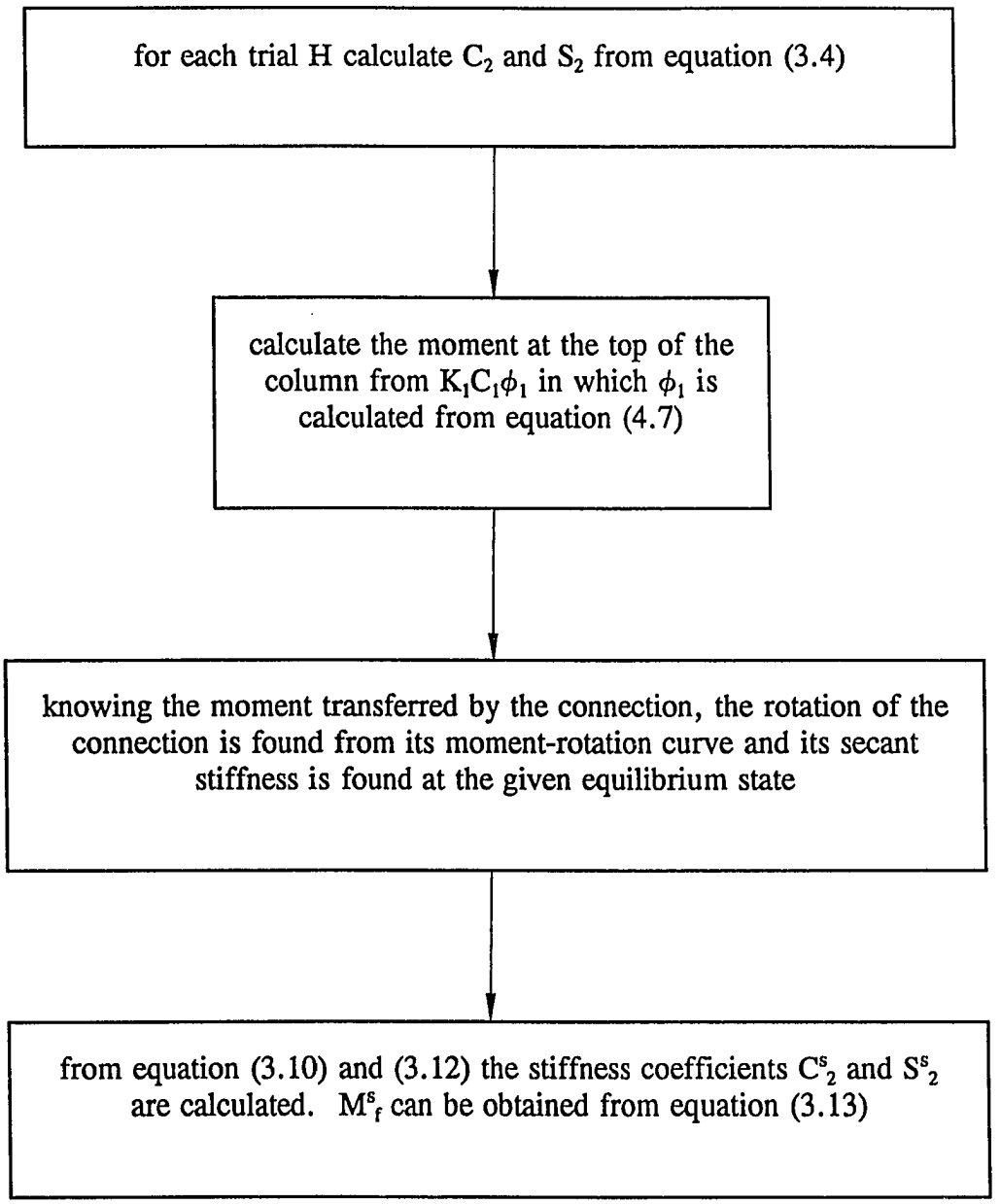
for each trial H calculate C_2 and S_2 from equation (3.4)
calculate the moment at the top of the column from $K_1C_1\phi_1$ in which ϕ_1 is calculated from equation (4.7)
knowing the moment transferred by the connection, the rotation of the connection is found from its moment-rotation curve and its secant stiffness is found at the given equilibrium state
from equation (3.10) and (3.12) the stiffness coefficients C^s_2 and S^s_2 are calculated. M^s_f can be obtained from equation (3.13)

Flow-chart 2

5.2. Two-Story Frames

5.2.1. Rigid Connections

As in the case of one-story frames, the equilibrium of a slightly buckled frame is considered to establish the conditions under which the frame initiates lateral instability. This is achieved by superimposing on the symmetrical deflection shape an infinitely small anti-symmetrical deformation associated with a lateral displacement ΔR_1 at joints 1 and 1′, and ΔR_2 at joints 2 and 2′, as shown in Figure 5.2. For the symmetrical deflection, the vertical reactions at supports 0 and 0′ are equal to the axial forces in columns 0-1 and 0′-1′, Figure 5.3, that is

$$P_1 = 2P = 2 \times \frac{WL_2}{2} \tag{5.13}$$

Equilibrium using summation of moments about point 0′ for the frame in Figure 5.3 gives

$$(2P_1+\Delta P_1)L_2+\Delta M_0-P(L_2-\Delta R_1)-P(L_2-\Delta R_1-\Delta R_2)+P(\Delta R_1+\Delta R_2)+P\Delta R_1+\Delta M_{0'}=0 \tag{5.13}$$

ΔM_0 and $\Delta M_{0'}$, as shown in Figure 5.3, are the moments induced at the supports 0 and 0′ due to a lateral displacement ΔR_1 at joints 1 and 1′, and ΔR_2 at joints 2 and 2′. From Figure 5.4, ΔM_0 and $\Delta M_{0'}$ can be written in the form

$$\Delta M_0 = \delta m_{10} + \delta m_{20}$$

$$\Delta M_{0'} = \delta m_{10'} + \delta m_{20'}$$

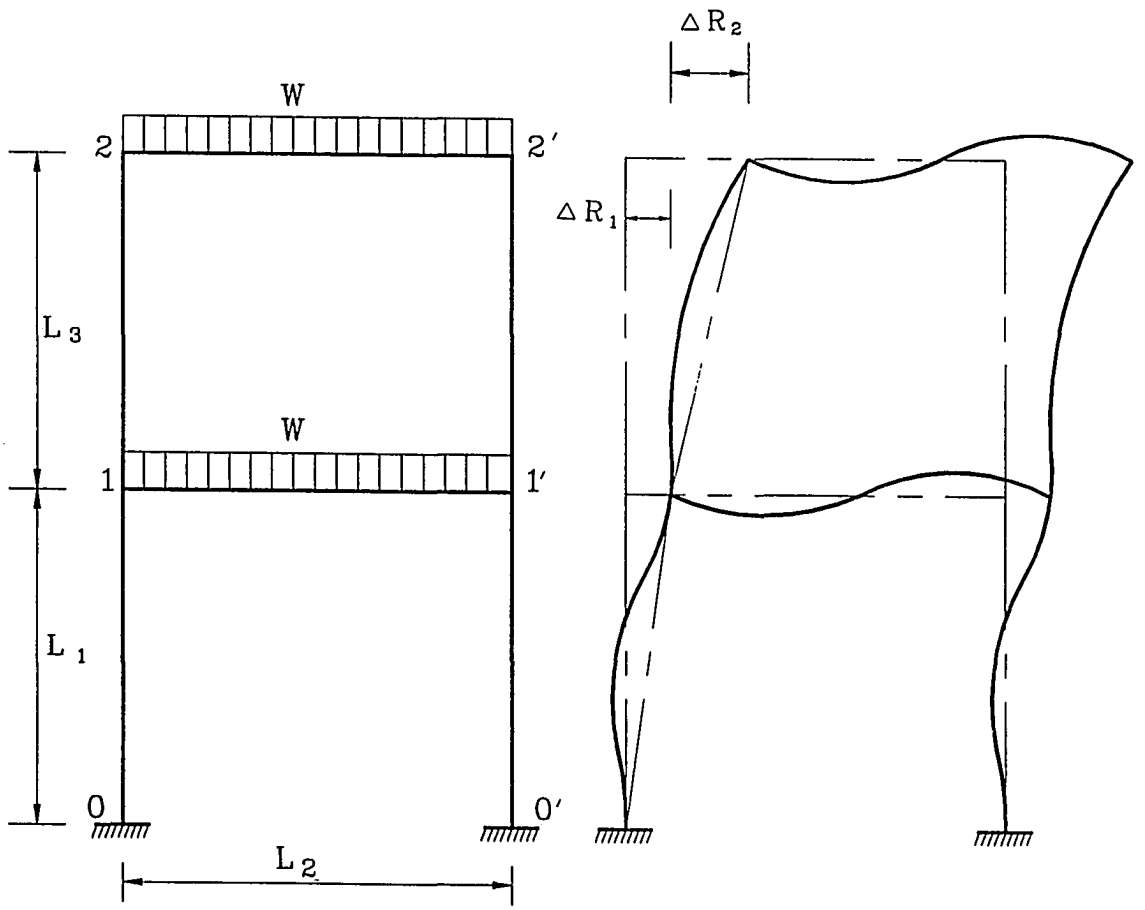

Figure 5.2, Two-Story Anti-Symmetric Mode

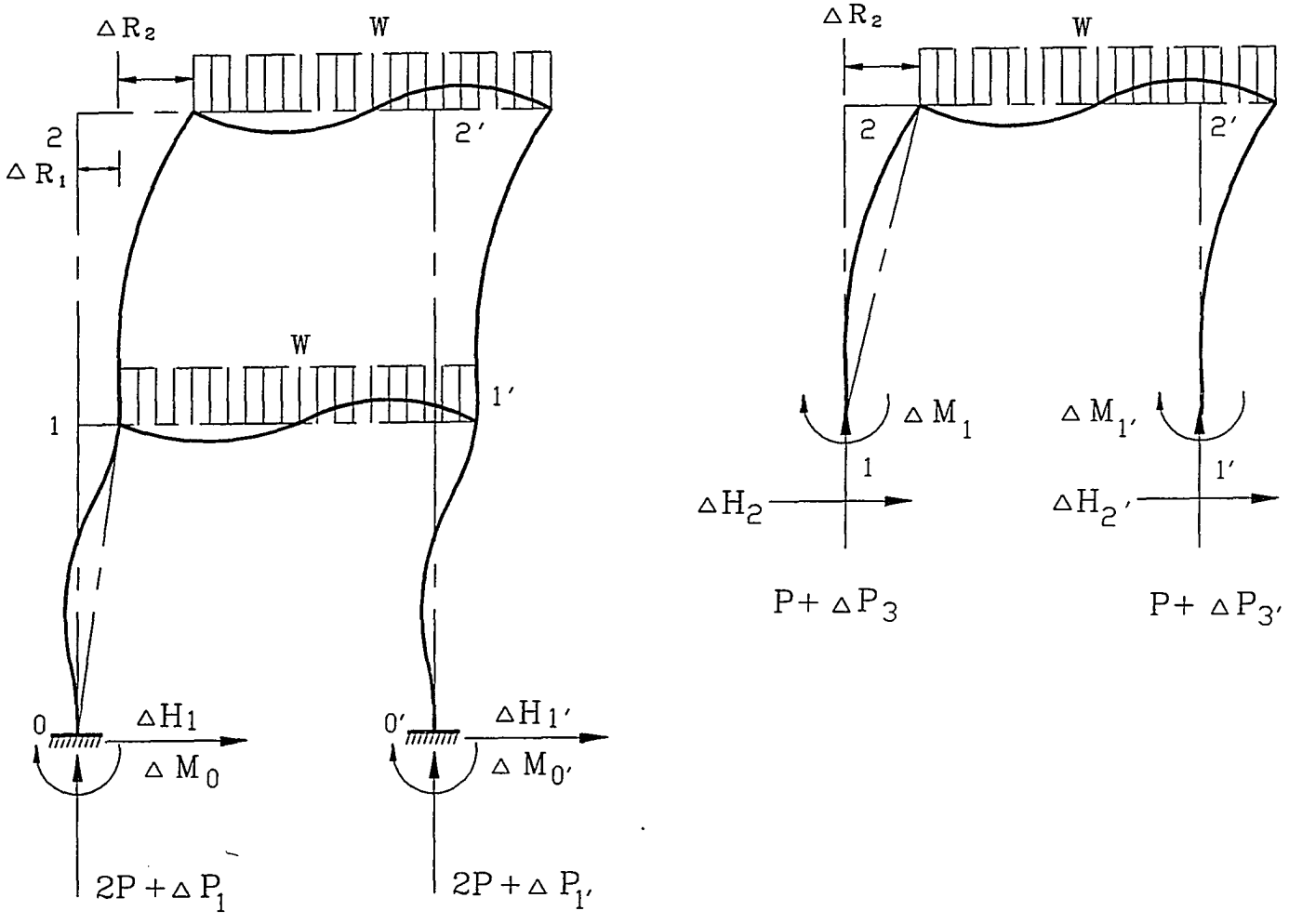

Figure 5.3, Equilibrium of a Two-Story Frame

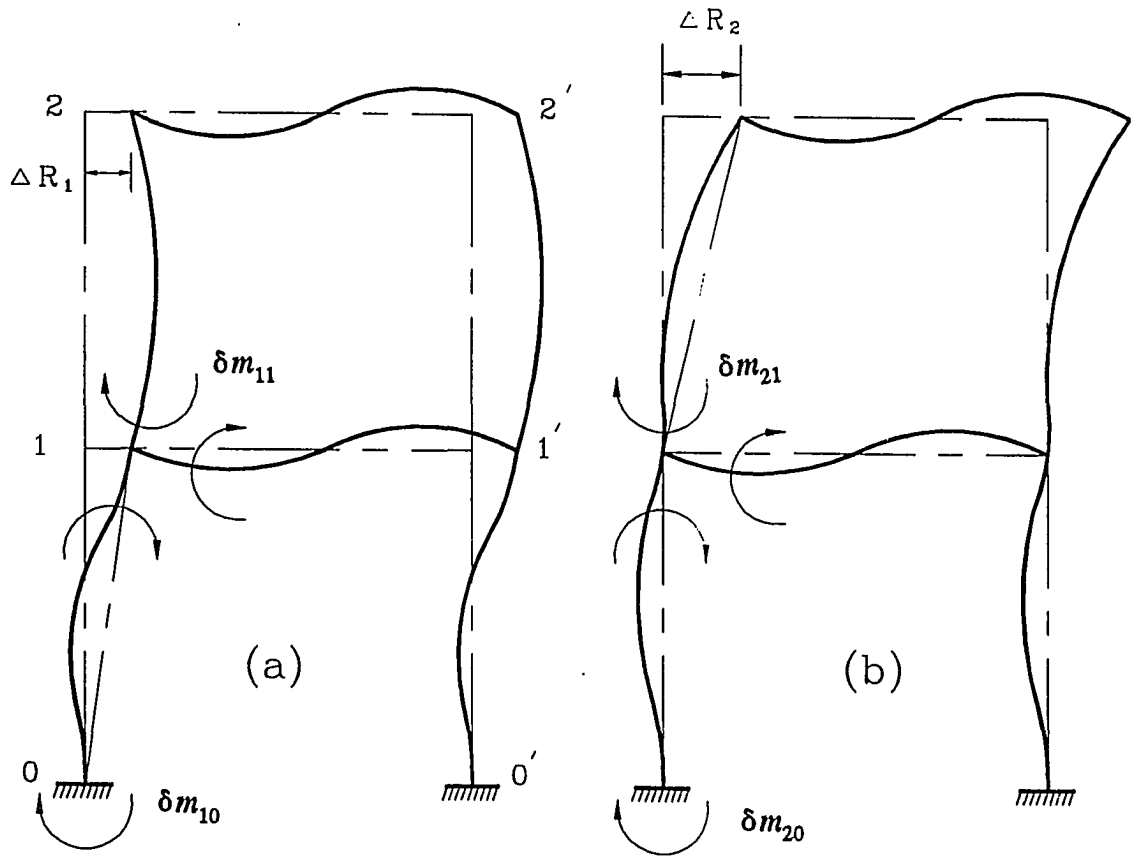

Figure 5.4, Incremental Moments Induced by Displacement ΔR_1 or ΔR_2

δm_{10} is the moment induced at point 0 by sidesway deformation of ΔR_1 only. δm_{20} is the moment induced at point 0 by sidesway deformation of ΔR_2 only. δm_{10} can be calculated in terms of ΔR_1 by solving the frame in Figure 5.4(a) by the moment distribution method for the applied displacement ΔR_1 at joint 1, as explained in Section 5.1.2. δm_{20} can be calculated in terms of ΔR_2 by solving the frame in Figure 5.4(b) by the moment distribution method for the applied displacement ΔR_2 at joint 2. Therefore, δm_{10} and δm_{20} can be written in the form

$$\delta m_{10} = -\frac{\eta_{10}}{L_1}\,\Delta R_1 \quad , \qquad \delta m_{20} = -\frac{\eta_{20}}{L_1}\,\Delta R_2$$

Substituting for ΔM_0 and $\Delta M_{0'}$ in Equation (5.13) and further simplifying, the following is obtained

$$\Delta P_1 = (2\eta_{10} - 4PL_1)\frac{1}{L_2}\,\frac{\Delta R_1}{L_1} + (2\eta_{20} - 2PL_1)\frac{1}{L_2}\,\frac{\Delta R_2}{L_1} \qquad (5.14)$$

In the above equation, Equation (5.14), ΔP_1 represents the change in axial force in column 0-1 due to a small anti-symmetrical deformation associated with a lateral displacement ΔR_1 at joints 1 and 1′, and ΔR_2 at joints 2 and 2′. Equilibrium using summation of moments about point 1′ of the free body 1-2-2′-1′ shown in Figure 5.3(b) gives the following in which P_3 is the axial force in column 1-2

$$(P_3+\Delta P_3)L_2+\Delta M_1-P(L_2-\Delta R_2)+P(\Delta R_2)+\Delta M_{1'} = 0 \qquad (5.15)$$

In which ΔM_1 and $\Delta M_{1'}$, as shown in Figure 5.3(b), are the moments induced at end 1 of column 1-2 and end 1′ of column 1′-2′, respectively, due to a lateral displacement ΔR_1 at joints 1 and 1′, and ΔR_2 at joints 2 and 2′. From Figure 5.4 ΔM_1 and $\Delta M_{1'}$ can be written in the form

$$\Delta M_1 = \delta m_{11} + \delta m_{21}$$

$$\Delta M_{1'} = \delta m_{11'} + \delta m_{21'}$$

δm_{11} is the moment induced at point 1 by sidesway deformation of ΔR_1 only. δm_{21} is the moment induced at point 1 by sidesway deformation of ΔR_2 only. Therefore, δm_{11} and δm_{21} can be written in the form

$$\delta m_{11} = -\frac{\eta_{11}}{L_1}\Delta R_1 \quad , \quad \delta m_{21} = -\frac{\eta_{21}}{L_1}\Delta R_2$$

Substituting for ΔM_1 and $\Delta M_{1'}$ in Equation (5.15) and further simplifying, the following is obtained

$$\Delta P_3 = (2\eta_{21} - 2PL_1)\frac{1}{L_2}\frac{\Delta R_2}{L_1} + \frac{2}{L_2}\eta_{11}\frac{\Delta R_1}{L_1} \qquad (5.16)$$

In the above equation, Equation (5.16), ΔP_3 expresses the change in axial force in column 1-2 due to a small anti-symmetrical deformation associated with a lateral displacement ΔR_1 at joints 1 and 1′, and ΔR_2 at joints 2 and 2′.

Because there is no net external horizontal force, the changes in horizontal forces, ΔH_1 at the support and ΔH_2 at end 1 of the free body 1-2-2′-1′, must all be zero to

satisfy both the equilibrium of the summation of horizontal forces and the condition for anti-symmetric deformation. Therefore, the terms including ΔS and ΔC and the term ΔM_f in Equation (5.1) are all zero. Moreover, the deformation configuration requires that $\phi_1 = -\phi_{1'}$ and $\phi_2 = -\phi_{2'}$ and $\rho_1 = \rho_2 = 0$ before buckling, since the loading and dimensions are symmetric. In addition, $\Delta\phi_1$ and $\Delta\phi_2$ should be equal to $\Delta\phi_{1'}$ and $\Delta\phi_{2'}$, respectively, because of the anti-symmetric configuration. Considering all of the above conditions, the terms for the change of moments expressed in Equation (5.1) for the beams and Equation (5.3) for the columns take the following forms

$$\Delta M_{1\text{-}0}=K_1C_1\Delta\phi_1+K_1[C'_1\phi_1(2\eta_{10}-4PL_1)\frac{1}{L_2}-(C_1+S_1)]\frac{\Delta R_1}{L_1} +K_1C'_1\phi_1(2\eta_{20}-2PL_1)\frac{1}{L_2}\frac{\Delta R_2}{L_1} \tag{5.17}$$

$$\Delta M_{0\text{-}1}=K_1S_1\Delta\phi_1+K_1[S'_1\phi_1(2\eta_{10}-4PL_1)\frac{1}{L_2}-(C_1+S_1)]\frac{\Delta R_1}{L_1} +K_1S'_1\phi_1(2\eta_{20}-2PL_1)\frac{1}{L_2}\frac{\Delta R_2}{L_1} \tag{5.18}$$

$$\Delta M_{1\text{-}2}=K_3C_3\Delta\phi_1+K_3S_3\Delta\phi_2+K_3(C'_3\phi_1+S'_3\phi_2)\frac{2}{L_2}\eta_{11}\frac{\Delta R_1}{L_1} +K_3[(C'_3\phi_1+S'_3\phi_2)(2\eta_{21}-2PL_1)\frac{1}{L_2}-(C_3+S_3)]\frac{\Delta R_2}{L_1} \tag{5.19}$$

$$\Delta M_{2\text{-}1}=K_3S_3\Delta\phi_1+K_3C_3\Delta\phi_2+K_3(S'_3\phi_1+C'_3\phi_2)\frac{2}{L_2}\eta_{11}\frac{\Delta R_1}{L_1} +K_3[(S'_3\phi_1+C'_3\phi_2)(2\eta_{21}-2PL_1)\frac{1}{L_2}-(C_3+S_3)]\frac{\Delta R_2}{L_1} \tag{5.20}$$

$$\Delta M_{1\text{-}1'}=K_2(C_2+S_2)\Delta\phi_1 \tag{5.21}$$

$$\Delta M_{2\text{-}2'}=K_4(C_4+S_4)\Delta\phi_2 \tag{5.22}$$

Equilibrium of column 0-1 gives

$$\Delta M_{1\text{-}0} + \Delta M_{0\text{-}1} = -2P\Delta R_1 \tag{5.23a}$$

Equilibrium of column 1-2 gives

$$\Delta M_{2\text{-}1} + \Delta M_{1\text{-}2} = -P\Delta R_2 \tag{5.23b}$$

Summation of moments of joint 2 produces

$$\Delta M_{2\text{-}1} + \Delta M_{2\text{-}2'} = 0 \tag{5.23c}$$

Summation of moments of joint 1 produces

$$\Delta M_{1\text{-}0} + \Delta M_{1\text{-}1'} + \Delta M_{1\text{-}2} = 0 \tag{5.23d}$$

Substitution of Equations (5.17) through (5.22) into Equations (5.23a), (5.23b), (5.23c) and (5.23d) leads to the following four homogeneous equations with four unknowns

$$\begin{aligned} &K_1(C_1+S_1)\Delta\phi_1+\{K_1[(C'_1+S'_1)\phi_1(2\eta_{10}-4PL_1)\frac{1}{L_2}-2(C_1+S_1)] \\ &+2PL_1\}\frac{\Delta R_1}{L_1}+K_1(C'_1+S'_1)\phi_1(2\eta_{20}-2PL_1)\frac{1}{L_2}\frac{\Delta R_2}{L_1} = 0 \end{aligned} \tag{5.24}$$

$$\begin{aligned} &K_3(C_3+S_3)\Delta\phi_1+K_3(C_3+S_3)\Delta\phi_2+K_3(C'_3+S'_3)(\phi_1+\phi_2)\frac{2}{L_2}\eta_{11}\frac{\Delta R_1}{L_1} \\ &+\{K_3[(C'_3+S'_3)(\phi_1+\phi_2)(2\eta_{21}-2PL_1)\frac{1}{L_2}-2(C_3+S_3)]+PL_1\}\frac{\Delta R_2}{L_1} = 0 \end{aligned} \tag{5.25}$$

$$K_3S_3\Delta\phi_1+[K_3C_3+K_4(C_4+S_4)]\Delta\phi_2+K_3(S'_3\phi_1+C'_3\phi_2)\frac{2}{L_2}\eta_{11}\frac{\Delta R_1}{L_1}$$
$$+K_3[(S'_3\phi_1+C'_3\phi_2)(2\eta_{21}-2PL_1)\frac{1}{L_2}-(C_3+S_3)]\frac{\Delta R_2}{L_1} = 0 \qquad (5.26)$$

$$[K_1C_1+K_2(C_2+S_2)+K_3C_3]\Delta\phi_1+K_3S_3\Delta\phi_2$$
$$+\{K_1[C'_1\phi_1(2\eta_{10}-4PL_1)\frac{1}{L_2}-(C_1+S_1)]+K_3(C'_3\phi_1+S'_3\phi_2)\frac{2}{L_2}\eta_{11}\}\frac{\Delta R_1}{L_1}$$
$$+\{K_1C'_1\phi_1(2\eta_{20}-2PL_1)\frac{1}{L_2}+K_3[(C'_3\phi_1+S'_3\phi_2)(2\eta_{21}-2PL_1)\frac{1}{L_2}-(C_3+S_3)]\}\frac{\Delta R_2}{L_1} = 0 \qquad (5.27)$$

In the case of frames with flexible connections the above equations apply after substituting C^s_2, C^s_4, S^s_2, S^s_4, M^s_{f1} and M^s_{f2} for C_2, C_4, S_2, S_4, M_{f1} and M_{f2}, respectively.

The vanishing of the determinant of the coefficients of Equations (5.24) through (5.27) produces the equation for the stability condition. The equation for the stability condition asserts the values of H_1 and H_2 as functions of P at the instant sidesway movement becomes possible. To compute the anti-symmetrical buckling load of the frame, the equation for the stability condition is solved simultaneously with the governing equation for the pre-buckling case, Equations (4.16a) and (4.16b). The following flow-chart, Flow-chart 3, presents the procedure for the calculation to establish the equilibrium path and to find the anti-symmetric buckling load for a two-story frame. Flow-chart 4 illustrates the method to find the connections' stiffnesses at each possible equilibrium state.

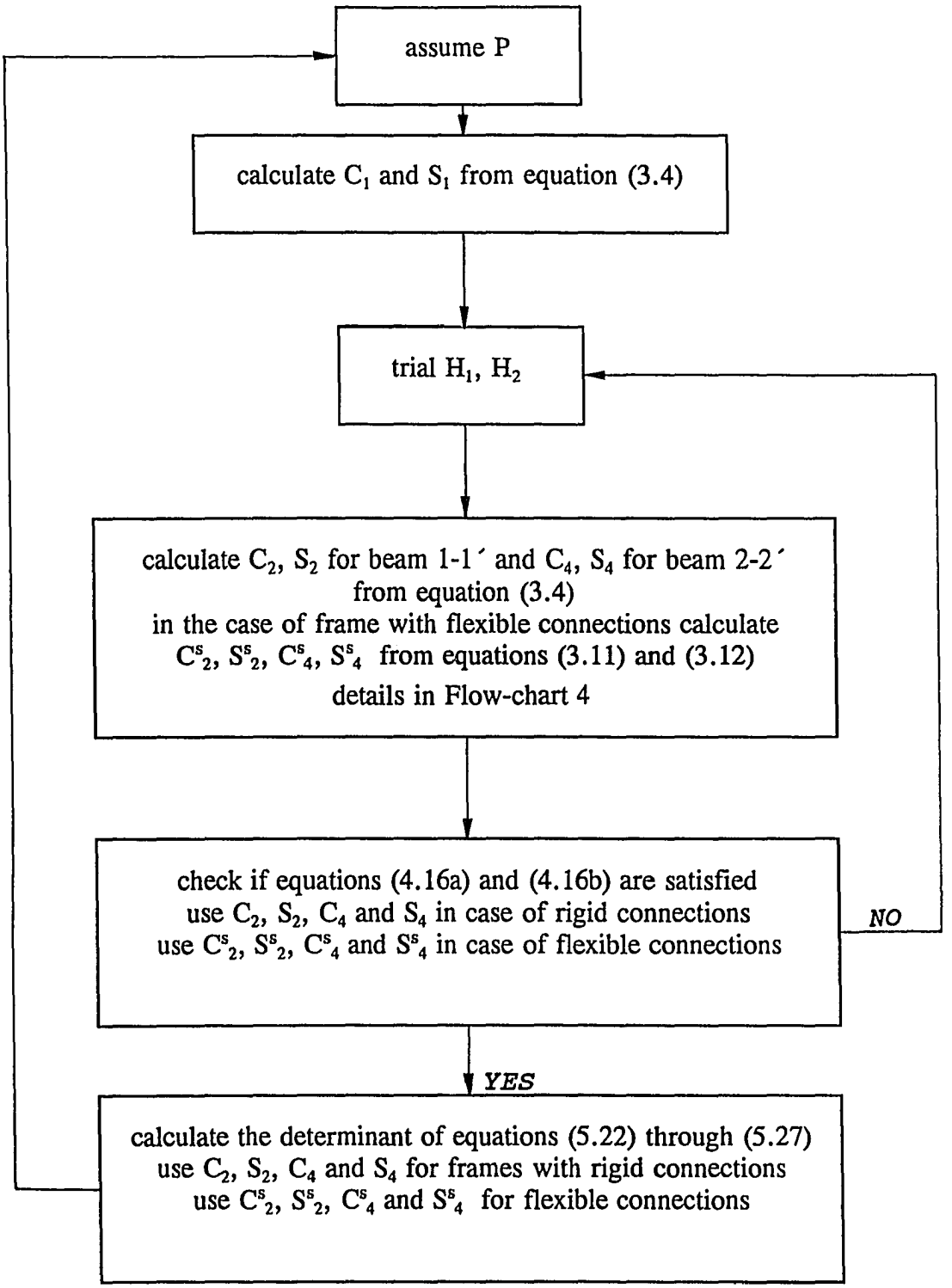
assume P
calculate C_1 and S_1 from equation (3.4)
trial H_1, H_2
calculate C_2, S_2 for beam 1-1′ and C_4, S_4 for beam 2-2′
from equation (3.4)
in the case of frame with flexible connections calculate
C^s_2, S^s_2, C^s_4, S^s_4 from equations (3.11) and (3.12)
details in Flow-chart 4
check if equations (4.16a) and (4.16b) are satisfied
use C_2, S_2, C_4 and S_4 in case of rigid connections
use C^s_2, S^s_2, C^s_4 and S^s_4 in case of flexible connections
NO
YES
calculate the determinant of equations (5.22) through (5.27)
use C_2, S_2, C_4 and S_4 for frames with rigid connections
use C^s_2, S^s_2, C^s_4 and S^s_4 for flexible connections

Flow-chart 3

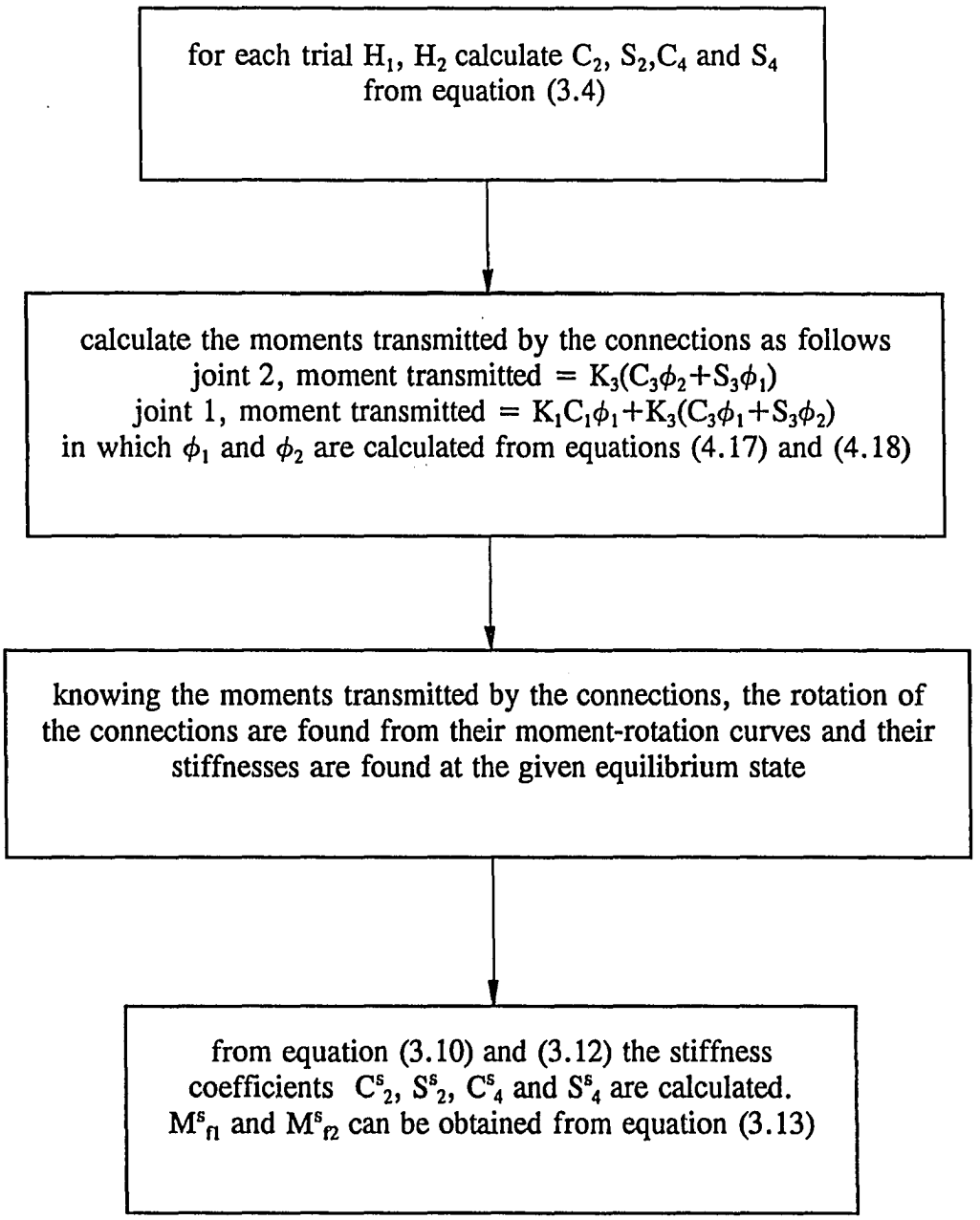
for each trial H_1, H_2 calculate C_2, S_2,C_4 and S_4 from equation (3.4)
calculate the moments transmitted by the connections as follows
joint 2, moment transmitted = $K_3(C_3\phi_2+S_3\phi_1)$
joint 1, moment transmitted = $K_1C_1\phi_1+K_3(C_3\phi_1+S_3\phi_2)$
in which ϕ_1 and ϕ_2 are calculated from equations (4.17) and (4.18)
knowing the moments transmitted by the connections, the rotation of the connections are found from their moment-rotation curves and their stiffnesses are found at the given equilibrium state
from equation (3.10) and (3.12) the stiffness coefficients C^s_2, S^s_2, C^s_4 and S^s_4 are calculated. M^s_{f1} and M^s_{f2} can be obtained from equation (3.13)

Flow-chart 4

CHAPTER 6

EFFECT OF LATERAL BRACING

Since the columns in the present study are considered to be inextensional, the presence of lateral bracing could have an effect on the buckling behavior of the structure only in the case of lateral instability. Therefore, only the case of anti-symmetrical buckling mode is considered in order to evaluate the influence of the bracing member on the stability of the structure.

6.1. One-Story Frames (Rigid Connections)

The analysis in this case follows that of Section 5.1.2. However, the terms involving the changes of axial forces, ΔP in Equation (5.6) and $\Delta H=0$, have to be modified for the effect of lateral bracing.

In general, the cross bracing is assumed to act only in tension. The diagonal brace under compression buckles slightly and becomes inactive. An infinitely small anti-symmetric deformation associated with a lateral displacement ΔR of joints 1 and 1′, shown in Figure 6.1, is superimposed on the symmetrical deflection shape to establish the conditions under which the frame with the bracing member initiates lateral instability. Since the displacement ΔR is a small quantity relative to the brace length L_b, the change in angle α, Figure 6.1, caused by the displacement ΔR is insignificant. Therefore, the angle between the new axis of the deformed brace and the horizontal is α. The elongation of the brace associated with a displacement ΔR is

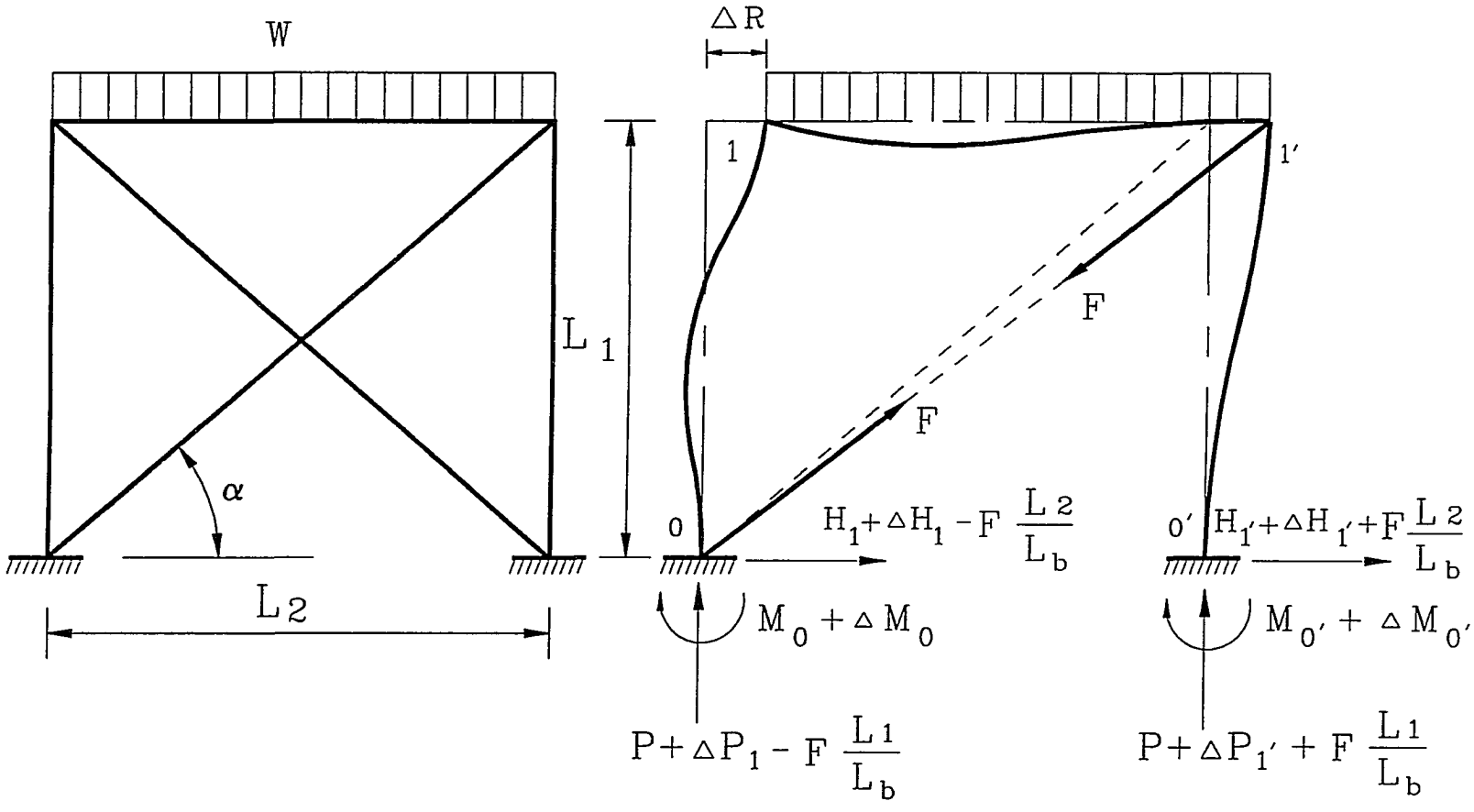

Figure 6.1 One-Story Frame with Lateral Brace

$$\Delta L_b = \Delta R \cos\alpha = \frac{L_2}{L_b} \Delta R \tag{6.1}$$

Under this elongation the brace force F is

$$F = \frac{E_b A_b}{L_b} \frac{L_2}{L_b} \Delta R \tag{6.2}$$

In which A_b is the cross sectional area of the brace. Equilibrium using summation of moments about point 0′ of Figure 6.1 gives the change in axial force in column 0-1 due to a lateral displacement ΔR

$$\Delta P_1 = (2\eta - 2PL_1 + K_b L_1^2 L_2^2) \frac{1}{L_2} \frac{\Delta R}{L_1} - K_b L_1 \Delta R^2 \tag{6.3}$$

In which η is as defined in Section 5.1.2. K_b is defined by

$$K_b = \frac{E_b A_b}{L_b^3}$$

Since ΔR is a small quantity, the term involving ΔR^2 in Equation (6.3) is very small relative to the terms that involve only ΔR. Therefore, the term involving ΔR^2 is neglected. Equation (6.3) becomes

$$\Delta P_1 = (2\eta - 2PL_1 + K_b L_1^2 L_2^2) \frac{1}{L_2} \frac{\Delta R}{L_1} \tag{6.4}$$

Summation of horizontal forces requires

$$\Delta H_1 + \Delta H_{1'} = 0 \tag{6.5}$$

Moreover, the assumed anti-symmetric configuration requires

$$\Delta H_1 = \Delta H_{1'} \tag{6.6}$$

Therefore, because there is no net external horizontal force, the change in horizontal reaction at the support 0, ΔH_1, must be zero and the change in horizontal reaction at the support $0'$, $\Delta H_{1'}$, must also be zero. The terms for the changes of moments in Equations (5.7a), (5.7b) and (5.8), after substitution for $\Delta H=0$ and for ΔP_1 from Equation (6.4), take the form

$$\Delta M_{1\text{-}0} = K_1 C_1 \Delta\phi_1 + K_1[C'_1\phi_1(2\eta - 2PL_1 + K_b L_1^2 L_2^2)\frac{1}{L_2} - (C_1 + S_1)]\frac{\Delta R}{L_1} \tag{6.7}$$

$$\Delta M_{0\text{-}1} = K_1 S_1 \Delta\phi_1 + K_1[S'_1\phi_1(2\eta - 2PL_1 + K_b L_1^2 L_2^2)\frac{1}{L_2} - (C_1 + S_1)]\frac{\Delta R}{L_1} \tag{6.8}$$

$$\Delta M_{1\text{-}1'} = K_2(C_2 + S_2)\Delta\phi_1 \tag{6.9}$$

Substitution of Equations (6.7), (6.8) and (6.9) into the equilibrium Equations (5.9) produces the following two homogeneous equations

$$K_1(C_1 + S_1)\Delta\phi_1 + \{K_1[(C'_1 + S'_1)\phi_1(2\eta - 2PL_1 + K_b L_1^2 L_2^2)\frac{1}{L_2} - 2(C_1 + S_1)] + PL_1\}\frac{\Delta R}{L_1} = 0 \tag{6.10}$$

$$[K_1 C_1 + K_2(C_2 + S_2)]\Delta\phi_1 + \{K_1[C'_1\phi_1(2\eta - 2PL_1 + K_b L_1^2 L_2^2)\frac{1}{L_2} - (C_1 + S_1)]\}\frac{\Delta R}{L_1} = 0 \tag{6.11}$$

In the case of frames with flexible connections C^s_2, S^s_2 and M^s_f are substituted for C_2, S_2 and M_f, respectively, in the above equations.

The vanishing of the determinant of the coefficients of Equations (6.10) and (6.11) produces the characteristic equation for the stability condition for the case of anti-symmetrical buckling, including the effect of the bracing member.

6.2. Two-Story Frames (Rigid Connections)

The analysis in this case follows that of Section 5.2. However, the terms involving the changes of axial forces due to lateral displacements ΔR_1 and ΔR_2; ΔP_1 in Equation (5.14), ΔP_3 in Equation (5.16), $\Delta H_1=0$ and $\Delta H_2=0$; have to be modified for the effect of lateral bracing. These changes can be obtained from the equilibrium of Figure 6.2 which gives, after dropping all terms involving ΔR_1^2 and ΔR_2^2

$$\Delta P_3 = (2\eta_{21}-2PL_1+K_{b2}L_1^2L_2^2)\frac{1}{L_2}\frac{\Delta R_2}{L_1}+\frac{2}{L_2}\eta_{11}\frac{\Delta R_1}{L_1} \tag{6.12}$$

$$\Delta H_2 = \Delta H_{2'} = 0 \tag{6.13}$$

$$\Delta P_1=(2\eta_{10}-4PL_1+K_{b1}L_1^2L_2^2)\frac{1}{L_2}\frac{\Delta R_1}{L_1}+(2\eta_{20}-2PL_1+K_{b2}L_1^2L_2^2)\frac{1}{L_2}\frac{\Delta R_2}{L_1} \tag{6.14}$$

$$\Delta H_1 = \Delta H_{1'} = 0 \tag{6.15}$$

In the above equations, $K_{b1}L_{b1}^2$ is the stiffness of the lateral brace of the first-story. $K_{b2}L_{b2}^2$ is the stiffness of the lateral brace of the second-story. K_{b1} and K_{b2} were defined in Equation (6.4). η_{10}, η_{11}, η_{20} and η_{21} are as defined in Section 5.2. With the introduction of Equations (6.12) through (6.15) to Equations (5.1) and (5.3), the expressions for the changes of moments in Equations (5.17) through (5.22) take the following form

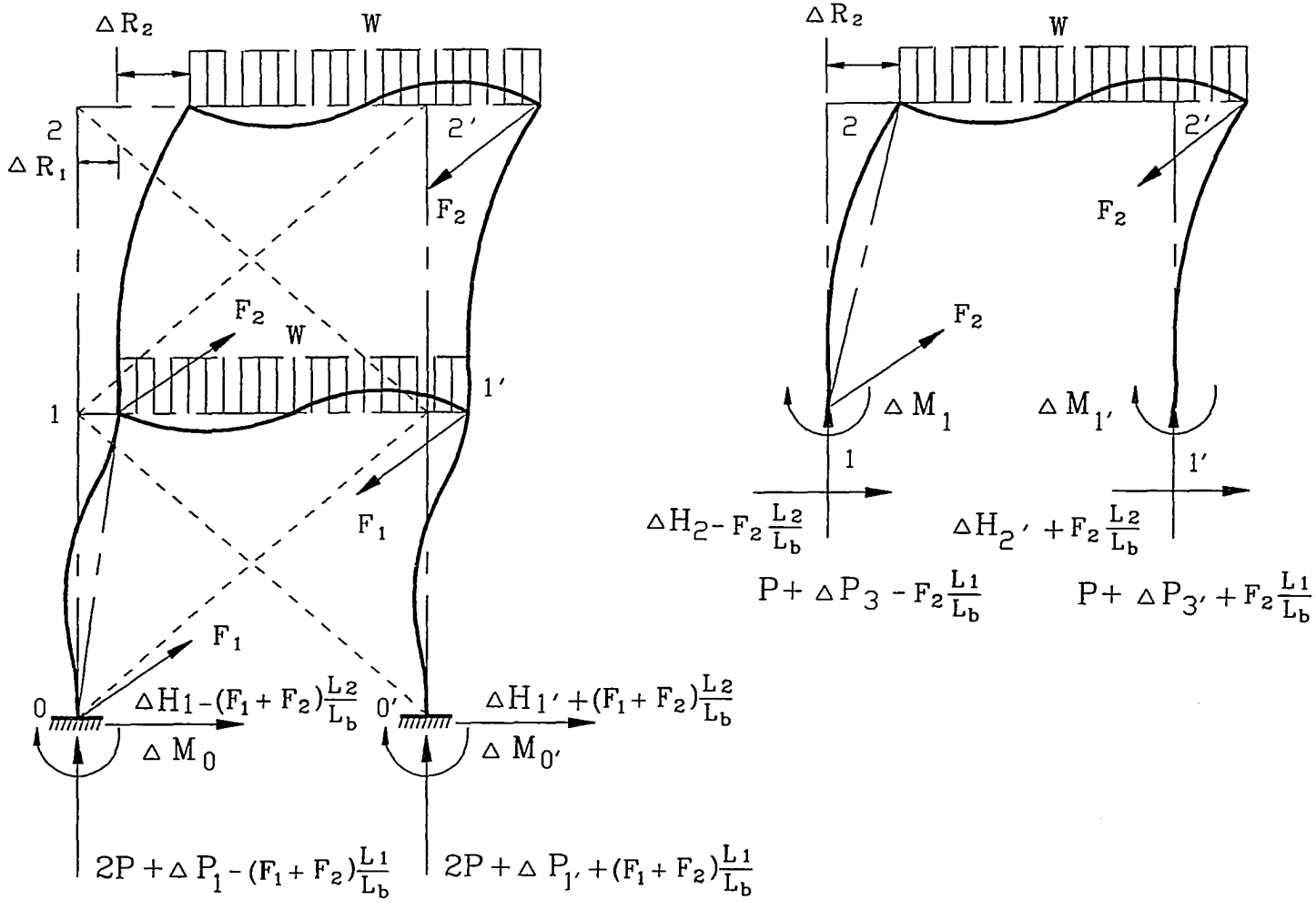

Figure 6.2 Two-Story with Lateral Bracing

$$\Delta M_{1-0} = K_1 C_1 \Delta\phi_1 + K_1[C'_1\phi_1(2\eta_{10} - 4PL_1 + K_{b1}L_1^2L_2^2)\frac{1}{L_2} - (C_1 + S_1)]\frac{\Delta R_1}{L_1}$$
$$+K_1 C'_1\phi_1(2\eta_{20} - 2PL_1 + K_{b2}L_1^2L_2^2)\frac{1}{L_2}\frac{\Delta R_2}{L_1}$$

(6.16)

$$\Delta M_{0-1} = K_1 S_1 \Delta\phi_1 + K_1[S'_1\phi_1(2\eta_{10} - 4PL_1 + K_{b1}L_1^2L_2^2)\frac{1}{L_2} - (C_1 + S_1)]\frac{\Delta R_1}{L_1}$$
$$+K_1 S'_1\phi_1(2\eta_{20} - 2PL_1 + K_{b2}L_1^2L_2^2)\frac{1}{L_2}\frac{\Delta R_2}{L_1}$$

(6.17)

$$\Delta M_{1-2} = K_3 C_3 \Delta\phi_1 + K_3 S_3 \Delta\phi_2 + K_3(C'_3\phi_1 + S'_3\phi_2)\frac{2}{L_2}\eta_{11}\frac{\Delta R_1}{L_1} + K_3[(C'_3\phi_1 + S'_3\phi_2)$$
$$(2\eta_{21} - 2PL_1 + K_{b2}L_1^2L_2^2)\frac{1}{L_2} - (C_3 + S_3)]\frac{\Delta R_2}{L_1}$$

(6.18)

$$\Delta M_{2-1} = K_3 S_3 \Delta\phi_1 + K_3 C_3 \Delta\phi_2 + K_3(S'_3\phi_1 + C'_3\phi_2)\frac{2}{L_2}\eta_{11}\frac{\Delta R_1}{L_1} + K_3[(S'_3\phi_1 + C'_3\phi_2)$$
$$(2\eta_{21} - 2PL_1 + K_{b2}L_1^2L_2^2)\frac{1}{L_2} - (C_3 + S_3)]\frac{\Delta R_2}{L_1}$$

(6.19)

$$\Delta M_{1\text{-}1'} = K_2(C_2+S_2)\,\Delta\phi_1 \tag{6.20}$$

$$\Delta M_{2\text{-}2'}=K_4(C_4+S_4)\Delta\phi_2 \tag{6.21}$$

Substitution of Equations (6.16) through (6.21) into the equilibrium Equations (5.23a), (5.23b), (5.23c) and (5.23d) produces the following four homogeneous equations, Equations (6.22), (6.23), (6.24) and (6.25)

$$K_1(C_1+S_1)\Delta\phi_1+\{K_1[(C'_1+S'_1)\phi_1(2\eta_{10}-4PL_1+K_{b1}L_1^2L_2^2)\frac{1}{L_2}-2(C_1+S_1)]+2PL_1\}\frac{\Delta R_1}{L_1}$$
$$+K_1(C'_1+S'_1)\phi_1(2\eta_{20}-2PL_1+K_{b2}L_1^2L_2^2)\frac{1}{L_2}\frac{\Delta R_2}{L_1}=0 \tag{6.22}$$

$$K_3(C_3+S_3)\Delta\phi_1+K_3(C_3+S_3)\Delta\phi_2+K_3(C'_3+S'_3)(\phi_1+\phi_2)\frac{2}{L_2}\eta_{11}\frac{\Delta R_1}{L_1}$$
$$+\{K_3[(C'_3+S'_3)(\phi_1+\phi_2)(2\eta_{21}-2PL_1+K_{b2}L_1^2L_2^2)\frac{1}{L_2}-2(C_3+S_3)]+PL_1\}\frac{\Delta R_2}{L_1}=0 \tag{6.23}$$

$$K_3S_3\Delta\phi_1+[K_3C_3+K_4(C_4+S_4)]\Delta\phi_2+K_3(S'_3\phi_1+C'_3\phi_2)\frac{2}{L_2}\eta_{11}\frac{\Delta R_1}{L_1}$$
$$+K_3[(S'_3\phi_1+C'_3\phi_2)(2\eta_{21}-2PL_1+K_{b2}L_1^2L_2^2)\frac{1}{L_2}-(C_3+S_3)]\frac{\Delta R_2}{L_1}=0 \tag{6.24}$$

$$[K_1C_1+K_2(C_2+S_2)+K_3C_3]\Delta\phi_1+K_3S_3\Delta\phi_2+\{K_1[C'_1\phi_1(2\eta_{10}-4PL_1+K_{b1}L_1^2L_2^2)\frac{1}{L_2}$$
$$-(C_1+S_1)]+K_3(C'_3\phi_1+S'_3\phi_2)\frac{2}{L_2}\eta_{11}\}\frac{\Delta R_1}{L_1}+\{K_1C'_1\phi_1(2\eta_{20}-2PL_1+K_{b2}L_1^2L_2^2)\frac{1}{L_2}$$
$$+K_3[(C'_3\phi_1+S'_3\phi_2)(2\eta_{21}-2PL_1+K_{b2}L_1^2L_2^2)\frac{1}{L_2}-(C_3+S_3)]\}\frac{\Delta R_2}{L_1}=0$$

(6.25)

In the case of frames with flexible connections C^s_2, S^s_2, M^s_{f1}, C^s_4, S^s_4 and M^s_{f2} are substituted for C_2, S_2, M_{f1}, C_4, S_4 and M_{f2}, respectively, in the above equations.

The vanishing of the determinant of the coefficients of Equations (6.22), (6.23), (6.24) and (6.25) produces the characteristic equation for the stability condition for the case of anti-symmetrical buckling, including the effect of the bracing member.

CHAPTER 7

NUMERICAL APPLICATIONS

The critical value of P is found by a numerical procedure that amounts to calculation of load deflection behavior up to the critical loading. In order to study how the introduction of primary bending moments, lateral bracing and the realistic behavior of the flexible connections affect the value of the critical load; several portal frames, with different beam-to-column rigidity and length ratios, were analyzed. The stiffness of the connections was increased gradually from connection A to connection C, as shown in Figures 7.2. Figure 7.1 presents a beam-connection model by Geschwindner (1991). Table 7.1 displays the ratio of beam length, L_B, to connection equivalent length, L_C, which may be calculated as shown in Figure 7.1. The smaller the ratio L_C/L_B the stiffer the connection with respect to the beam. The results of the analyses are given in Tables 7.2 to 7.13 showing the effective length factor k, where kL is the equivalent pinned-end length referred to as the effective length (Salmon and Johnson, 1986).

One factor that affects the critical behavior of framed structures is the introduction of primary moments to the buckling load analysis. To illustrate the impact of this factor, the values of k for one-story and two-story frames considering the influence of primary bending moments are compared to the corresponding values obtained by Bleich (1952) and the AISC for frames loaded only on the columns. This comparison is illustrated in Table 7.12 for single-bay portal frames and in Table 7.13 for two-story frames for both symmetric and antisymmetric modes of buckling. The results show the deteriorating

effect on frames stability by the primary bending moments . To further illustrate this point , the buckling load analysis was performed on frames with various beam-to-column length ratios. Three ratios were adopted, $L_2/L_1=1.0$, $L_2/L_1=2.0$ and $L_2/L_1=3.0$, in which L_2 is the beam span and L_1 is the column length. Increasing the beam-to-column length ratio results in increasing the primary moments. The results, shown in tables 7.2 through 7.7 for one-story frames, support the cited conclusion on the influence of primary moments on the value of the critical load.

An important factor in this study is to assess the influence of the realistic non-linear behavior of the connections on the stability of framed structures. To make this assessment several flexible connections were adopted. These connections are identified by their moment-rotation curves, presented in Figure 7.2. The stiffness is increased gradually from connection A up to connection C. A comparison of the k values that are given in Tables 7.2 through 7.7 for one-story frames and in Tables 7.10 and 7.11 for two-story frames assert the superiority of rigid connections over flexible connections for both modes of buckling, symmetric and anti-symmetric. The results in the above tables point to the fact that a slight increase in the connection stiffness causes a slight increase in the critical load value. only when the beam is extremely flexible with respect to the column the slight increase of the connection stiffness will not result in an increase of the critical load value.

In general, frames with no lateral brace buckle in an anti-symmetric mode. This is evident from comparing the results of tables 7.2 through 7.7. Therefore, it is of interest to this investigation to assess the influence of the bracing members on the critical

behavior of frames. It is also of interest to find the values of frame stiffness to brace stiffness at which the frame buckles symmetrically. Hence, increasing the brace stiffness over this ratio would have no effect on the critical load value. The buckling load analysis for one-story frames and two-story frames with lateral bracing were given in Chapter 6. Results for some numerical applications of this analysis are displayed in Table 7.8 for one-story frames with rigid connections and Table 7.9 for one-story frames with flexible connection C. A Fortran program was developed which involves a numerical procedure to solve Equations (4.8) for one-story frames, (4.16a) and (4.16b) for two-story frames. In the case of two-story frames there are two homogeneous equations to be solved simultaneously for each case. In the case of multi-story frames with n-stories there are n non-linear equations (non-linear in the coefficients) that have to be solved simultaneously. The Newton procedure is utilized to find the solutions. When the number of non-linear equations are increased, meaning higher multi-story frames, the domain of the solution is decreased. Consequently, one numerical difficulty is encountered since the starting values for the Newton procedure should be chosen in this domain to guarantee convergence. Solving the mentioned equations for the entire range of loading, the load-deflection curve is obtained from which the critical load is determined. Each point on the load deflection curve represents an equilibrium state of the symmetrical configuration. Therefore, at each equilibrium state the determinant of Equations (5.11) and (5.12) is evaluated to check if the equilibrium state is stable with regard to the anti-symmetrical configuration. Also, the determinant of Equations (6.10) and (6.11) is calculated to inspect the lateral stability of braced one-story frames.

The variations of the stiffness coefficients of column 0-1 ,C_1 and S_1, with the load are given in Figure 7.3. Variation of stiffness coefficients for the beam-connection element are given in Figures 7.4 through 7.10. Some curves of load versus horizontal reaction for one-story frames, with beam-to-column length ratio $L_2/L_1 = 1.0$ and beam-to-column rigidity ratio $G = 0.2$, are given in Figures 7.11 for connection A, 7.12 for connection B, 7.12 for connection C, and 7.14 for rigid connection. Figure 7.34 gives the load versus base horizontal reaction for a two-story frame with flexible connection C. Figure 7.35 give the load versus base horizontal reaction for a two-story frame with rigid connection. The top-end rotation the column 0-1 versus the vertical load for some cases are given in Figures 7.15 for connection A, 7.16 for connection B and 7.17 for connection C. The connections rotation versus the vertical load for some cases are given in Figures 7.18 for connection A, 7.19 for connection B and 7.20 for connection C. Some curves for the load versus the moment on the beam-to-column connections are given in Figures 7.21 for connection A, 7.22 for connection B and 7.23 for connection C. The curves for the determinant of Equations (5.11) and (5.12) for one-story frames with flexible connections B and C are provided in Figures 7.24 and 7.25, respectively. Figure 7.26 provides the curve for the determinant of Equations (6.10) and (6.11) for a one-story frame with flexible connection C. The curves for the determinant versus loading for one-story frames with connection C and varying bracing members are given in Figures 7.26 through 7.29. Figure 7.30 provides the curve for the determinant of Equations (6.10) and (6.11) for a one-story frame with rigid connections. The curves for the determinant versus loading for one-story frames with rigid connections and

varying bracing members are given in Figures 7.31 through 7.33. Figures 7.36 and 7.37 provide the curves for the determinant of Equations (6.22) through (6.25) for a two-story frame with connection C and rigid connection, respectively. The curve for the determinant for a two-story frame with a bracing member is given in Figure 7.38. Finally, it should be mentioned that a section with EI = 210,000 kip-in^2 is adopted for the column in all the cited examples, a column length of 180 inches. Some of the values given in Tables 7.2 through 7.11 for the length factor are verified for column sections W 36x135 and W 24x104.

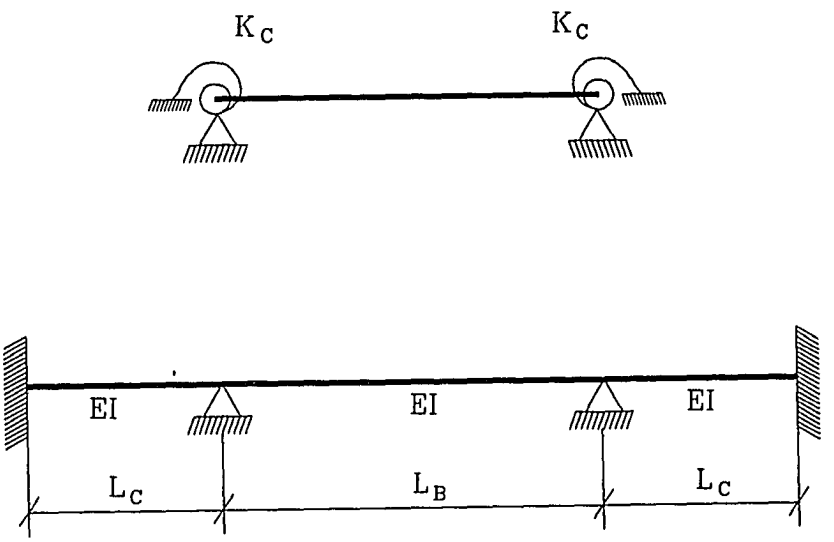

Figure 7.1, Beam-Connection Model (Geschwindner, 1991), $K_c = 4EI/L_c$

TABLE 7.1
Ratio of Beam Length to Connection Equivalent Length, L_C/L_B

G	Connection		
	A	**B**	**C**
0.1	1.80	0.36	0.18
0.2	0.90	0.18	0.09
0.5	0.36	0.07	0.04
1.0	0.18	0.04	0.02

TABLE 7.2
Length Factor k for Single-bay Portal Frame, Fixed at Base.
Symmetric Buckling, $L_2 = L_1$ $G = I_1L_2/I_2L_1$ion Equivalent Length, L_C/L_B

G	Connection			
	A	**B**	**C**	**Rigid**
0.1	0.663	0.609	0.586	0.527
0.2	0.669	0.629	0.611	0.558
0.5	0.688	0.674	0.664	0.658
1.0	0.729	0.759	0.774	0.784

TABLE 7.3
Length Factor k for Single-bay Portal Frame, Fixed at Base.
Anti-symmetric Buckling, $L_2 = L_1$

G	Connection			
	A	**B**	**C**	**Rigid**
0.1	1.940	1.806	1.713	1.054
0.2	1.934	1.745	1.713	1.102
0.5	1.923	1.788	1.717	1.225
1.0	1.923	1.811	1.745	1.368

TABLE 7.4
Length Factor k for Single-bay Portal Frame, Fixed at Base.
Symmetric Buckling, $L_2=2L_1$

G	Connection			
	A	**B**	**C**	**Rigid**
0.1	0.665	0.615	0.593	0.530
0.2	0.678	0.648	0.633	0.585
0.5	0.743	0.798	0.832	0.873
1.0	0.916	1.079	1.144	1.204

TABLE 7.5
Length Factor k for Single-bay Portal Frame, Fixed at Base.
Anti-symmetric Buckling, $L_2=2L_1$

G	Connection			
	A	**B**	**C**	**Rigid**
0.1	1.951	1.834	1.784	1.054
0.2	1.951	1.820	1.745	1.104
0.5	1.934	1.811	1.745	1.239
1.0	1.934	1.835	1.784	1.415

TABLE 7.6
Length Factor k for Single-bay Portal Frame, Fixed at Base.
Symmetric Buckling, $L_2=3L_1$

G	Connection			
	A	**B**	**C**	**Rigid**
0.1	0.669	0.623	0.602	0.535
0.2	0.707	0.681	0.674	0.669
0.5	0.855	1.021	1.107	1.210
1.0	1.238	1.536	1.646	1.709

TABLE 7.7
Length Factor k for Single-bay Portal Frame, Fixed at Base.
Anti-symmetric Buckling, $L_2=3L_1$

G	Connection			
	A	**B**	**C**	**Rigid**
0.1	1.957	1.845	1.801	1.054
0.2	1.940	1.839	1.775	1.108
0.5	1.934	1.849	1.811	1.281
1.0	1.885	1.934	1.957	1.709

TABLE 7.8

Length Factor k for Single-bay Portal Frame, Fixed at Base.
Anti-symmetric Buckling with Lateral Brace and Rigid Connections, $L_2=L_1$

K_b/K_f	Symm.	0.	1.0	3.0	4.0	5.0
E_bA_b		0.	440	1320	1720	2200
G = 0.1	0.527	1.054	0.963	0.894	0.883	0.867
G = 0.2	0.558	1.102	0.949	0.873	0.853	0.843
G = 0.5	0.658	1.225	0.942	0.843	0.829	0.816
G = 1.0	0.784	1.368	0.956	0.825	0.808	0.796

$$K_b = \frac{E_B A_B L_2^2}{(L_1^2+L_2^2)^{3/2}} \quad , \quad K_f = \frac{24\, EI_1}{L_1^3}$$

TABLE 7.9

Length Factor k for Single-bay Portal Frame, Fixed at Base.
Anti-symmetric Buckling with Lateral Brace and Flexible Connection C, $L_2=L_1$

K_b/K_f	Symm.	0.	1.0	3.0	4.0	5.0
E_bA_b		0.	440	1320	1720	2200
G = 0.1	0.586	1.713	1.352	1.120	1.069	1.032
G = 0.2	0.611	1.713	1.249	1.032	0.992	0.956
G = 0.5	0.664	1.717	1.167	0.956	0.917	0.889
G = 1.0	0.774	1.745	1.120	0.905	0.867	0.833

$$K_b = \frac{E_B A_B L_2^2}{(L_1^2+L_2^2)^{3/2}} \quad , \quad K_f = \frac{24\, EI_1}{L_1^3}$$

TABLE 7.10
Length Factor k for Two-story Rectangular Frame, Fixed at Base.
Symmetric Buckling, $L_2=L_1$

G	Connection		
	B	**C**	**Rigid**
0.1	0.838	0.804	0.746
0.2	0.867	0.829	0.780
0.5	0.923	0.878	0.853
1.0	0.969	0.923	0.900

TABLE 7.11
Length Factor k for Two-story Rectangular Frame, Fixed at Base.
Anti-symmetric Buckling, $L_2=L_1$

G	Connection		
	B	**C**	**Rigid**
0.1	1.525	1.498	1.473
0.2	1.616	1.584	1.553
0.5	1.811	1.766	1.766
1.0	2.031	2.031	1.969

TABLE 7.12
Length Factor K for Single-bay Portal Frame, Fixed at Base.
Results Comparison of Different Studies
$L_2 = L_1$ $G = I_1L_2/I_2L_1$

G		0.1	0.2	0.5	1.0
Symmetric Buckling	This Study	0.527	0.558	0.658	0.784
	Bleich	0.524	0.545	0.590	0.626
	AISC	0.525	0.545	0.588	0.625
Anti-symmetric Buckling	This Study	1.054	1.102	1.225	1.368
	Bleich	1.016	1.030	1.082	1.156
	AISC	1.025	1.042	1.083	1.150

Bleich, AISC Alignment Charts, Loads are Applied on Columns
This Study, Loads are Applied on Columns and Beams

TABLE 7.13
Length Factor k for Two-story Portal Frame, Fixed at Base.
Results Comparison of Different Studies
$L_2 = L_1$ $G = I_1L_2/I_2L_1$

G		0.1	0.2	0.5	1.0	2.0
Symmetric Buckling	**This Study**	0.746	0.780	0.853	0.900	0.956
	Bleich	0.507	0.668	0.689	0.753	0.803
	AISC	0.567	0.625	0.730	0.825	0.890
Lateral Buckling	**This Study**	1.473	1.553	1.766	1.969	2.262
	Bleich	1.033	1.065	1.160	1.310	1.515
	AISC	1.050	1.100	1.230	1.450	1.800

Bleich, AISC Alignment Charts, Loads are Applied on Columns
This Study, Loads are Applied on Columns and Beams

The Richard equation for defining moment-rotation relationships is

$$M(\psi) = \frac{(K - K_p)\psi}{(1 + |\frac{(K-K_p)\psi}{M_0}|^N)^{\frac{1}{N}}} + K_p\psi$$

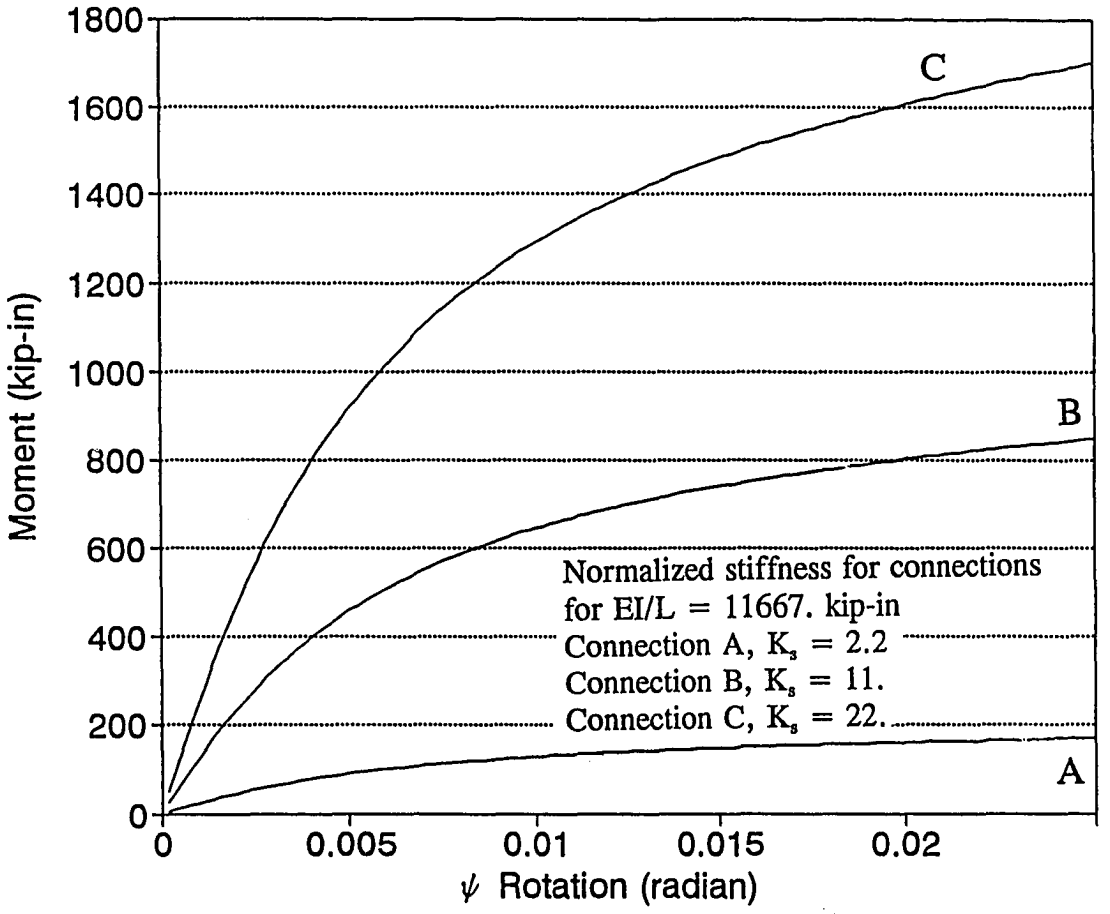

connection C, K = 257060., K_p = 11077.0, M_0 = 1541.10, N =1.5
connection B, K = 128530., K_p = 5538.5, M_0 = 770.55, N =1.5
connection A, K = 25706., K_p = 1107.7, M_0 = 154.11, N =1.5

K initial stiffness, K_p plastic stiffness, M_0 reference moment, N curve shape factor

Figure 7.2, Moment-Rotation for Connections A, B and C

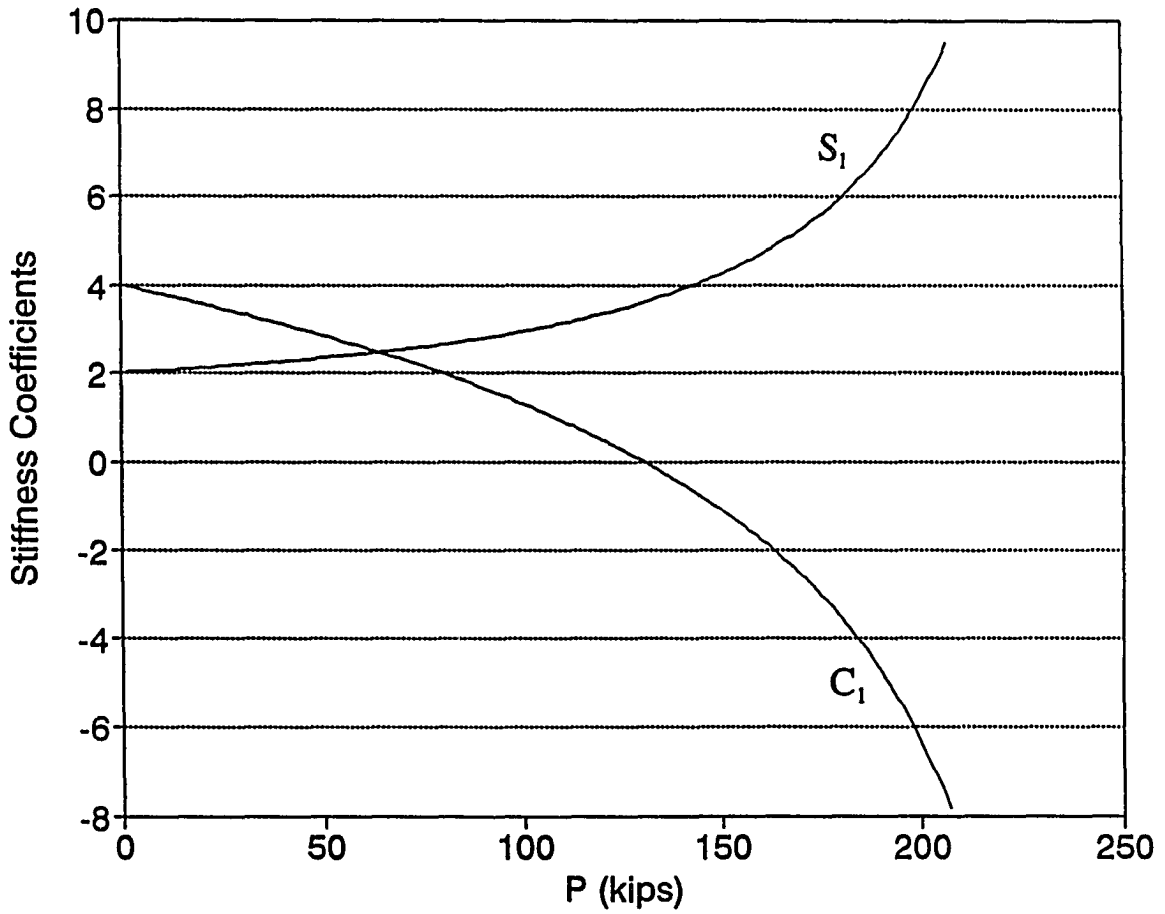

Figure 7.3, Load $P = WL_2/2$ versus Stiffness Coefficients C_1 and S_1 for Column 0-1,

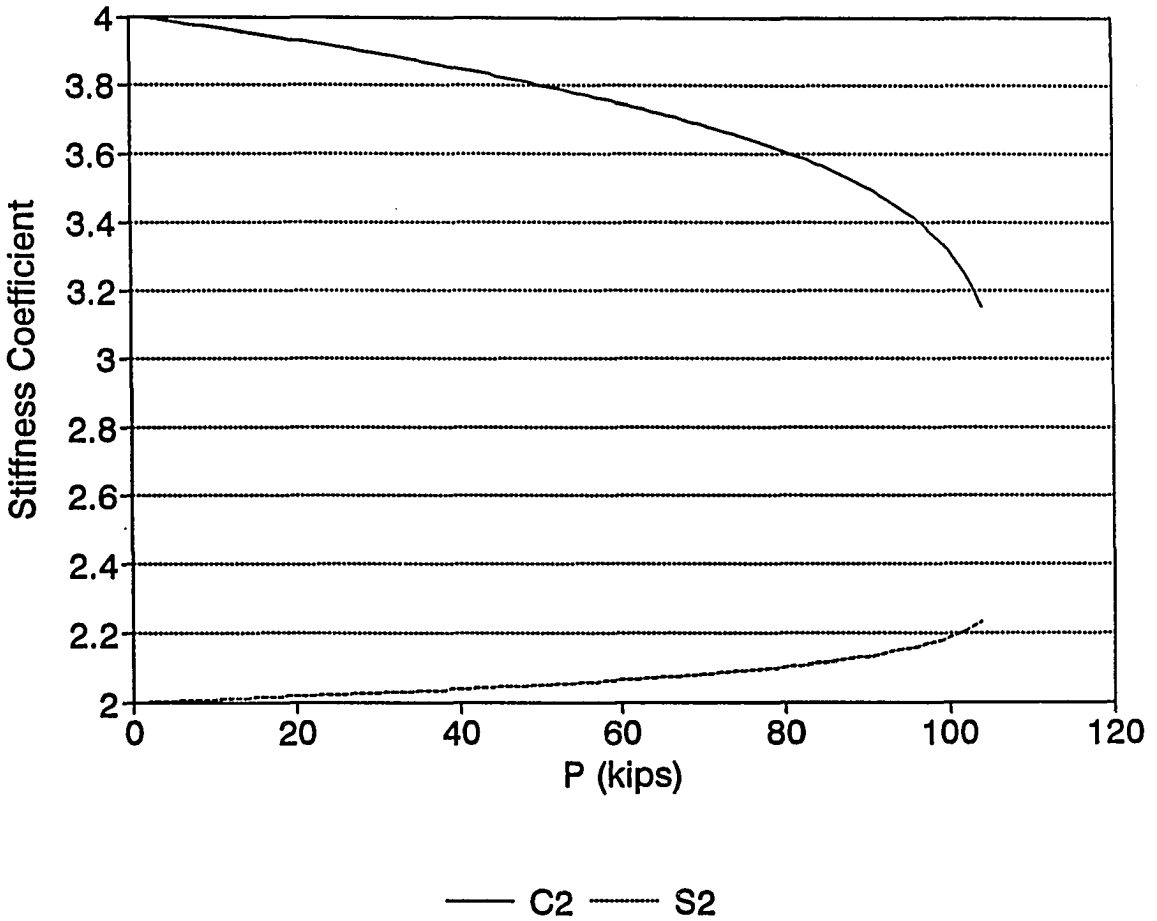

Figure 7.4, Load versus Stiffness Coefficients C_2 and S_2 for Beam 1-1′, G = 1.0

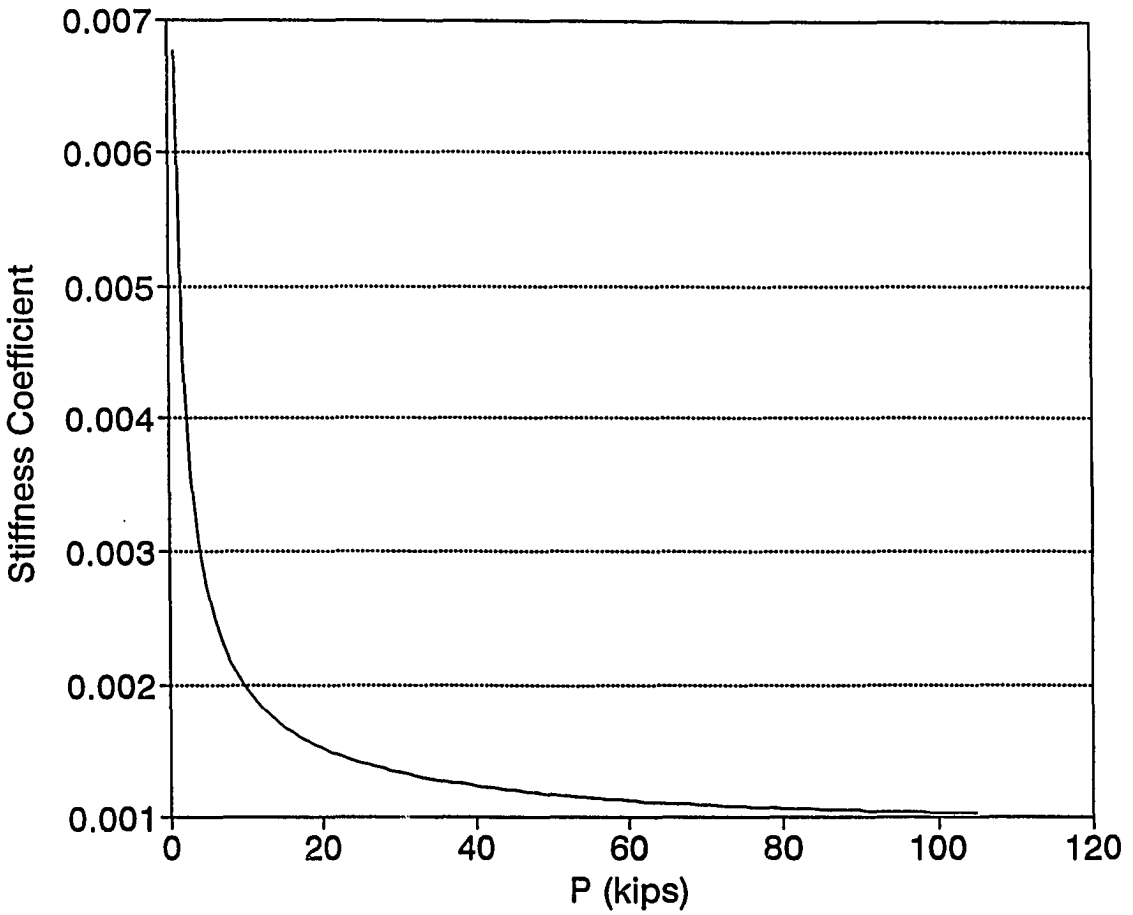

Figure 7.5, Load versus C^s_2 for Beam-Connection Element 1-1′, G = 1.0, L_2=L_1

One-story, Connection A

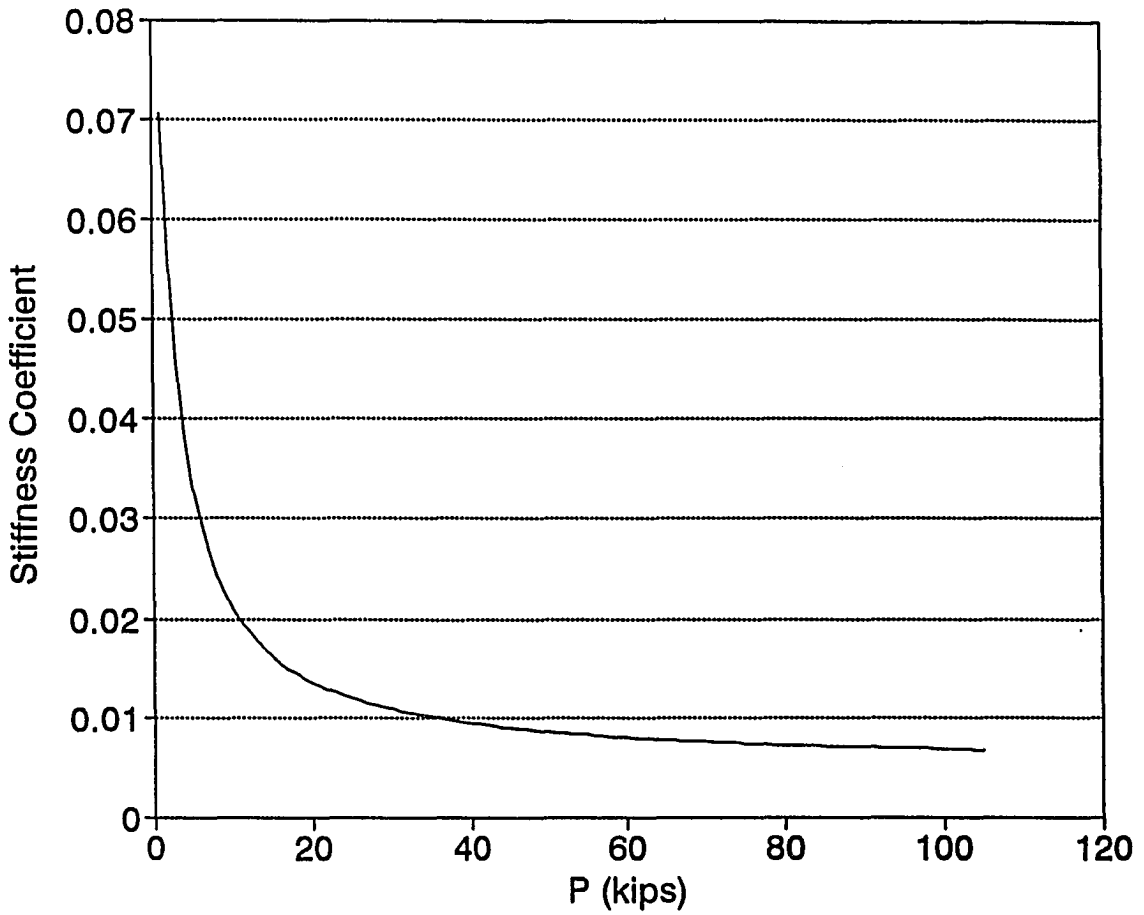

Figure 7.6, Load versus C^s_2 for Beam-Connection Element 1-1′, G = 1.0, L_2=L_1

One-story, Connection B

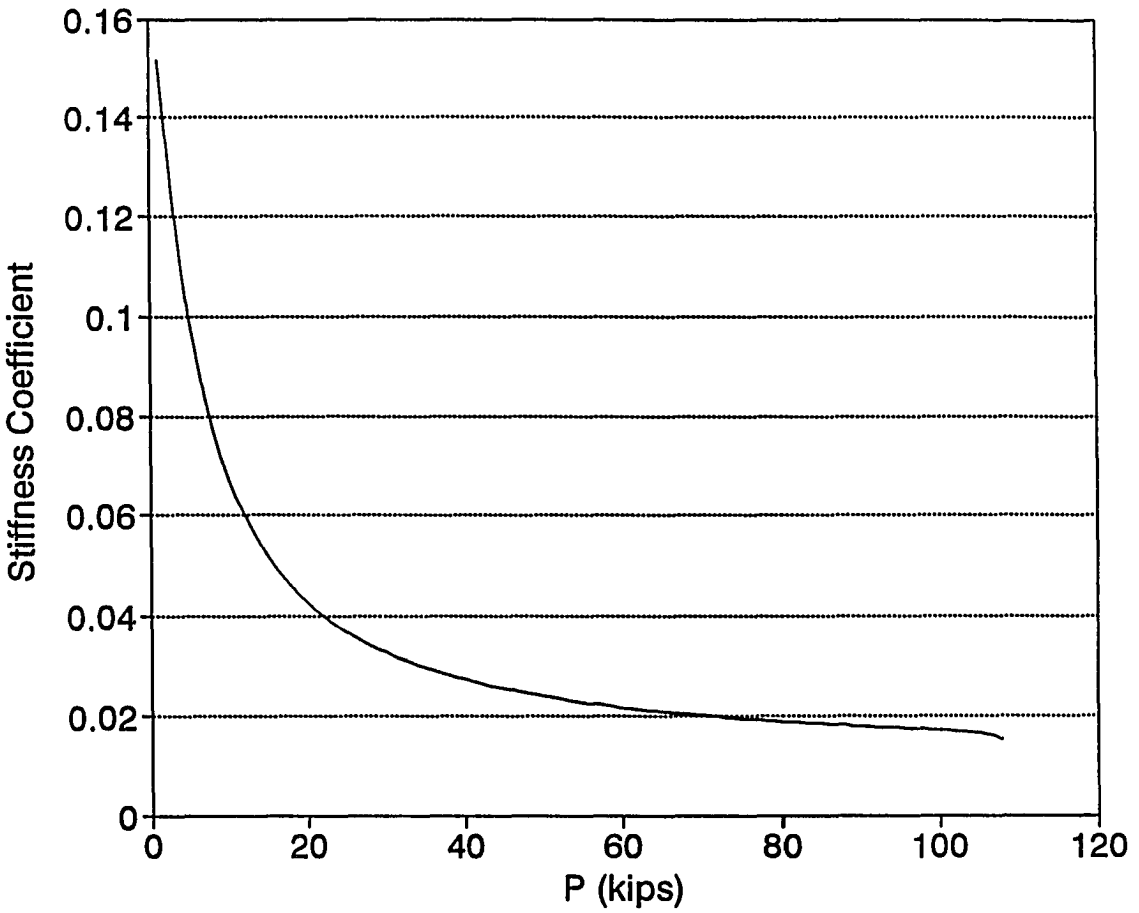

Figure 7.7, Load versus C^s_2 for Beam-Connection Element 1-1´, G = 1.0, L_2=L_1

One-story, Connection C

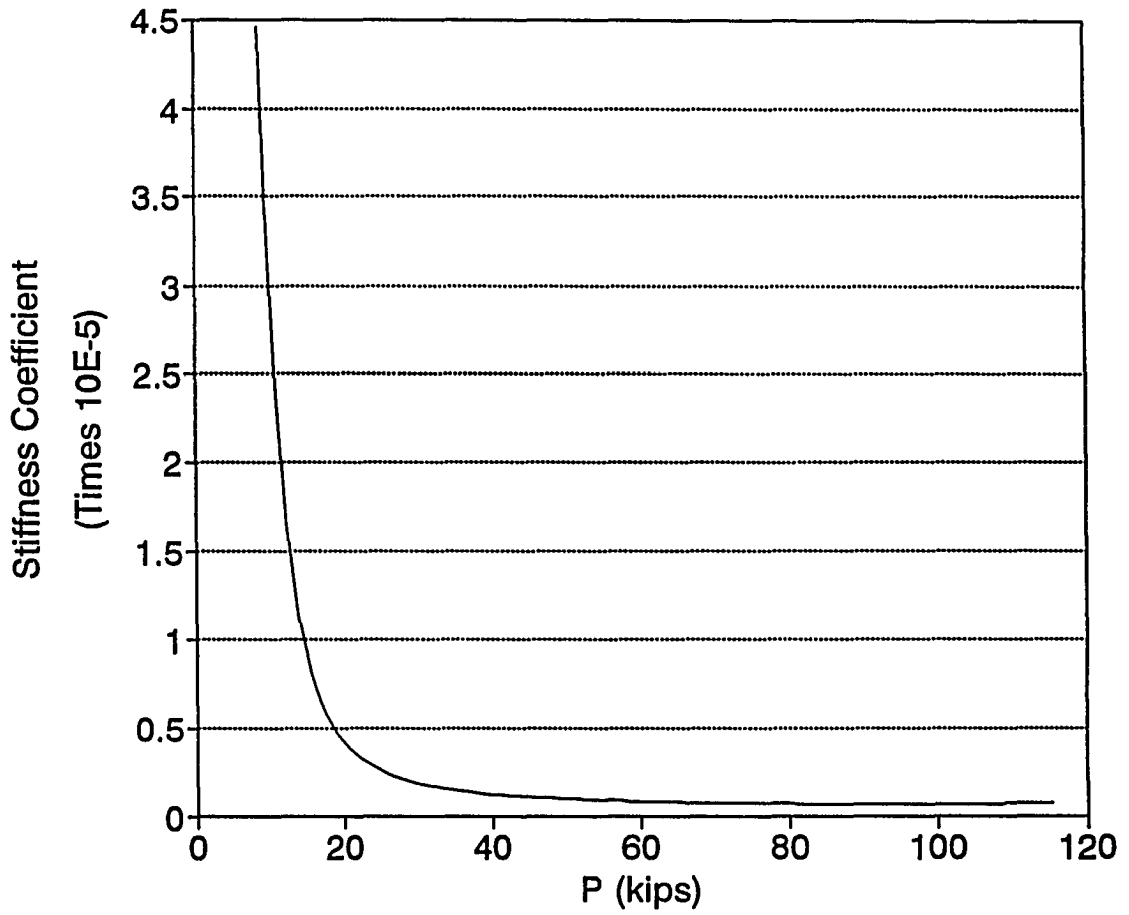

Figure 7.8, Load versus S^s_2 for Beam-Connection Element 1-1′, G = 1.0, $L_2=L_1$

One-story, Connection A

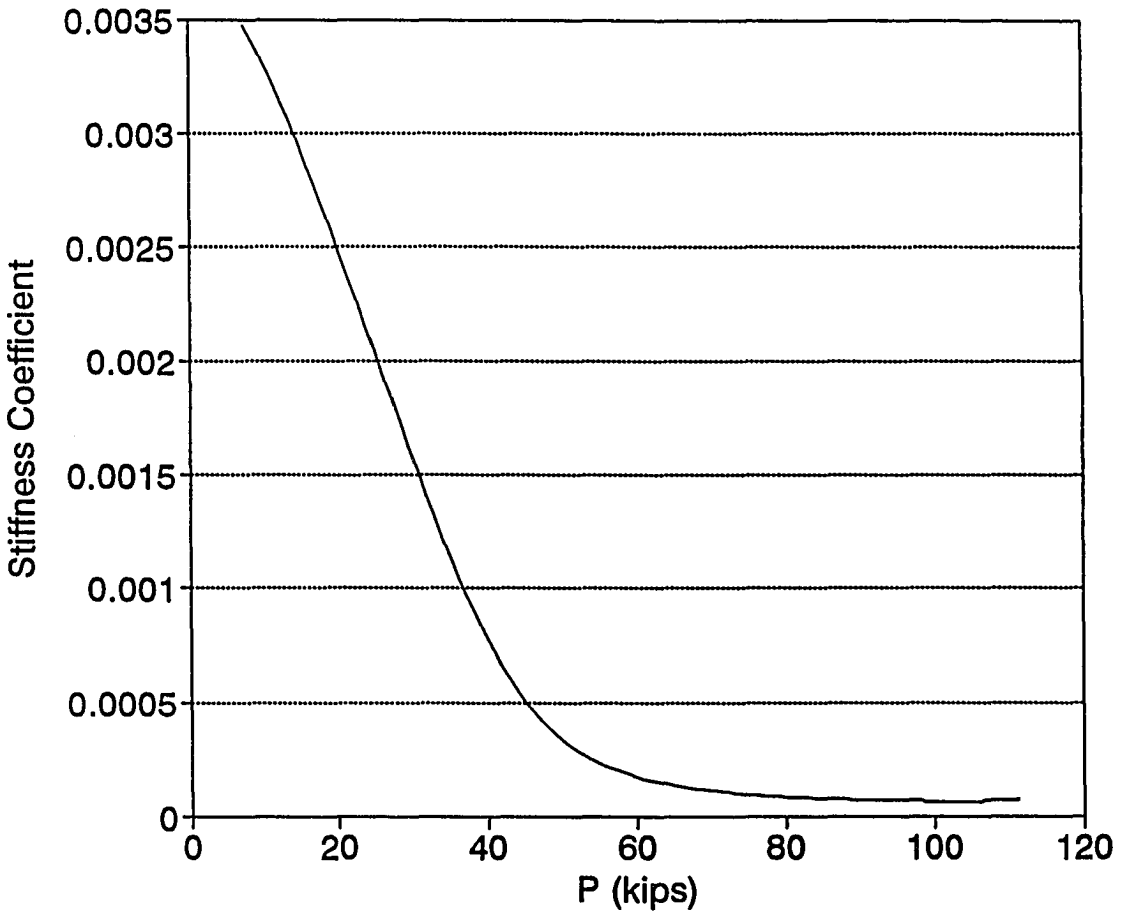

Figure 7.9, Load versus S^s_2 for Beam-Connection Element 1-1′, G = 1.0, L_2=L_1

One-story, Connection B

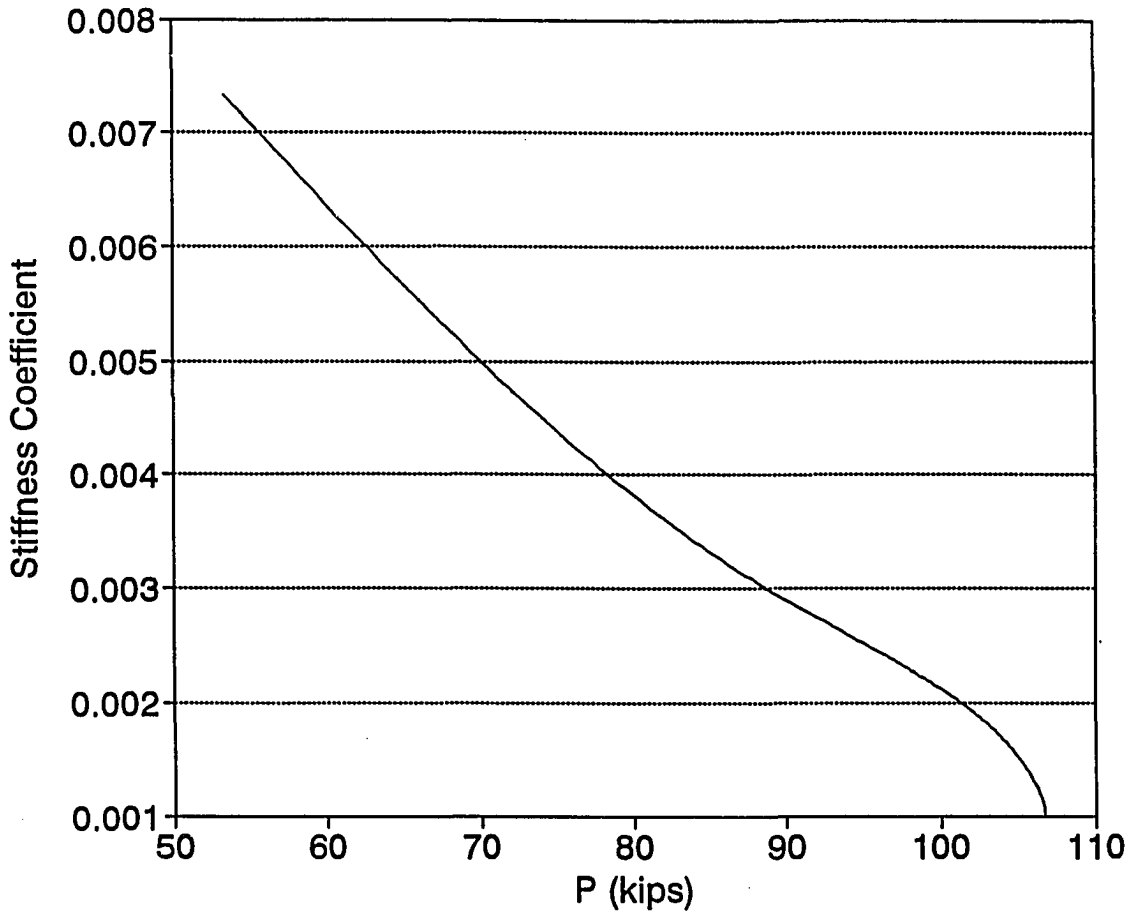

Figure 7.10, Load versus S^s_2 for Beam-Connection Element 1-1′, G = 1.0, L_2=L_1

One-story, Connection C

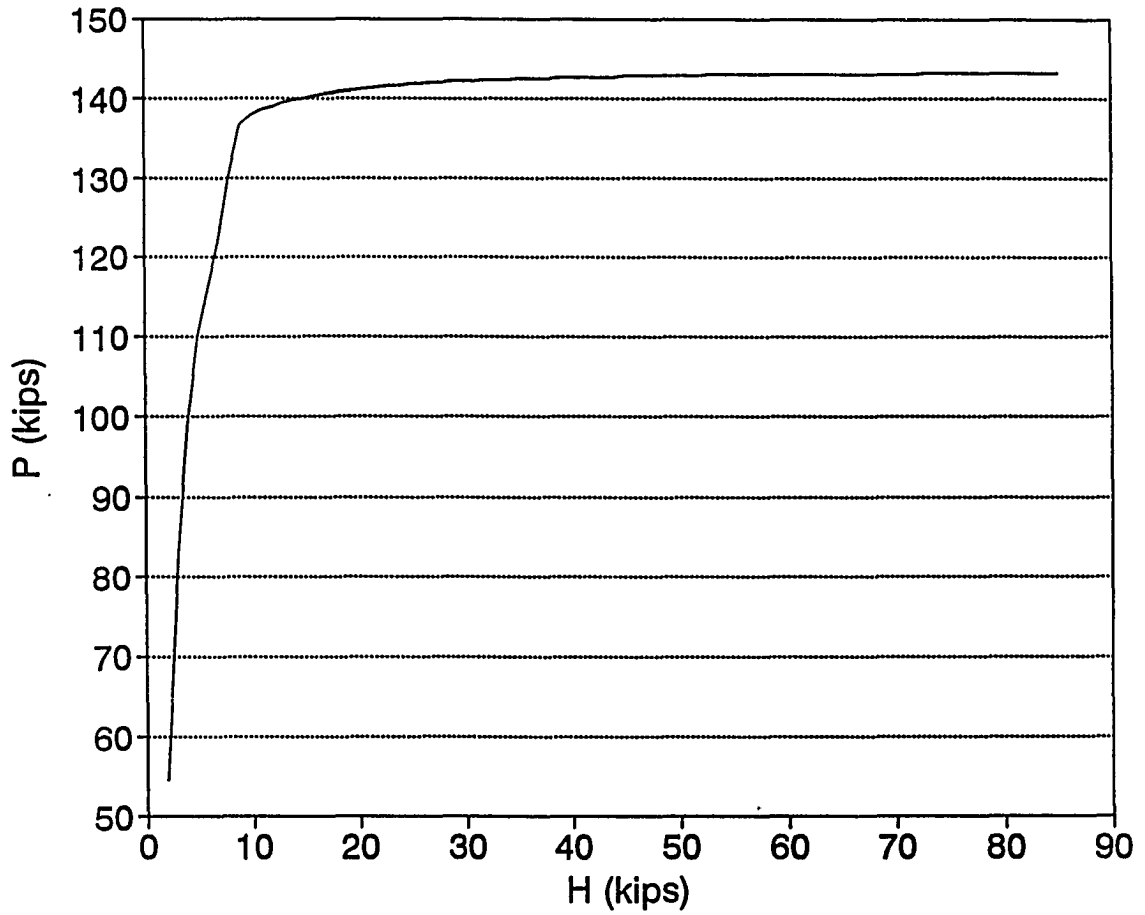

Figure 7.11, Load versus Horizontal Reaction, One-story , G=0.2, $L_2=L_1$

Connection A

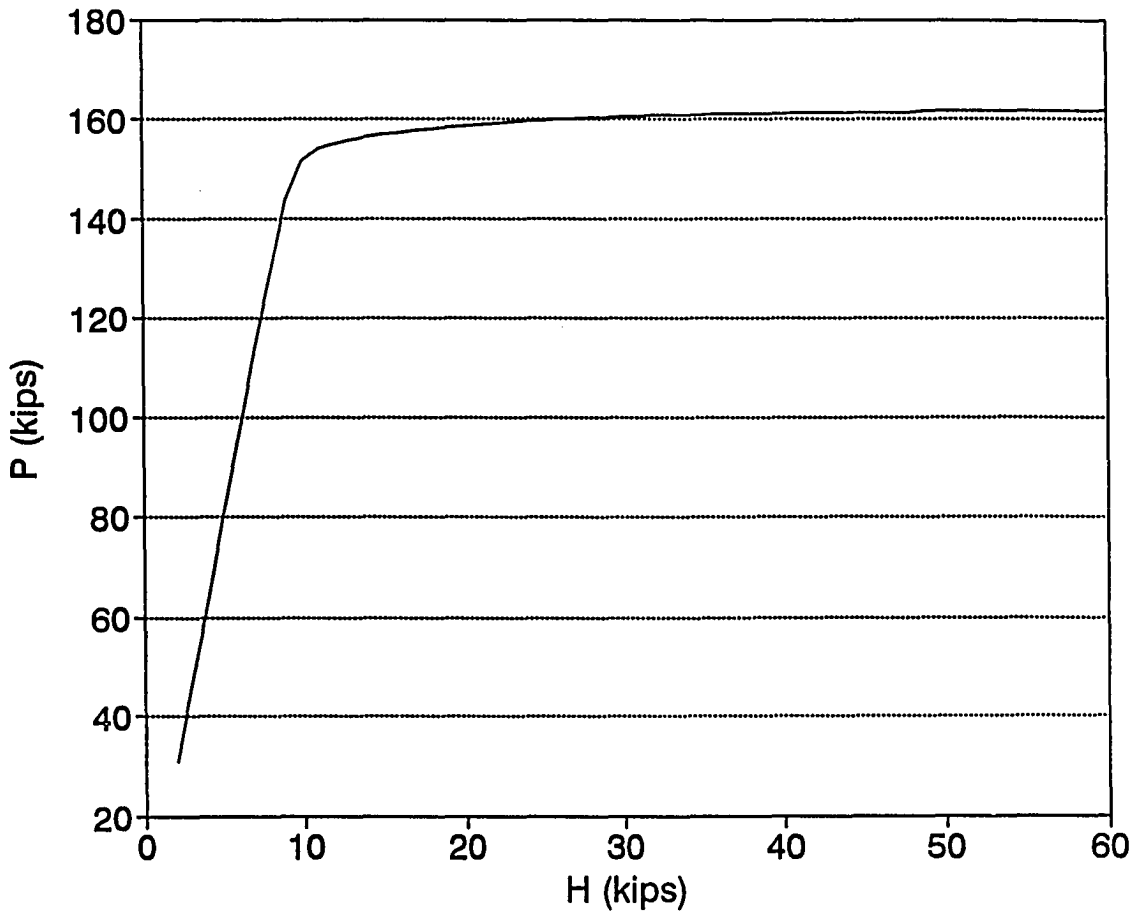

Figure 7.12, Load versus Horizontal Reaction, One-story, G=0.2, L_2=L_1

Connection B

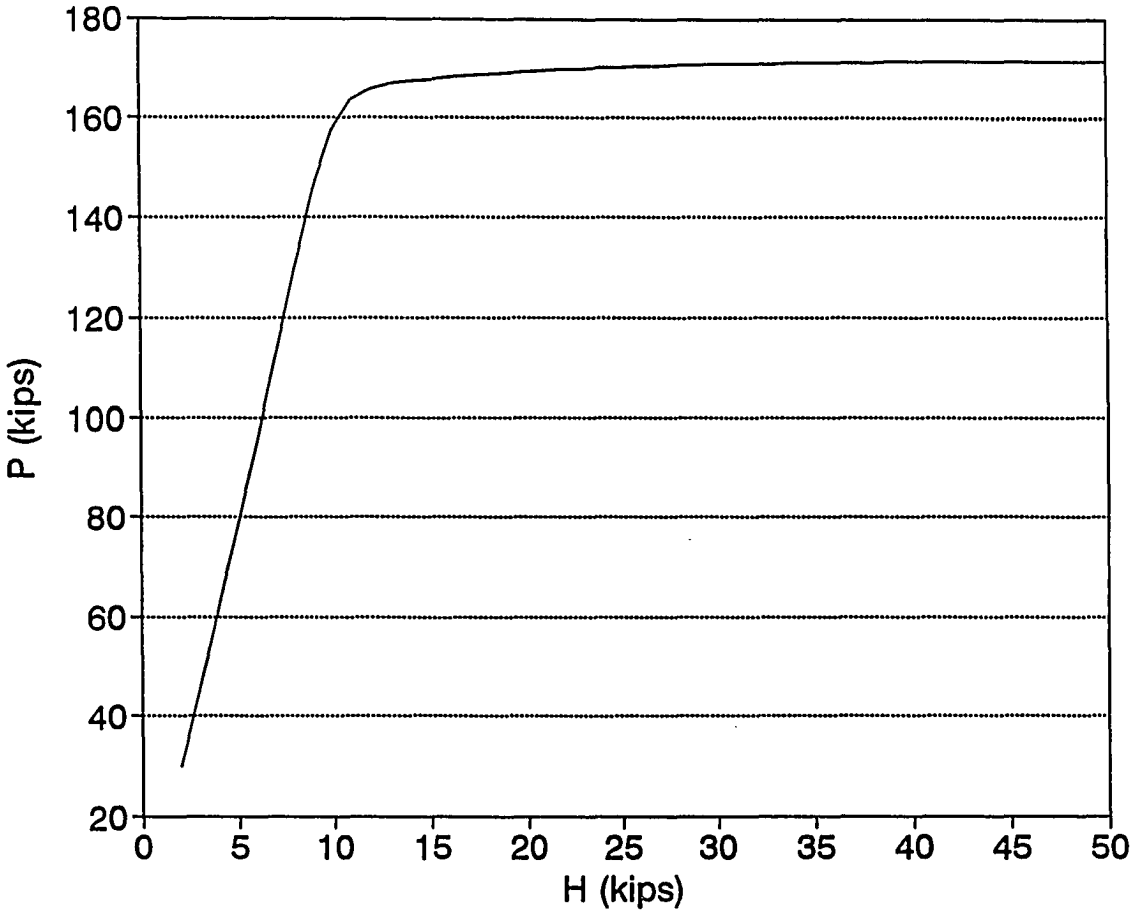

Figure 7.13, Load versus Horizontal Reaction, One-story , G=0.2, $L_2=L_1$

Connection C

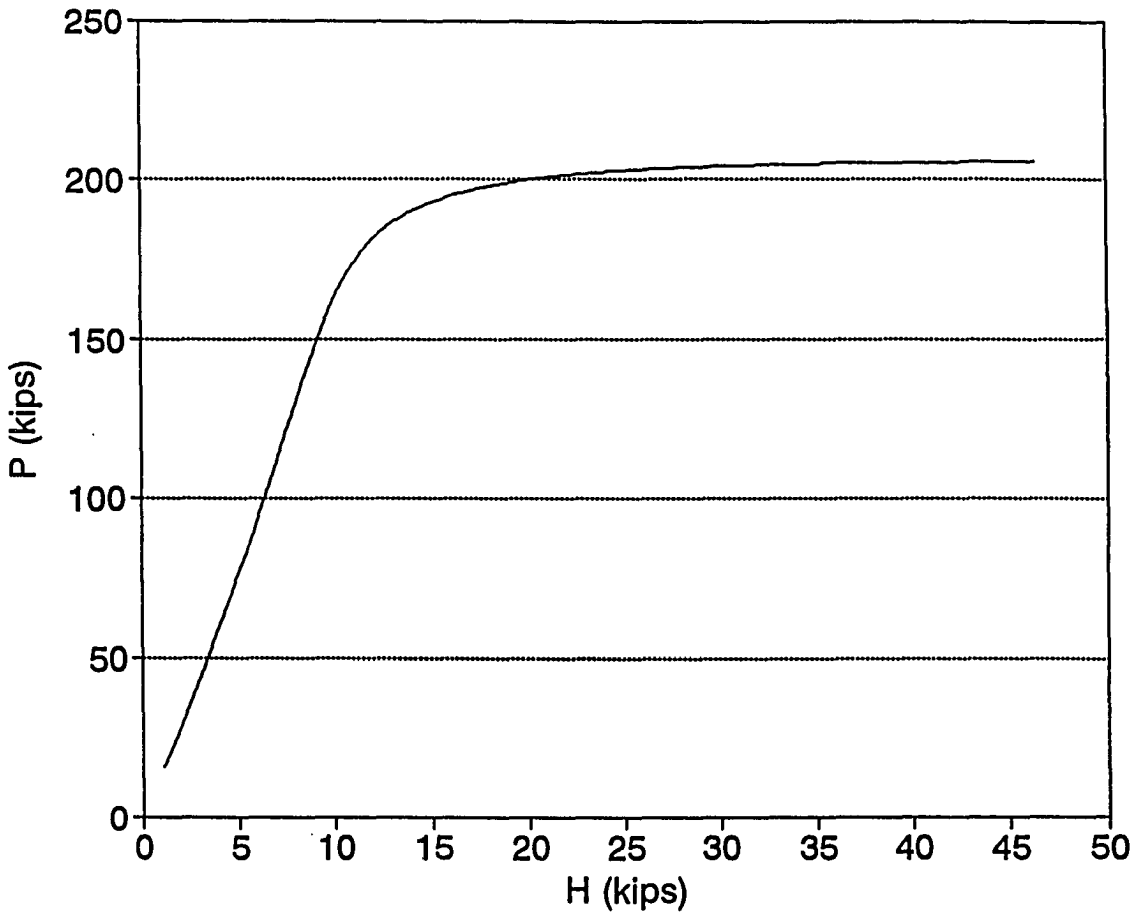

Figure 7.14, Load versus Horizontal Reaction, One-story , G=0.2, $L_2=L_1$

Rigid Connection

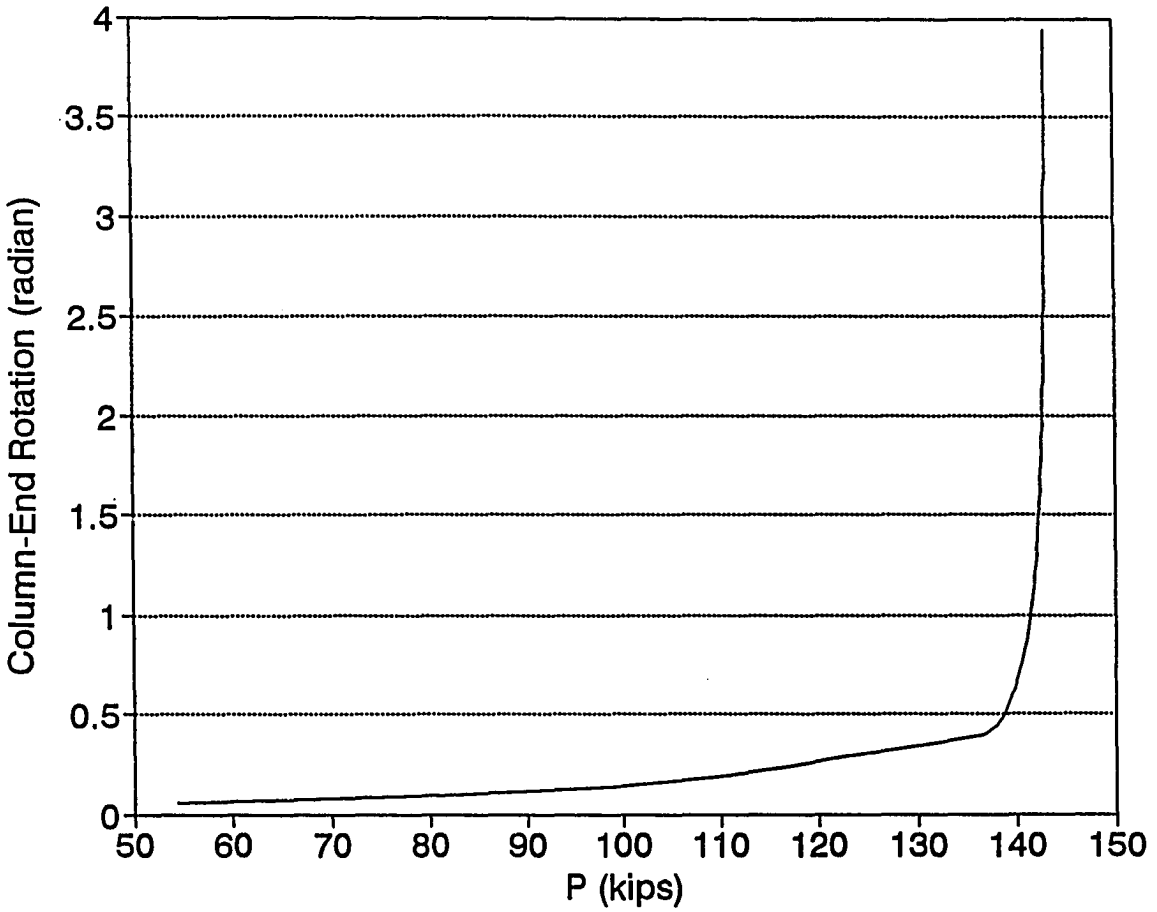

Figure 7.15, Load versus Column 0-1 Top-End Rotation, One-story, G=0.2, $L_2=L_1$

Connection A

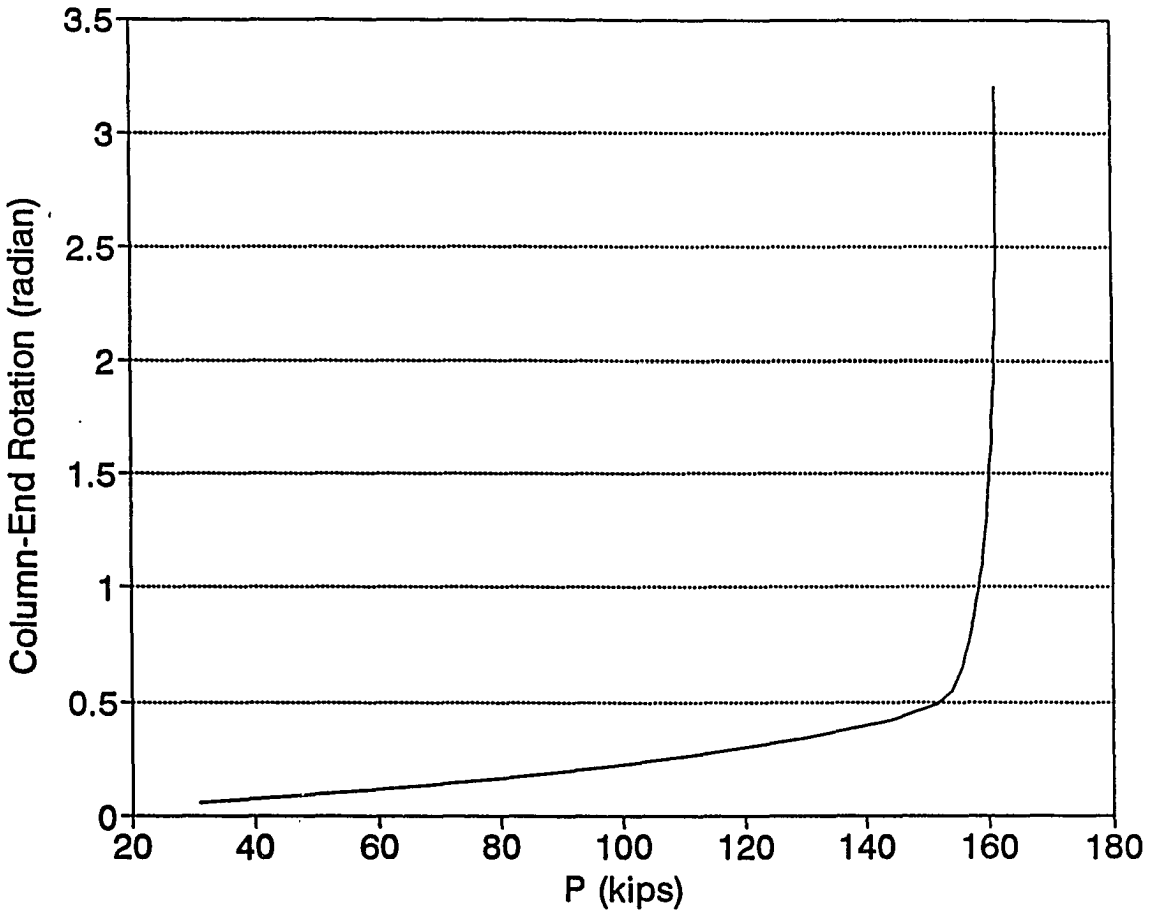

Figure 7.16, Load versus Column 0-1 Top-End Rotation, One-story, G=0.2, L_2=L_1

Connection B

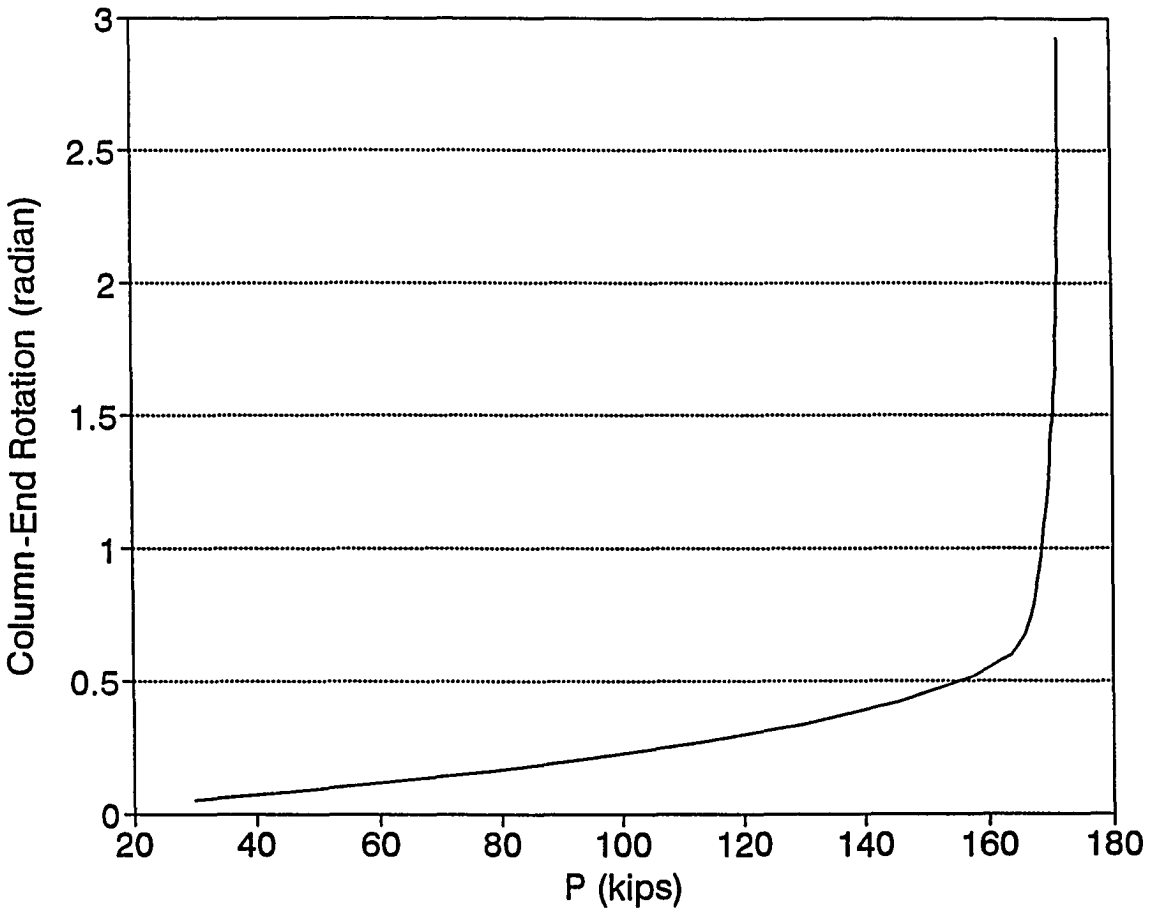

Figure 7.17, Load versus Column 0-1 Top-End Rotation, One-story, G=0.2, L_2=L_1

Connection C

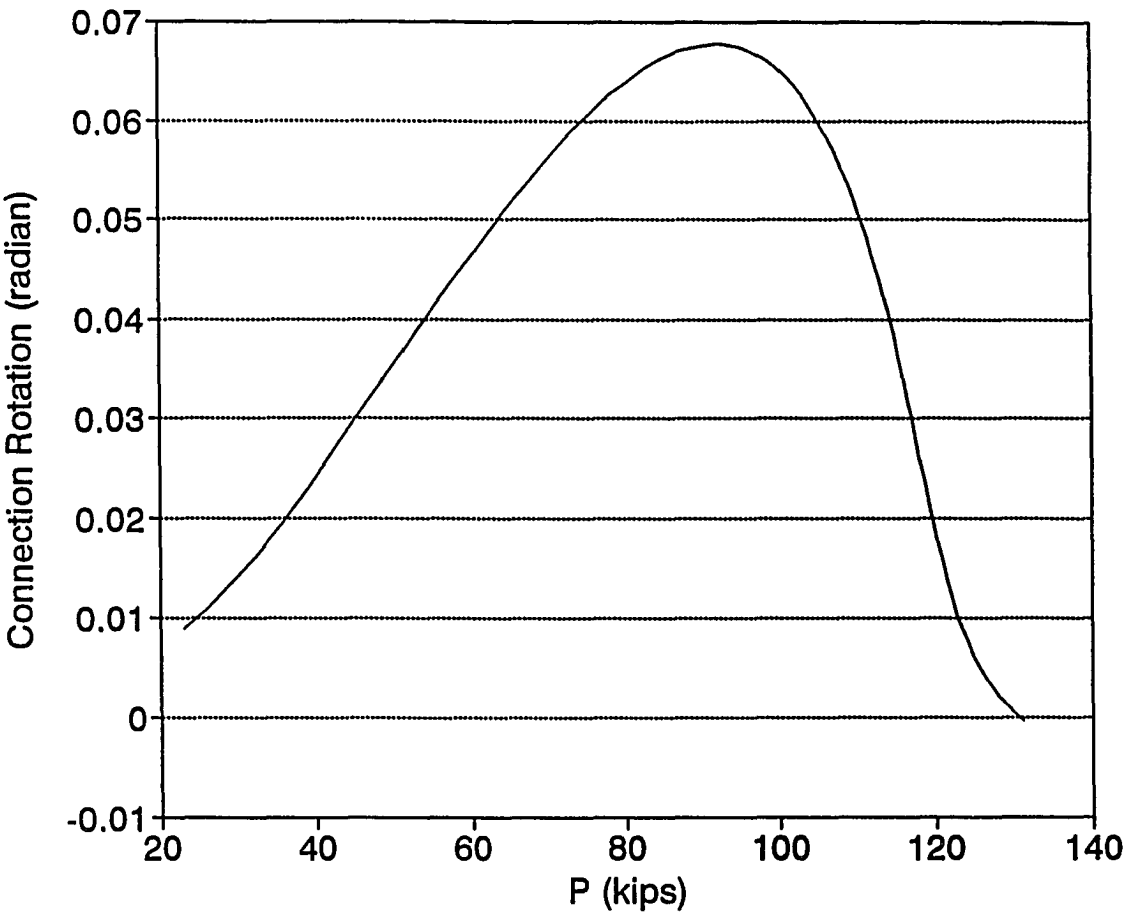

Figure 7.18, Load versus Connection Rotation, One-story, G=0.2, $L_2=L_1$

Connection A

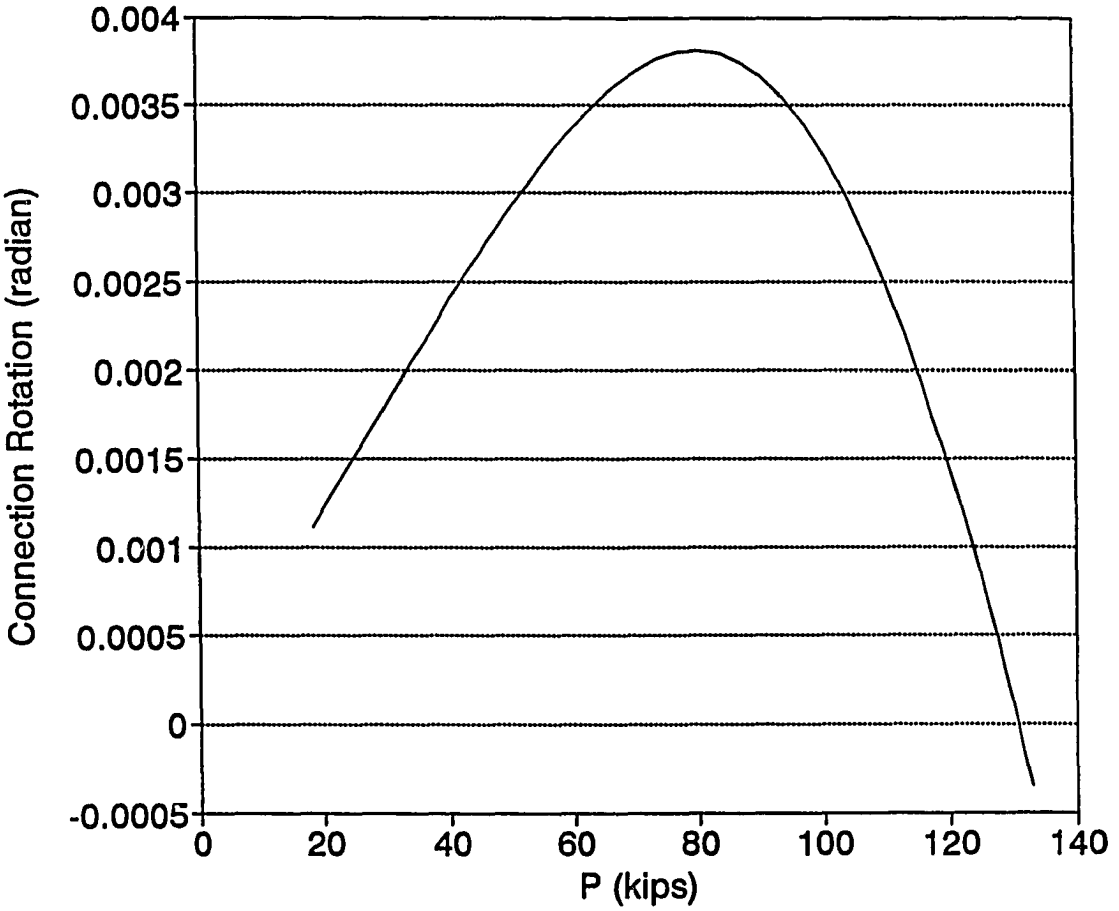

Figure 7.19, Load versus Connection Rotation, One-story, G=0.2, $L_2=L_1$

Connection B

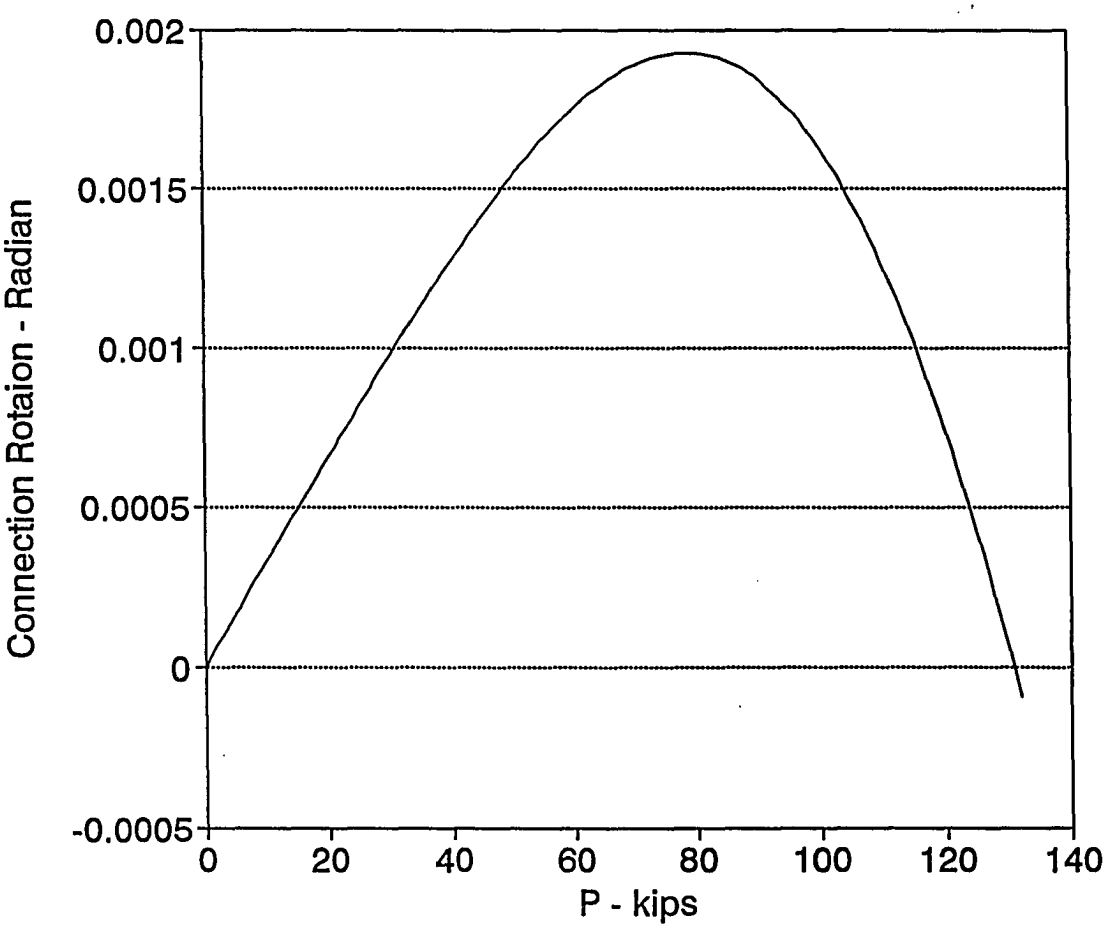

Figure 7.20, Load versus Connection Rotation, One-story, G=0.2, $L_2=L_1$

Connection C

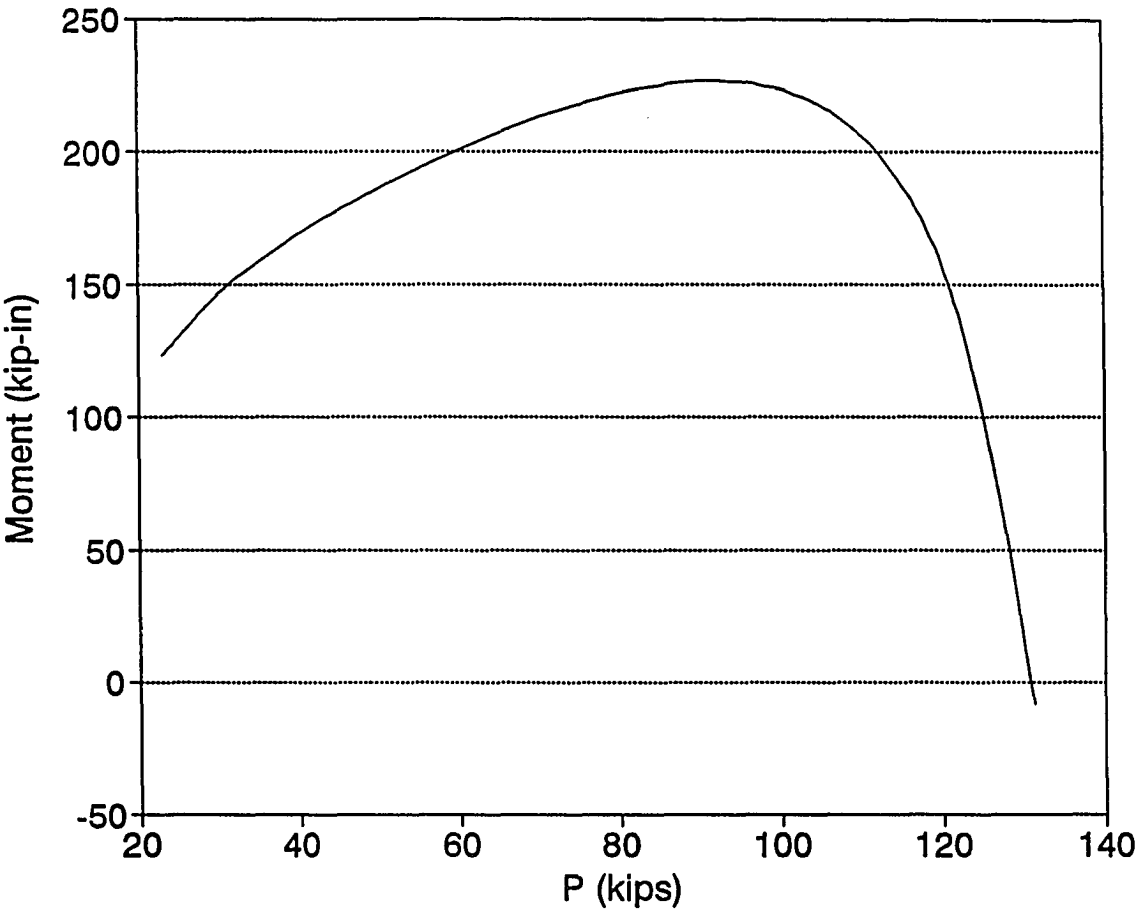

Figure 7.21, Load versus Moment on Connection, One-story, G=0.2, $L_2=L_1$

Connection A

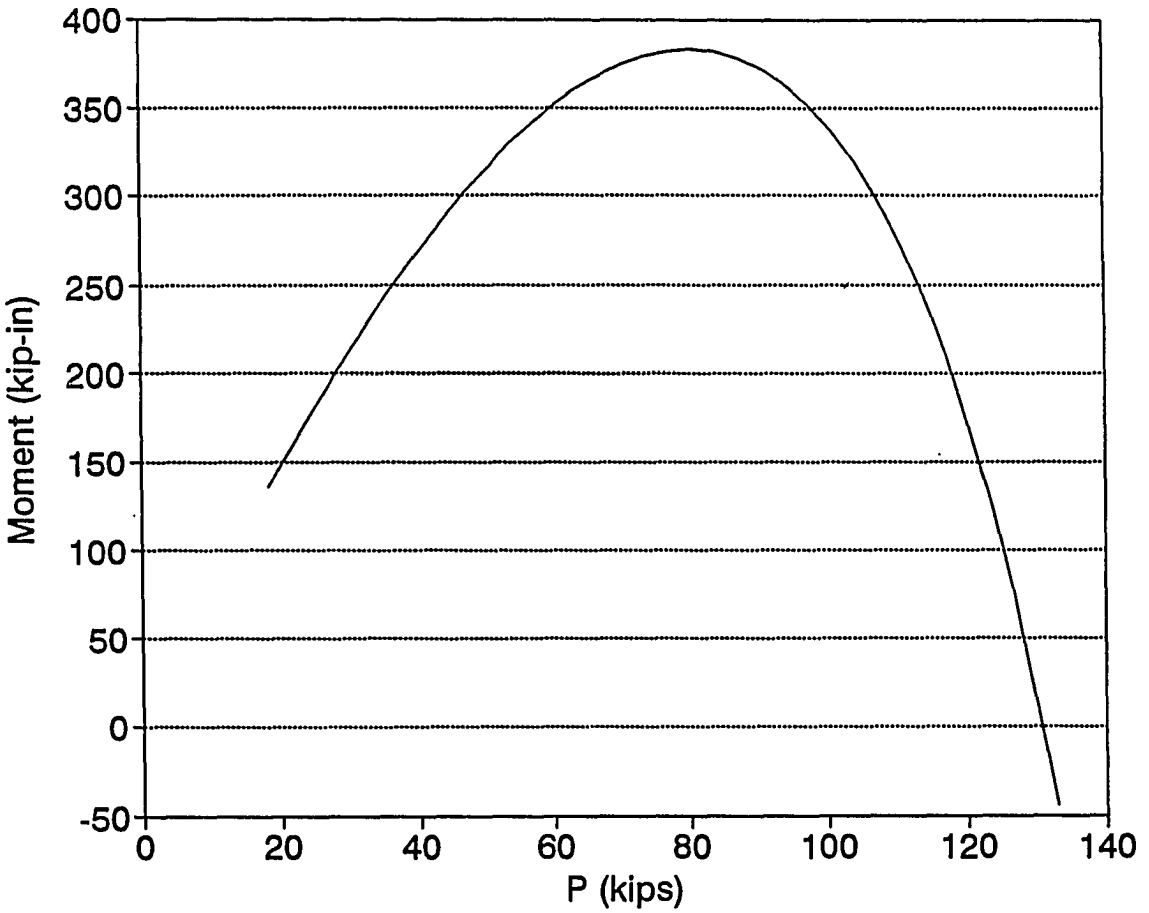

Figure 7.22, Load versus Moment on Connection, One-story, G=0.2, L_2=L_1

Connection B

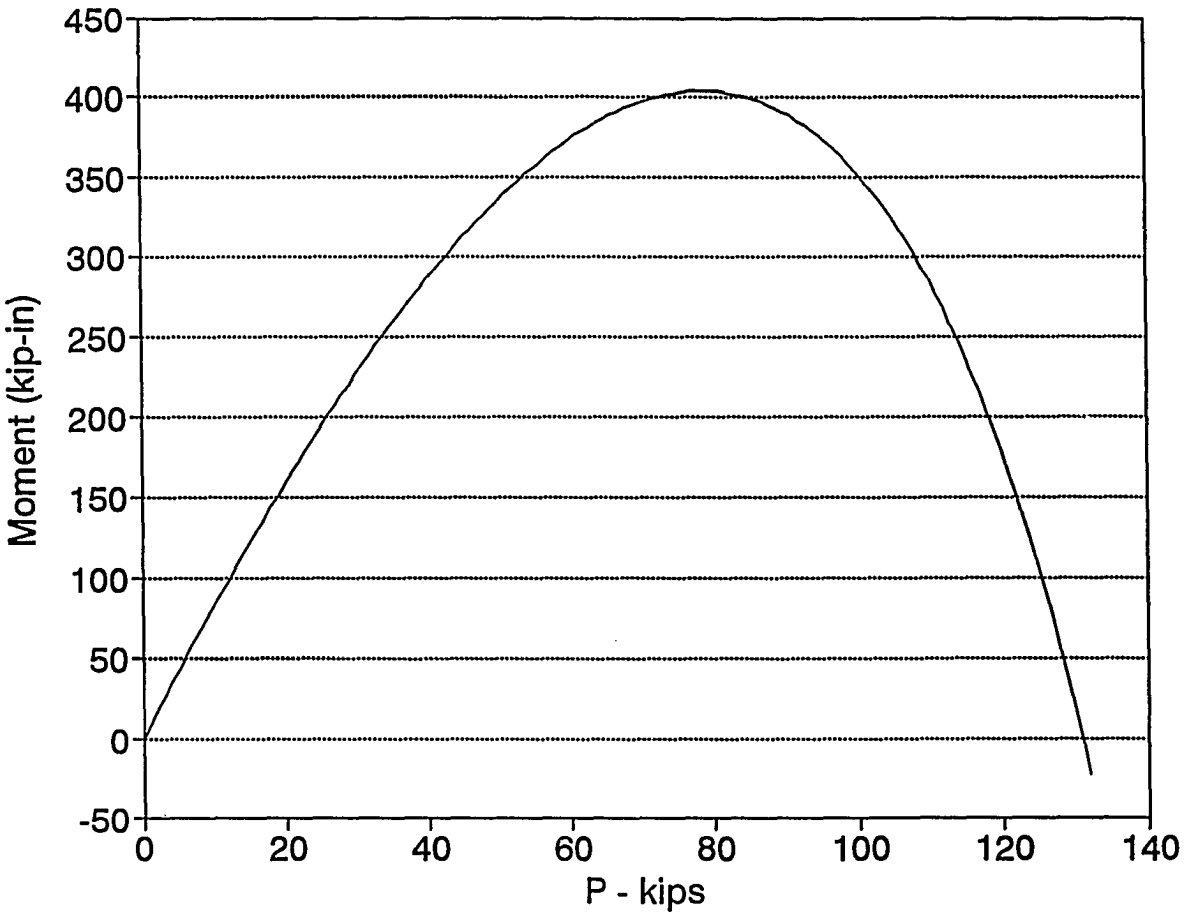

Figure 7.23, Load versus Moment on Connection, One-story, G=0.2, L_2=L_1

Connection C

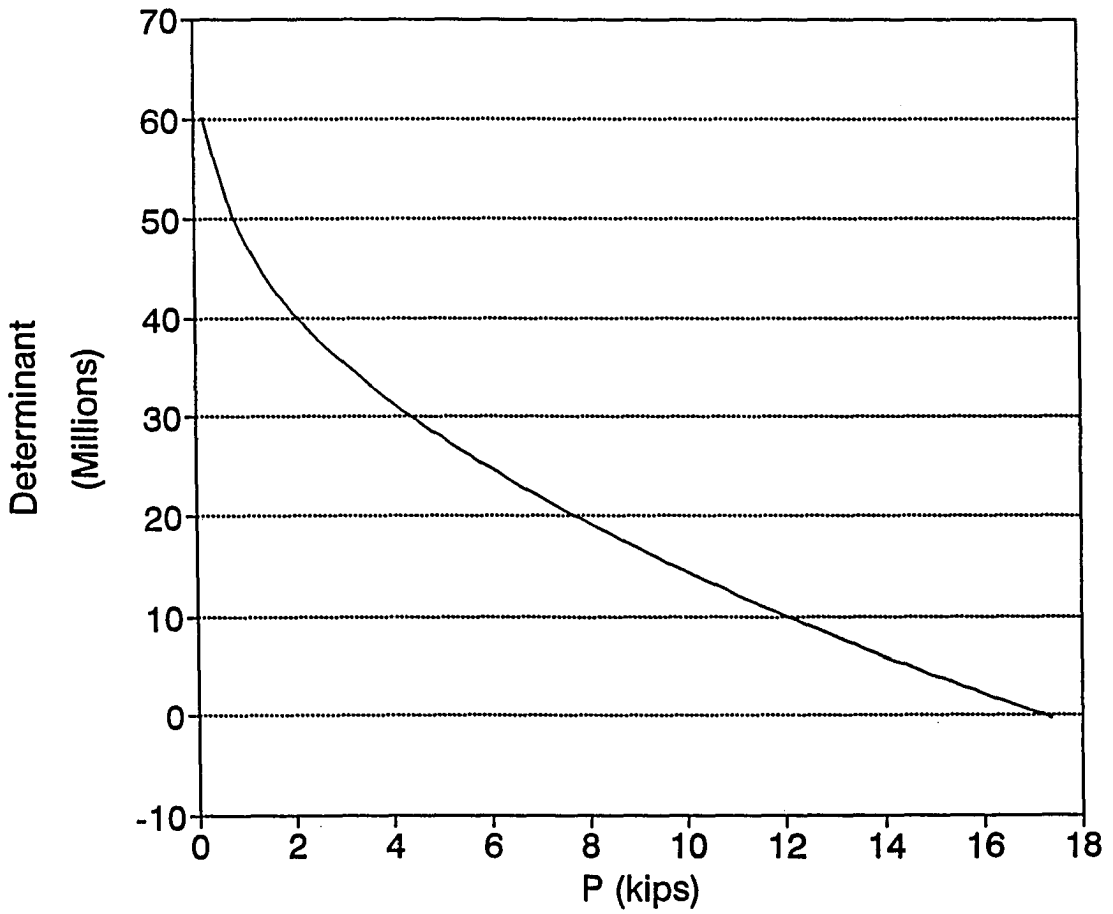

Figure 7.24, Load versus Determinant, One-story, G=1.0, $L_2=L_1$

Anti-symmetric Buckling, Connection B

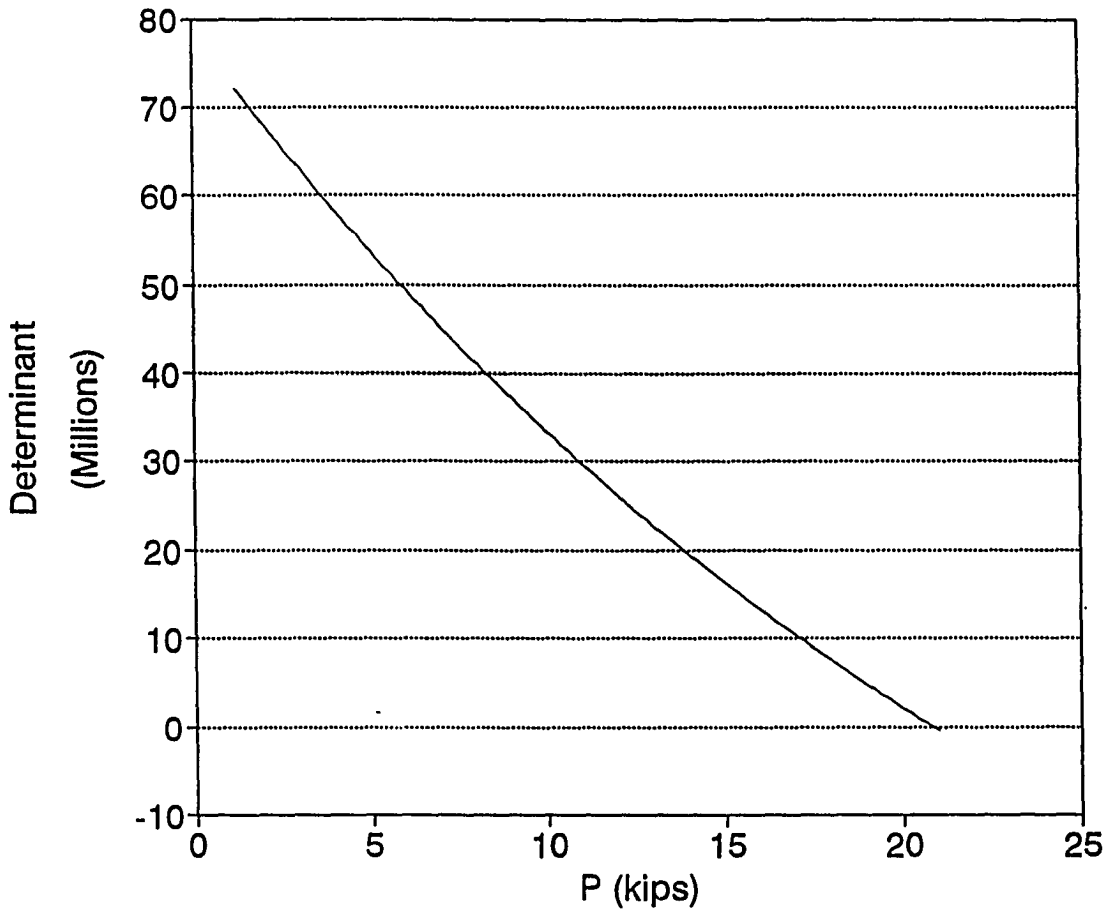

Figure 7.25, Load versus Determinant, One-story, G=1.0, L_2=L_1

Anti-symmetric Buckling, Connection C

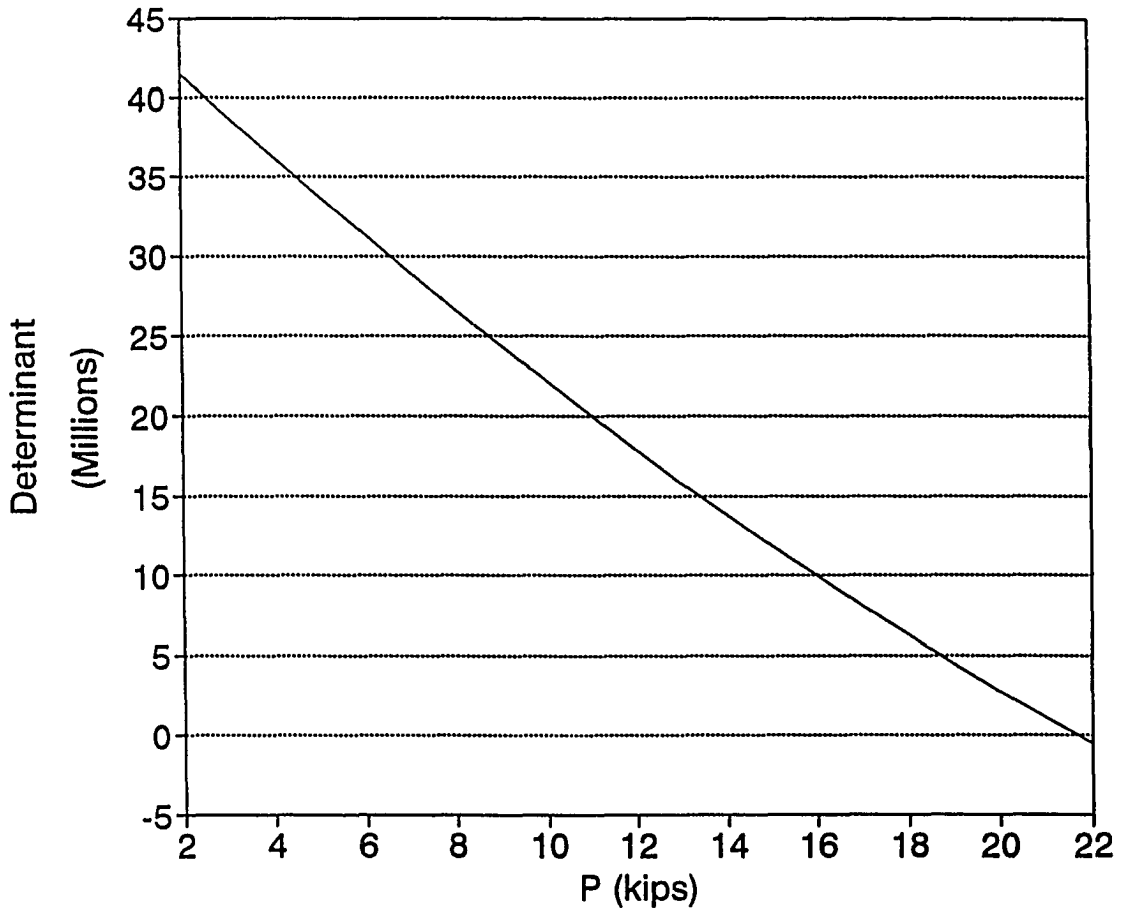

Figure 7.26, Load versus Determinant, One-story, G=0.5, $L_2=L_1$

Anti-symmetric Buckling, Connection C

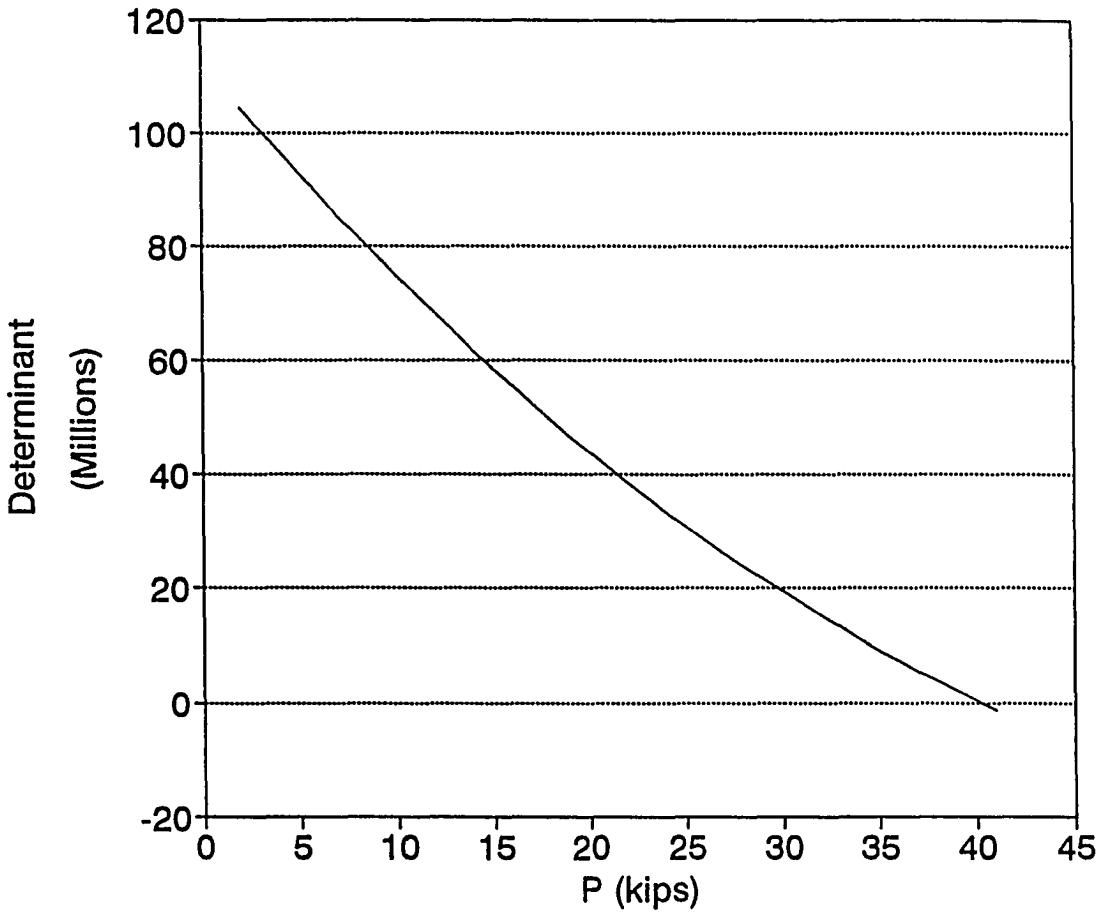

Figure 7.27, Load versus Determinant, One-story, G=0.5, L_2=L_1

Connection C, Anti-symmetric Buckling with Lateral Bracing, K_b/K_f = 1.0

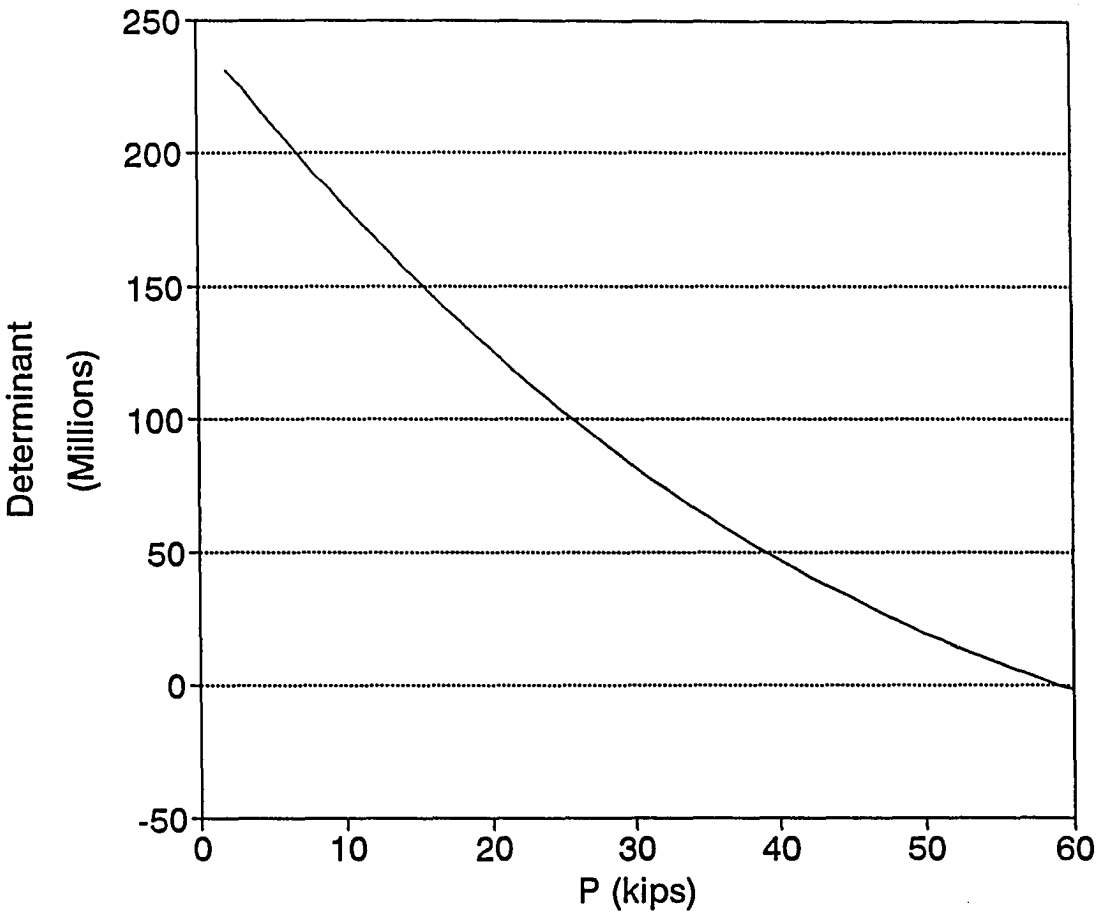

Figure 7.28, Load versus Determinant, One-story, G=0.5, L_2=L_1

Connection C, Anti-symmetric Buckling with Lateral Bracing, K_b/K_f = 3.0

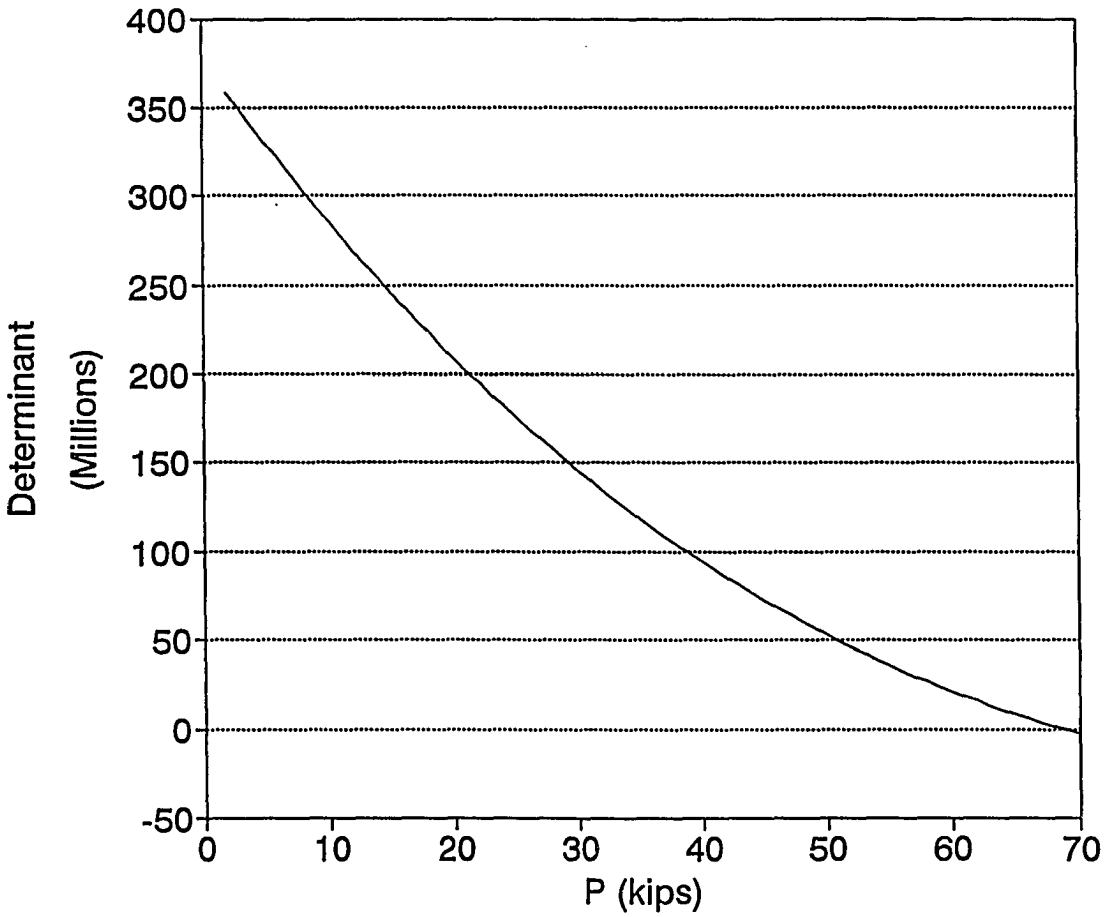

Figure 7.29, Load versus Determinant, One-story, G=0.5, L_2=L_1

Connection C, Anti-symmetric Buckling with Lateral Bracing, K_b/K_f = 5.0

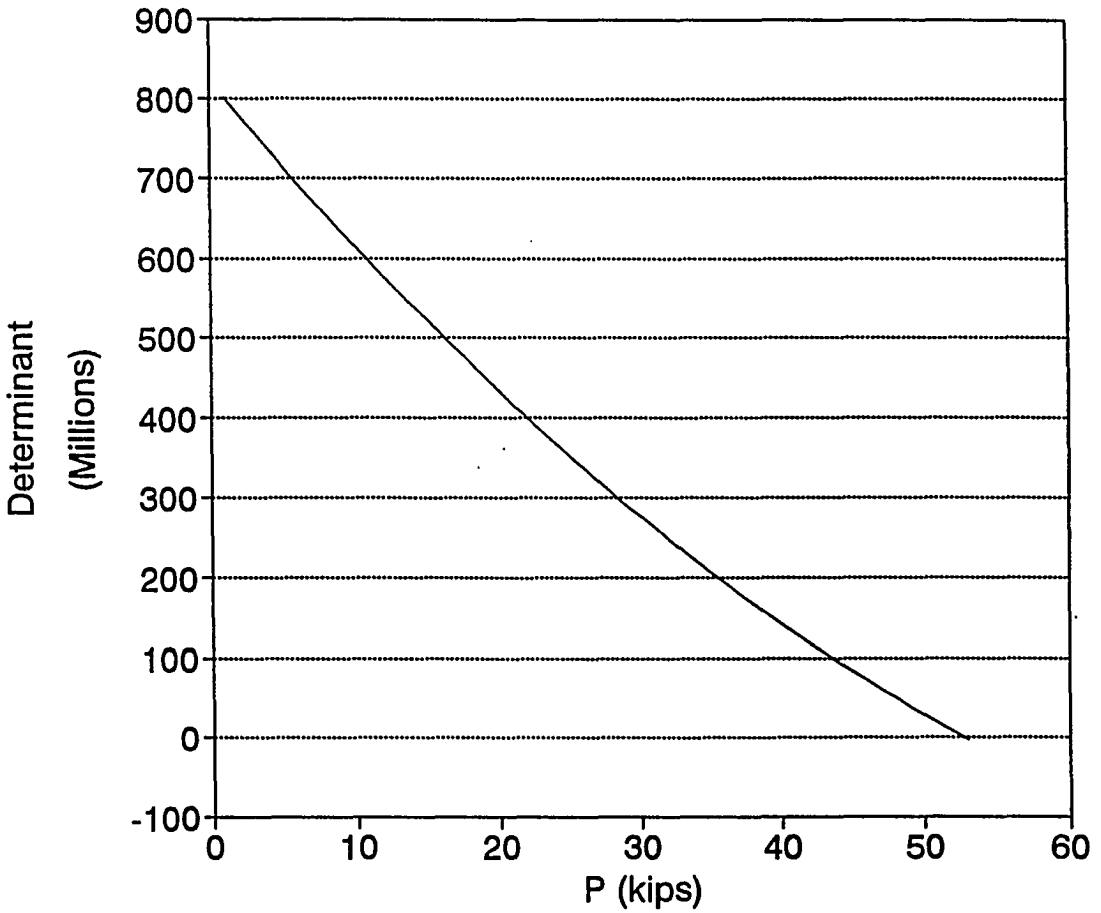

Figure 7.30, Load versus Determinant, One-story, G=0.5, $L_2=L_1$

Anti-symmetric Buckling, Rigid Connection

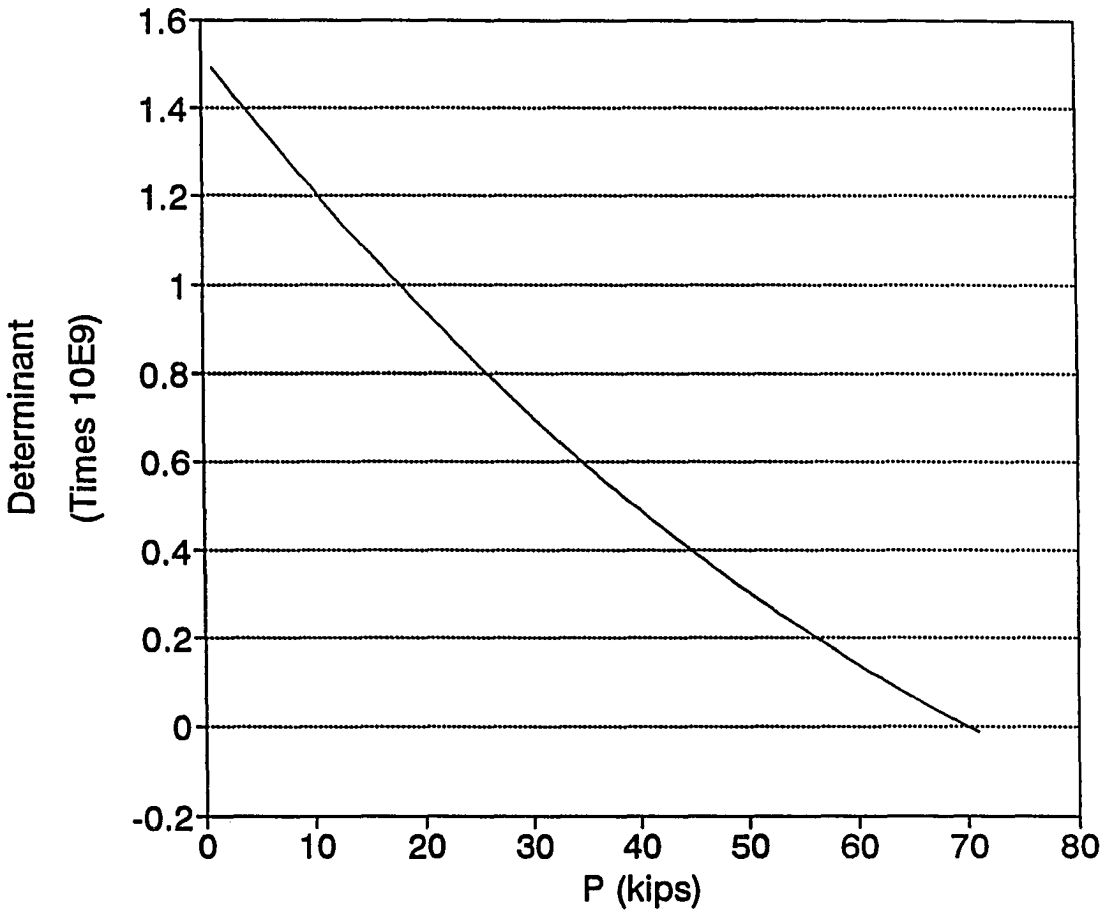

Figure 7.31, Load versus Determinant, One-story, G=0.5, $L_2=L_1$

Rigid Connection, Anti-symmetric Buckling with Lateral Bracing, $K_b/K_f = 1.0$

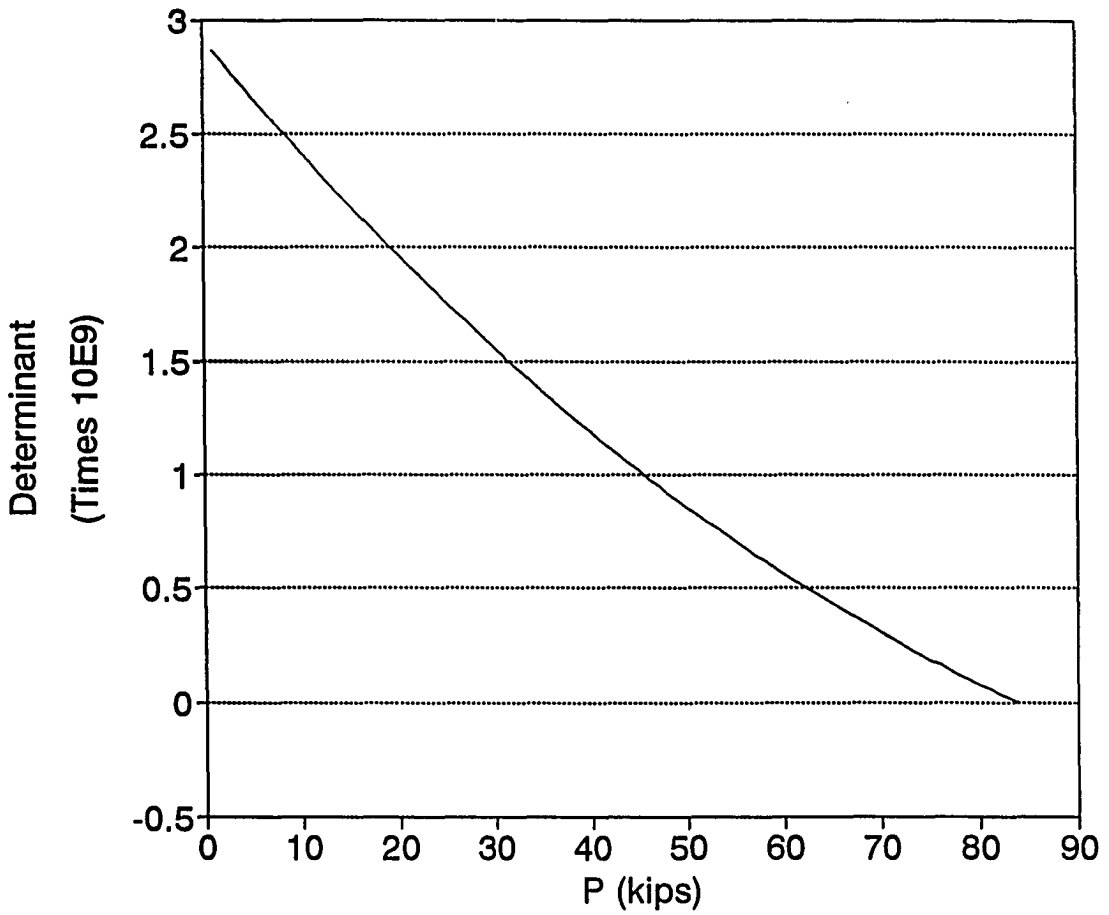

Figure 7.32, Load versus Determinant, One-story, G=0.5, L_2=L_1

Rigid Connection, Anti-symmetric Buckling with Lateral Bracing, K_b/K_f = 3.0

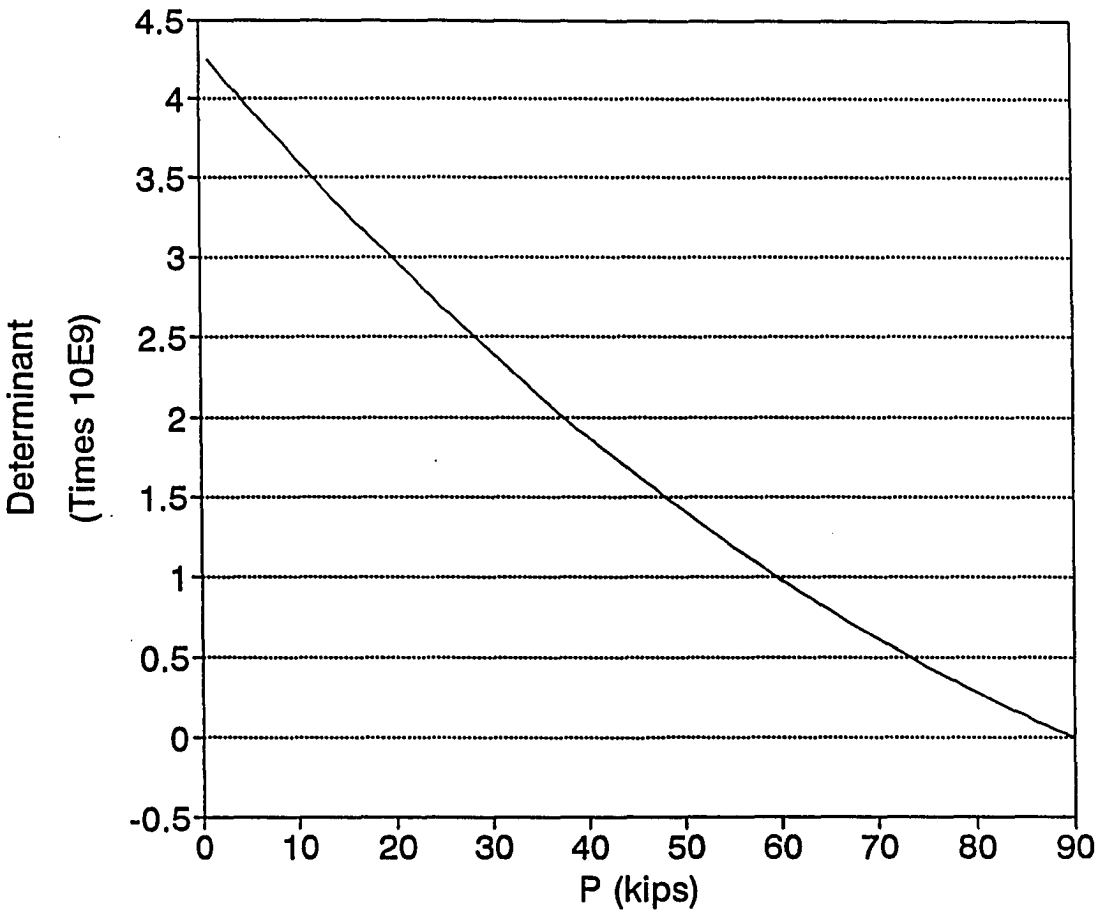

Figure 7.33, Load versus Determinant, One-story, G=0.5, L_2=L_1

Rigid Connection, Anti-symmetric Buckling with Lateral Bracing, K_b/K_f = 5.0

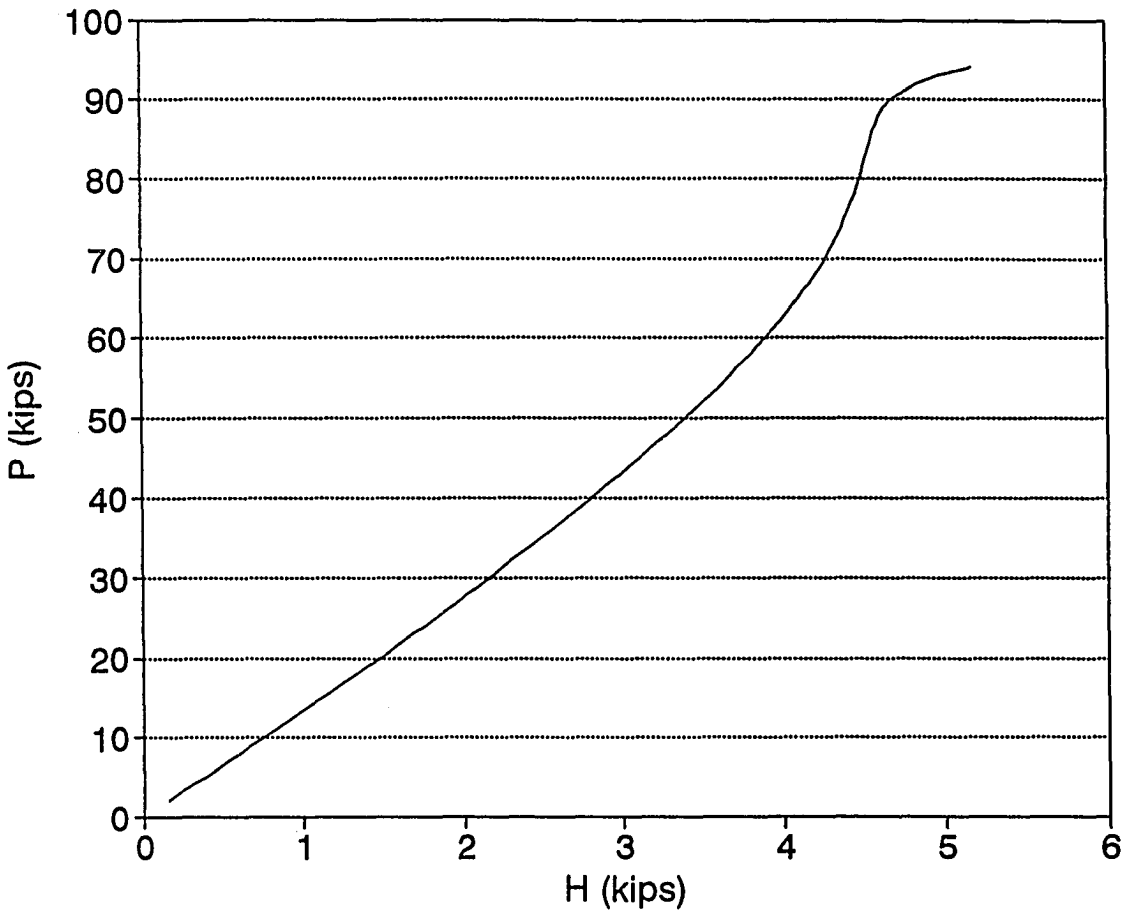

Figure 7.34, Load versus Base Horizontal Reaction, Two-story, G=0.1, $L_2=L_1$

Connection C

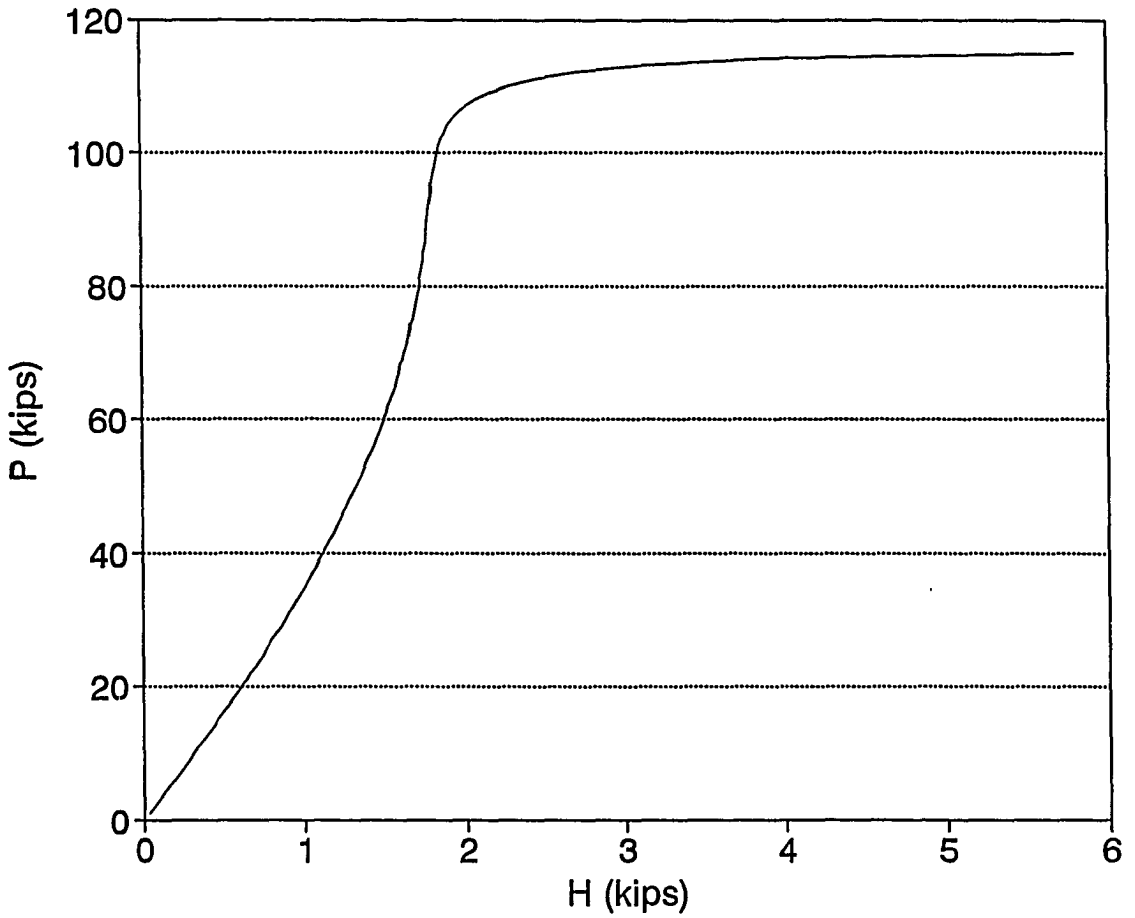

Figure 7.35, Load versus Base Horizontal Reaction, Two-story, G=0.1, $L_2=L_1$

Rigid Connection

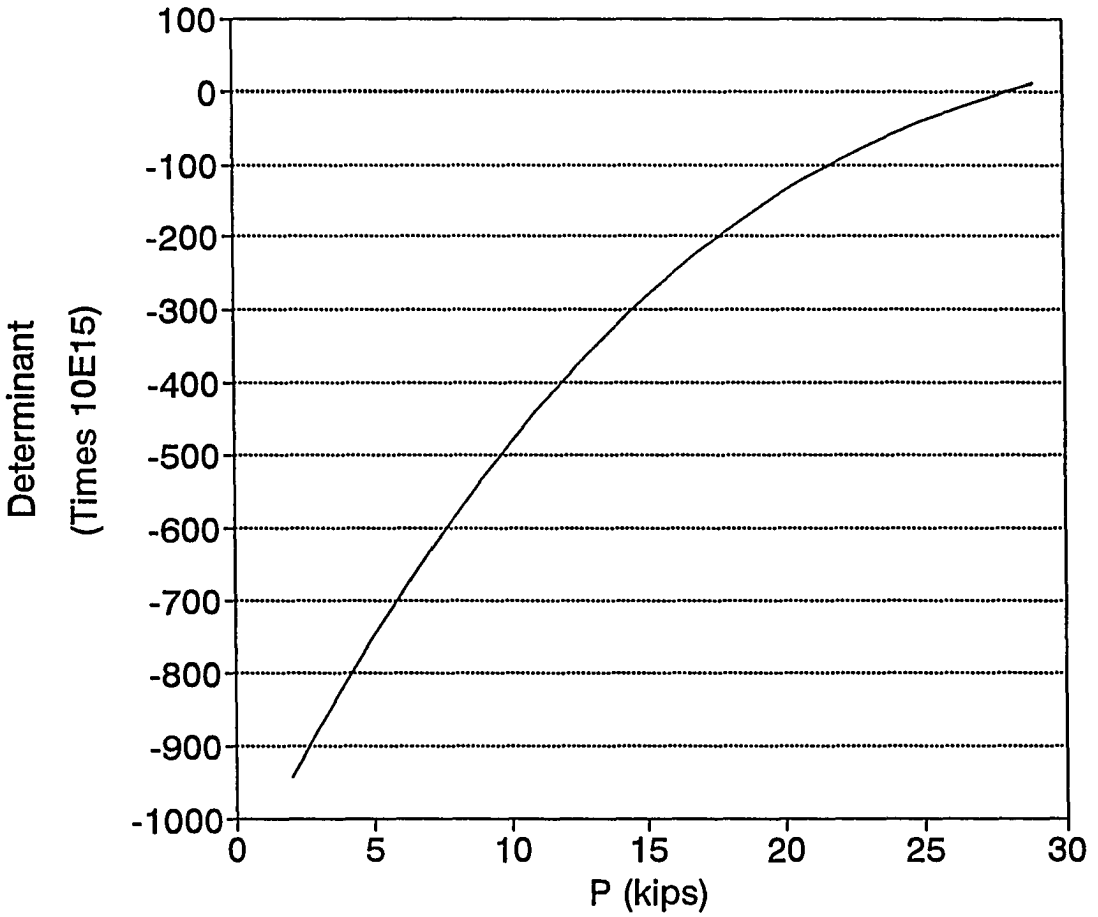

Figure 7.36, Load versus Determinant, Two-story, G=0.1, $L_2=L_1$

Anti-symmetric Buckling, Connection C

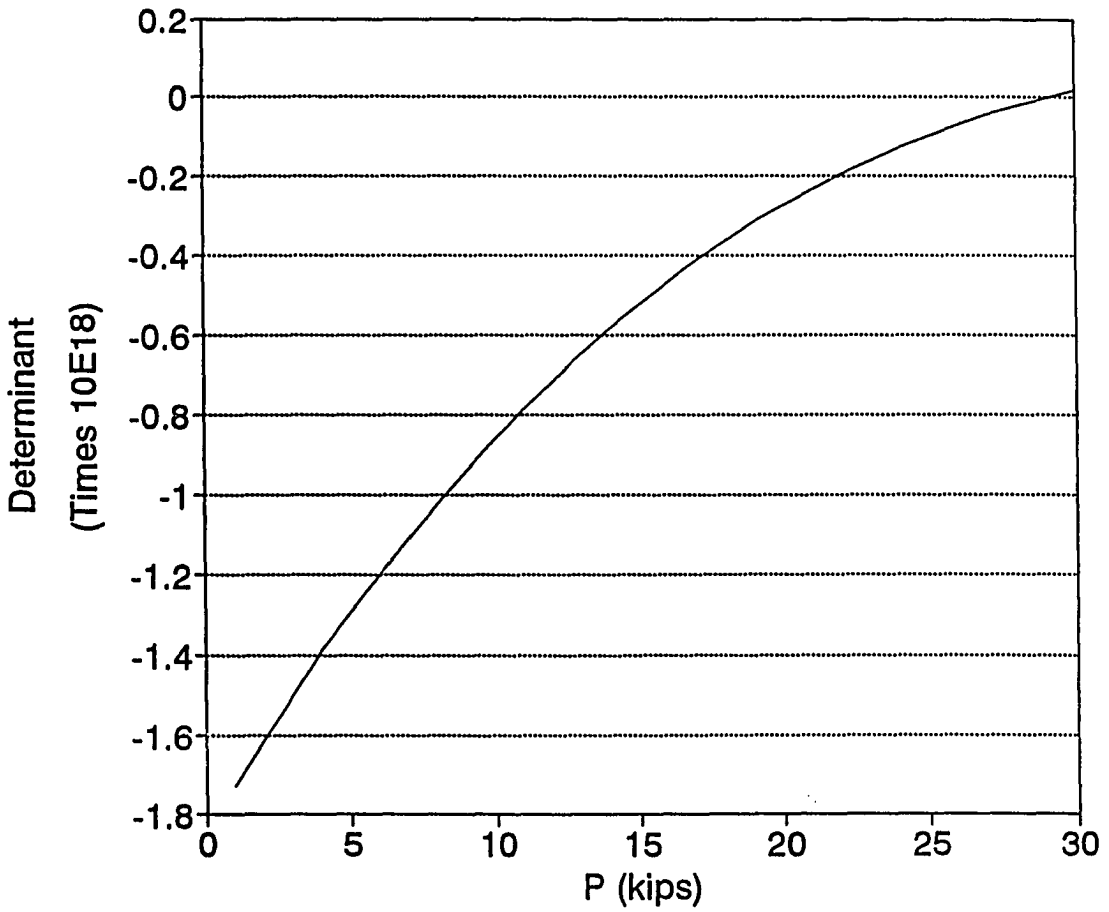

Figure 7.37, Load versus Determinant, One-story, G=0.1, $L_2=L_1$

Anti-symmetric Buckling, Rigid Connection

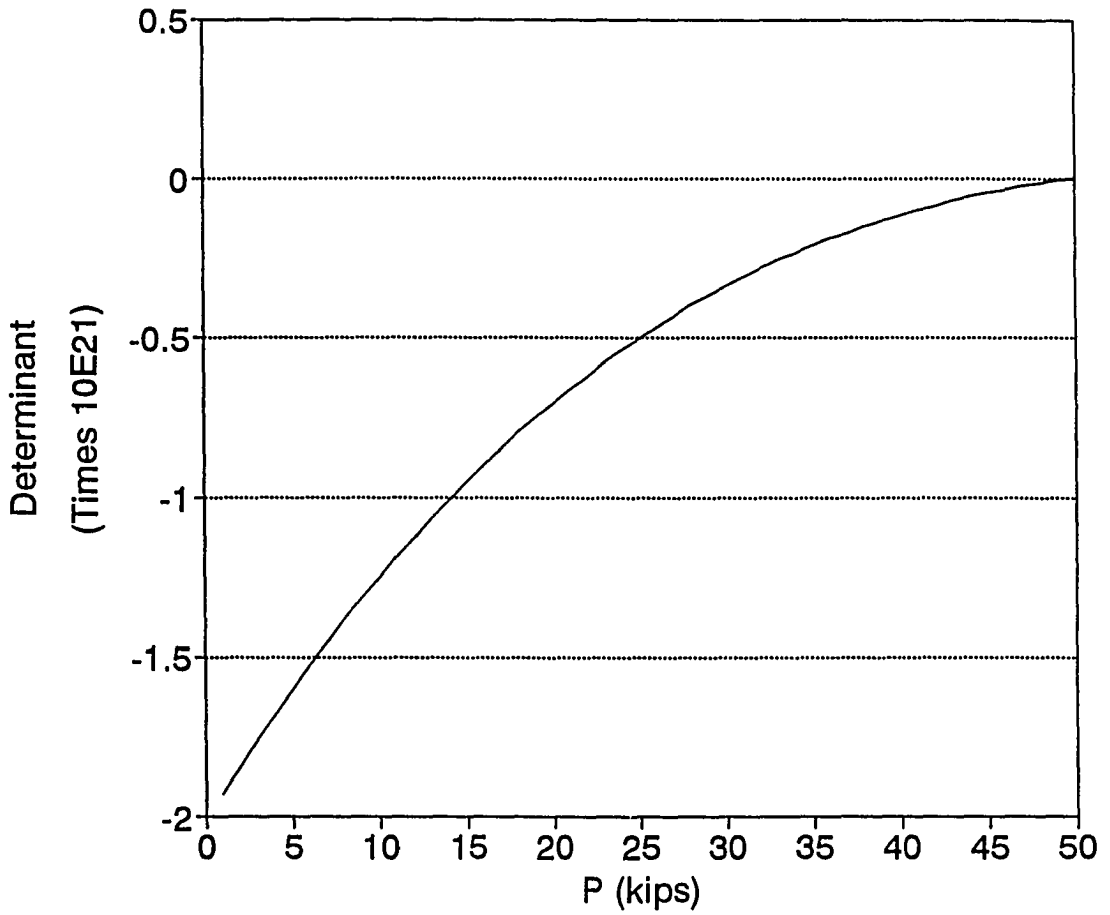

Figure 7.38, Load versus Determinant, Two-story, G=0.1, $L_2=L_1$

Rigid Connection, Anti-symmetric Buckling with Lateral Bracing, $A_b=1.0$ in^2

CHAPTER 8

CONCLUSION

The concern among some engineers that an increase in connection stiffness may impair the stability of framed structures is investigated in this study. It is pointed out that when primary bending moments are not considered in the analysis, the increase of connection stiffness enhances the stability of frames. This conclusion is supported by several studies. Some of these studies are cited in Chapter 2. The above concern becomes valid only when primary moment is contemplated in the buckling load analysis of frames. However, the conclusion of this study is that the critical buckling load increases with the stiffness of the connection. The critical buckling load does not increase with connection stiffness when the ratio of beam-to-column stiffness equals 1 or less. The connection behavior is considered to be non-linear. Chapter 2 gives a summary on modeling flexible connections. The Richard model is selected in this study to represent the connection behavior in the buckling load analysis of frames. The non-linear behavior was accounted for by using the Richard equation to find the slip angle of the flexible connection for a given state of load, known bending moment on the joint. The analysis was performed for one-story frames and for two-story frames. The method of the slope-deflection equations constitutes the basis for the analysis. The resulting non-linear set of equations is solved by implementing the Newton iterative procedure.

The topics in this study are divided into five major parts: (1) parameters involving the analysis for frame stability, (2) symmetrical mode of buckling, (3) anti-symmetrical

mode of buckling, (4) effect of lateral bracing, (5) numerical application for the critical analysis of frames using the developed Fortran program.

The first topic is accomplished in Chapter 3 in which all parameters entering the slope deflection equations are defined and modified to account for the introduction of flexible connections in the analysis. The second topic is achieved in Chapter 4, the third in Chapter 5, and the fourth in Chapter 6. The analyses in all of these chapters are furnished for one-story frames and two-story frames having either rigid beam-to-column connections or flexible ones. The last topic is completed in Chapter 7, in which a numerical analysis of frames with different connections' stiffness, diverse beam-to-column stiffness, and various frame-to-brace stiffness are provided. The connection and column behaviors are assumed to be elastic over the entire range of loading.

Some of the conclusions that can be made are:

1. For the loading and structures considered in the analysis, stronger and stiffer beam-to-column connections enhance the stability of frames.
2. Critical buckling load increases with the stiffness of the connection except when the beams are very flexible with regard to the columns.
3. The reduction in the stiffness of a member because of considering the effect of axial force in the buckling load analysis is significant. In other words, the buckling load is reduced when the effect of axial compressive force is accounted for in the buckling load analysis.
4. Frames that have no lateral bracing, in general, buckle in anti-symmetrical mode.
5. For certain values of the brace-to-frame stiffness, the frame buckles only in

symmetrical mode; increasing the stiffness of the lateral brace over this value has no effect on frame stability.

6. The above observations apply to one-story and two-story frames.

Some suggestions for future research include:

1. The effect of inelastic behavior of the connections with unloading and reloading the joints on the buckling load.

2. The effect of dynamic loading on stability of frames having flexible beam-to-column connections.

3. Considering the effect of inelastic behavior of the column on the buckling load analysis.

NOMENCLATURE

A	Cross-Sectional Area
C	Stiffness Coefficient for Member's Near-End
E	Young's Modulus
E_t	Inelastic Modulus of Elasticity
[F]	Flexibility Matrix
f	Flexibility Coefficient
F	Force
G	Ratio of Column-to-Beam Rigidity
H	Horizontal Force
I	Moment of Inertia
K	Flexural Stiffness K = EI/L
k	Effective Length Ratio
L	Member Length
M	Bending Moment
P	Axial Force
ΔR_1	Sidesway of First Story
ΔR_2	Sidesway of Second Story
[S]	Stiffness Matrix
S	Stiffness Coefficient for Member's Far-End
V	Vertical Reaction
W	Load per Linear ft.

α	Lateral Brace Angle with the Horizontal
η	Moment Factor
θ	Total Joint Rotation
λ	End-Rotation of Simply Supported Member
μ	Stability Angle , $\mu = L(P/EI)^{1/2}$
ρ	Chord Rotation
ϕ	Joint Rotation
ψ	Slip Angle of Flexible Connection

Superscripts

s	Semi-Rigid

Subscripts

1, 3	Column 1, 3
2, 4	Beam 2, 4
b	Brace
i-j	Member i-j
i, j	End i, j
f	Frame
f1	Fixed at End 1
f2	Fixed at End 2

REFERENCES

Ackroyed, M.H. and Gerstle, K.H., " Elastic Stability of Flexibly Connected Frames," Journal of Structural Engineering, 109, No. 1, Jan.,1983.

Alkhatib, A.M., " Effect of Semi-Rigid Connections, Tension Members and Yielded Columns on Frame Stability," Advanced independent study report submitted in partial fulfillment for the degree of Master of Science, University of Wisconsin-Madison, May, 1987.

Bergquist, D.J., " Test on Columns Restrained by Beams with Simple Connections," Department of Civil Engineering, University of Texas at Austin, Jan. 1977.

Bleich, F., " Buckling Strength of Metal Structures," McGraw-Hill Book Co., Inc., New York, N. Y.,1952.

Chang, I.C., " On the Buckling Strength of Frames," Thesis Presented to the Illinois Inst. of Tech., in Chicago, Ill., 1958, in Partial fulfillment of the requirements for the degree of Doctor of Philosophy.

Chapuis, J. and T.V. Galambos., " Restrained Crooked Aluminum Columns," Journal of Structural Division, ASCE, Vol. 108, No. ST3, March 1982, 511-524.

Chen, W.F., " Semi-Rigid Connections in Steel Frames," Structural Engineering Report, Purdue University, West Lafayette, IN, 1987.

Chen, W.F., " Semi-Rigid Connections in Steel Frames," Tall Building and Urban Environment Series, McGraw-Hill, New York, 1993.

Frye, M.J., " Analysis of Frames with Flexible Connections," MSC Thesis, Department of Civil Engineering, University of Manitoba, Winnipeg, Manitoba, Canada, 1971.

Frye, M.J., and G.A. Morris, "Analysis of Flexible Connected Steel Frames," Canadian Journal of Civil Engineers, 2, No.3, September 1975, 280-91.

Geschwinder, Louis F., " A Simplified Look at Partially Restrained Beams," Engineering Journal, American Institute of Steel Construction, Second Quarter, 1991.

Grundy, P., " Stability and Design of Frames with Flexible Connections," J. Institution of Engineers, Australia, Civil Engineering Transaction v, CE28, No.2,Apr. 1986, p. 190-194.

Halldorsson, P. and Wang, C.K., " Stability Analysis of Frameworks by Matrix Methods," Journal of Structural Division, ST7, July, 1968.

Johnston, B.G., " Guide to Stability Design Criteria for Metal Structures," Wiley Interscience, New York, 1976.

Kounadis, A.N., Giri, J. and Simitses, G.J., " Nonlinear Stability Analysis of an Eccentrically Loaded Two-bar Frame," Journal of Applied Mechanics, Vol. 44, Series E, No. 4, 1977, p. 701-706.

Le-Wu Lu, A.M., " Stability of Frames Under Primary Bending Moments," Journal of the Structural Division, No. ST 3, June, 1963, pp. 35-62

Lionberger, S.R., "Statics and Dynamics of building Frames with Non-Rigid Connections," Ph.D. Thesis, Stanford University, 1967.

Lionberger, S.R. and W. Weaver, "Dynamics Response of Frames with Non-Rigid Connections," Journal of Engineering Mechanics Division, American Society of Civil Engineers, 95, EM. 1, February 1969, 95-114.

LRFD, "Load and Resistance Factor Design Specification For Structural Steel Buildings", AISC, Chicago, IL, Oct.,1986.

Lui, E.M., " Effect of Connection Flexibility and Panel Zone Deformation on the Behavior of Plane Steel Frames," Ph.D. Dissertation, School of Civil Engineering, Purdue University, West Lafayette, IN, 1985.

Masur, E.F., Chang, I. C. and Donnell,L.H., "Stability of Frames in the Presence of Primary Bending Moments," Journal of the Engineering Mechanics Division, ASCE, Vol. 87, No. EM4, proc. Paper 2442, August, 1961.

Rashed, A., Machaly, B. and Niazy, A.S., " Stability of Space Frames with Semi-Rigid Connections," Journal of Computer and Structures, Vol. 36, No. 4, pp 613-622, 1990

Richard, R.M. and Abbott, B.J., " Versatile Elastic-Plastic Stress-Strain Formula," J. Engineering Mechanics Division, ASCE, Vol. 101, No. EM4,Aug., 1975, pp. 511-515.

Romstad, K.M. and C.V. Subramanian, " Analysis of Frames with Partial Connection Rigidity," Journal of Engineering Mechanics Division, American Society of Civil Engineers, 96, ST. 11, November 1970, 2283-2300.

Simitses, G.J. and Vlahinos, A.S., " Stability Analysis of a Semi-Rigidly Connected Simple Frame," Journal of Constructional Steel Research. Vol.2, No. 3, September 1982.

Sommer,W.H., " Behavior of Welded Header Plate Connections," Masters Thesis, University of Toronto, Ontario, Canada, 1969.

Timoshenko, S.P. and Gere, J.M., " Theory of Elastic Stability," McGraw-Hill Book Co., New York, N. Y., 1961, Chapter 1.

Wang, C.K., " Intermediate Structural Analysis," McGraw Hill Inc., New York, 1983, Chapter 20, pp. 721-740.

Yu, C.H. and Shanmugam, N.E., " Stability of Frames with Semi-Rigid Joints," Journal of Computer and Structures, Vol. 23, No. 5, pp 639-648, 1986.

Yu, C.H. and Shanmugam, N.E., " Stability of Semi-Rigid Space Frames," Journal of Computer and Structures, Vol. 28, No. 1, pp 85-91, 1988.

Yura, Joseph A., " The Effective Length of Columns in Unbraced Frames", AISC Engineering Journal (April, 1971).